

Explorations of Black Hole Thermodynamics in de Sitter Spacetime

by

Saoussen Mbarek

A thesis
presented to the University of Waterloo
in fulfillment of the
thesis requirement for the degree of
Doctor of Philosophy
in
Astrophysics and Gravitation

Waterloo, Ontario, Canada, 2019

© Saoussen Mbarek 2019

Examining Committee Membership

The following served on the Examining Committee for this thesis. The decision of the Examining Committee is by majority vote.

- External Examiner: Valeri P. Frolov
Professor, Dept. of Physics,
University of Alberta
- Supervisor(s): Robert B. Mann
Professor, Dept. of Physics and Astronomy,
University of Waterloo
- Internal Member: Niayesh Afshordi
Associate Professor, Dept. of Physics and Astronomy,
University of Waterloo
- Internal-External Member: Florian Girelli
Associate Professor, Dept. of Mathematics,
University of Waterloo
- Other Member(s): Avery Broderick
Associate Professor, Dept. of Physics and Astronomy,
University of Waterloo

Author's Declaration

This thesis consists of material all of which I authored or co-authored: see Statement of Contributions included in the thesis. This is a true copy of the thesis, including any required final revisions, as accepted by my examiners.

I understand that my thesis may be made electronically available to the public.

Statements of Contribution

1. This thesis is based on the following publications
 - Chapter 3 is based on:
R. A. Hennigar., R. B. Mann and S. Mbarek ,*Thermalon mediated phase transitions in Gauss-Bonnet gravity*, *JHEP* **02** (2016)034, [1512.02611].
This work was in collaboration with Robie A. Hennigar and Robert B. Mann.
 - Chapter 4 is based on:
S. Mbarek and R. B. Mann,*Thermodynamic Volume of Cosmological Solitons*, *Phys. Lett. B* **765** (2017)352-358, [1611.01131].
This work was in collaboration Robert B. Mann.
 - Chapter 5 is based on:
S. Mbarek and R. B. Mann,*Reverse Hawking-Page Phase Transition in de Sitter Black Holes*, [1808.03349].
This work was in collaboration with Robert B. Mann.
2. With permission granted by the authors Robert B. Mann and David Kubiznak, the figures in Chapter 2 are reproduced from:
M. Teo, D. Kubiznak and R. B. Mann,*Black hole chemistry: thermodynamics with Lambda*, *Class. Quant. Grav.* **34** (2017)6-063001, [1608.06147].

Abstract

In this thesis I map out two approaches that are foundational to studying black hole thermodynamics in de Sitter spacetime. The first is to understand the “thermodynamic volume” of cosmological horizons in isolation. Fortunately a broad class of exact solutions having only a cosmological horizon exists: Eguchi-Hanson de Sitter solitons. I carried out the first study of thermodynamic volume associated with the cosmological horizon for Eguchi-Hanson de Sitter solitons in general dimensions. This work illustrated that the cosmological volume is a well-defined concept, and that cosmological horizons indeed have meaningful thermodynamic properties.

The second approach is to move on and include black hole horizons. My first step along this path is to understand the phase transitions of thermalons: objects that describe a transition from a black hole in Anti de Sitter spacetime to one in de Sitter spacetime. This indicated that asymptotically de Sitter black holes do have phase transitions which inspired my second project where I exploit a class of exact hairy black hole solutions to Einstein gravity with conformally coupled scalar fields to overcome the two-horizon problem. By adding hair to the black hole, the thermodynamic equilibrium could be maintained between the two horizons. These solutions make it possible to explore a range of black hole phase transitions in de Sitter spacetime. I found that this hairy charge black hole system, and the de Sitter space surrounding it, undergo a “Reverse” Hawking-Page phase transition within the grand-canonical ensemble. This is the first approach that successfully addressed the two-horizon problem whilst including all contributions of energy from every part of the system.

Acknowledgements

To my role-model, my life-coach and my best friend, my mother Nejia: I wouldn't have come this far without you Mama, may *Allah* bless your heart. I love you!

I am thankful to the rest of my family for their never-ending support: my father Mohamed who always believed in me. My brother Bessem who is always there for me. He is the best brother anyone can ever hope for. Last but not least, my sister Sabria who always made me want to be a better version of myself.

I am so grateful to my supervisor Dr. Robert B. Mann for giving me this amazing opportunity to learn from him, for all his continuous support and encouragement and for making all of us feel like a family.

Many thanks to all my friends who have been there for me during this rough journey especially Katherine White, Kim-Tuyen Hoang , Chengyu Xi, Ridha Soua, Ibrahim Ben Daya. I couldn't be happier having such caring and supportive friends.

I would like to acknowledge the friendship and assistance of many of my colleagues here at the University of Waterloo. A special thanks goes to Erickson Tjoa for reading the first draft of this thesis and providing feedback, and to Robie Hennigar for tirelessly answering many of my questions about black holes throughout the years.

Finally, to my fiancé Marwen Ben Rejeb: no words can ever express how thankful I am to you. Your unconditional love, support and understanding made this experience rather easy. I hope I can make you as happy as you make me, I love you!

Dedication

In memory of a great man.. my high school physics teacher Mr. *Abdallah El Fersi*
May his soul rest in peace.

Table of Contents

List of Tables	xi
List of Figures	xii
Notations and Conventions	1
1 Introduction	1
1.1 A Gravity Overview: from Einstein to Lovelock	2
1.2 A promenade in de Sitter Land	5
2 Black Hole Chemistry in a Nutshell	8
2.1 Standard Black Hole Thermodynamics: Overview	8
2.2 Thermodynamics with Λ	11
2.3 Black Hole Volume Dilemma	13
2.3.1 Thermodynamic Volume	13
2.3.2 Reverse Isoperimetric Inequality	15
2.4 Black Hole Chemistry	17
2.4.1 Hawking-Page Phase Transition	17
2.4.2 Other AdS black hole phase transitions	20
2.4.2.1 Van der Waals phase transitions	20
2.4.2.2 Reentrant phase transitions	23

2.4.2.3	Triple points: a solid/liquid/gas phase transition	24
2.4.3	Thermodynamics of asymptotically de Sitter black holes	25
2.4.3.1	Multiple Horizons: First laws and Smarr Formulae	26
2.4.3.2	Multiple Horizons: Effective thermodynamics	28
I	Cosmological Horizons	31
3	Thermodynamic Volume of Cosmological Solitons	32
3.1	EHdS solitons	34
3.2	Soliton Thermodynamics	35
3.2.1	Inside the cosmological horizon	37
3.2.2	Outside the cosmological horizon	39
3.3	Discussion	44
II	Black Hole Chemistry in de Sitter Spacetime	46
4	Thermalons	47
4.1	Thermalons in Lovelock gravity	48
4.2	Gauss-Bonnet case	51
4.2.1	Stability	53
4.2.2	Thermodynamic picture	54
4.2.3	Criticality & phase phenomena	57
4.2.3.1	Negative pressure: thermal AdS to dS black hole transitions	57
4.2.3.2	Vanishing pressure: thermal AdS to asymptotically flat black hole transitions	64
4.2.3.3	Positive pressures: thermal AdS to AdS black hole transitions	66
4.3	Discussion	67

5	Hairy Black Holes	68
5.1	Conformal Scalar Coupling and Hairy Black Hole Thermodynamics	69
5.2	Asymptotically de Sitter Hairy black holes	71
5.2.1	Setup	72
5.2.2	The Grand Canonical Ensemble: Thermodynamics with Fixed Potential	75
5.2.3	Canonical Ensemble: Thermodynamics with Fixed Charge	78
5.3	Discussion	80
6	General Conclusions	81
	References	84
	Appendices	94
A	Generalized first law of black hole mechanics	95
B	Van de Waals Fluids: A brief review	98
C	Eguchi-Hanson Solitons	100
D	Themalons	102

List of Tables

3.1	General results	40
3.2	Results with the regularity condition $y^2 = \frac{3}{4}$ imposed	41
3.3	Mass and Volume computed outside the cosmological horizon. The constant $m_{\frac{D}{2}}$ is chosen to yield the mass of de Sitter spacetime when $a = 0$	44

List of Figures

2.1	Hawking–Page phase transition. A plot of the Gibbs free energy of a Schwarzschild-AdS black hole as a function of temperature for fixed pressure $P = 1/(96\pi)$	18
2.2	The Hawking-Page phase transition coexistence diagram: A plot displaying a $P - T$ coexistence line of the thermal radiation/large black hole state.	19
2.3	Swallowtail behaviour of RN–AdS black hole A plot of the Gibbs free energy of a Reissner–Nordstrom-AdS black hole at a fixed charge $Q = 1$	21
2.4	Coexistence line of RN–AdS black hole A plot of the $P - T$ phase diagram illustrating the small/large black hole phase transition.	22
2.5	Reentrant phase transition diagram A plot of the Gibbs free energy of a singly spinning Kerr-AdS black hole in $d = 6$. The arrows in this figure indicate the increasing size of the event horizon r_+	23
2.6	Coexistence line of singly spinning Kerr–AdS black hole A plot of the $P - T$ phase diagram of a singly spinning rotating black hole.	25
2.7	Coexistence line of doubly spinning Kerr–AdS black hole A plot of the $P - T$ phase diagram in $d = 6$ for a doubly-spinning Kerr-AdS black hole at fixed angular momenta ratio $J_2/J_1 = 0.05$. The diagram displays a triple-critical point where the three states could coexist.	26
3.1	Plots of the isoperimetric ratio \mathcal{R} (for a representative dimension $D = 6$) as a function of the parameter $y = \frac{a}{l}$. The plots, from left to right, correspond respectively to case 1, case 2, and case 4 discussed in Table 3.1. The dashed line corresponds to the regularity condition $y = \sqrt{3/4}$	38

3.2	A plot of the isoperimetric factor \mathcal{R} for the cases 1, 2 and 4 of the cosmological volume as a function of the spatial dimension D when the regularity condition is imposed (see Table 3.2). The first case is (blue), the second is in (red) and the fourth is in (green).	39
4.1	A plot of r_h (blue), r_c (red) and a_* (green) as functions of a_* for $d = 5$, $\lambda = 0.1$, $\Lambda = 0.5$, $\sigma = 1$. I see that the bubble location, a_* , is always found between the event horizon and the cosmological horizon until all three meet at the Nariai bound, $a_* = 1/\sqrt{4\Lambda}$. The plot is qualitatively the same for $d > 5$	55
4.2	A plot displaying a_* (black), the cosmological horizon (cyan), the event horizon (red) and the mass parameter M_- (purple) as functions of a_* , in units of the Planck length. The Nariai limit corresponds to the point where the black, cyan, and red curves meet. This plot corresponds to $P = -0.1$ and $\lambda = 1.35$; plots for other parameter values are qualitatively similar.	58
4.3	AdS to dS transition: pressure effects: $\lambda = 1.35$. The red curves correspond to $P = -0.1$ while the blue curves correspond to $P = -1$. <i>Upper left:</i> A plot of the free energy vs. T_+ . For $P = -0.1$ a thermalon mediated phase transition is possible over a range of temperature, while it is not possible for $P = -1$. In each case the thin upper branch is unphysical, corresponding to $\Pi^+ = -\Pi^-$. The dotted black line corresponds to the Gibbs free energy for the Nariai limit as a function of pressure. <i>Upper right:</i> A plot of the temperature, T_+ vs. a_* n both the blue and red curve, the cusp corresponds to the Nariai limit. <i>Bottom:</i> A plot showing the Gibbs free energy as a function of a_* with the cusps again corresponding to the Nariai limit. All quantities are measured in units of the Planck length. The thick lines correspond to the physical curves.	59
4.4	AdS to dS transition: λ effects: $P = -0.1$. The above plots show the free energy vs temperature (T_+) for $\lambda = 0.05, 0.1, 0.2, 1.35$ (from right to left) with the right plot being just a zoomed-in version of the left. Thermalon mediated phase transitions are possible over a wider range of temperatures for larger values of λ . The physical parts of the curves are the thick ones to the left of the cusps. The dotted black line corresponds to the Nariai limit as a function of λ . Quantities are measured in units of the Planck length.	61

4.5	AdS to dS transition: $P - T$ plane: $\lambda = 0.1$. For parameter values inside the red curve a thermalon mediated phase transition is permitted, while parameters outside of this wedge correspond to thermal AdS space—no phase transition is possible. The cusp corresponds to the Nariai limit; the physical curve is the thick one at the left.	62
4.6	AdS to dS transition: Nariai Gibbs free energy. The dotted lines display the Gibbs free energy at the Nariai limit for $\lambda = 0.1, 0.2, 0.4, 0.8, 1.35$ (right to left, respectively). The solid black curve displays the locus of points corresponding the limit $P \rightarrow -\infty$ of the Nariai Gibbs free energy. The quantities are measured in units of the Planck length.	63
4.7	AdS to flat space transition: <i>Left:</i> G vs. T plot for $P = 0$ showing $\lambda = 0.1, 0.2, 0.4, 0.8, 1.35$ (bottom to top in y -intercept). For each value of λ there is a temperature above which the thermalon-mediated transition can occur. <i>Right:</i> The coexistence plot in $\lambda - T$ space for the AdS to asymptotically flat black hole transition. Below the red line, the thermodynamically preferred state is thermal AdS space, while above the red line an asymptotically black hole is thermodynamically preferred. The coexistence plot can only be read from left to right, and not from right to left, since the thermalon is dynamically unstable.	65
5.1	The thermodynamic parameters of the charged hairy asymptotically de Sitter black holes: for $P = -0.0001$. The $\{red, blue, green, purple\}$ curves correspond to the potential $\Phi_+ = \{0.1, 1, 2, 3\}$ respectively. The dotted line represents the Nariai limit.	73
5.2	The thermodynamic parameters of the charged hairy asymptotically de Sitter black holes for fixed potential: the case of $\Phi_+ = 0.1$. The $\{red, blue, green, purple\}$ curves correspond respectively to the pressure $P = \{-0.0001, -0.0003, -0.0005, -0.0008\}$. The dotted line represents the Nariai limit.	74
5.3	Gibbs Free Energy with fixed potential. The green curve represents G_+ , corresponding only to the black hole, as a function of temperature. The blue curve represents G_c as measured at the cosmological horizon r_c and the red curve is that of G_{Total} for the total system <i>i.e.</i> of the black hole in a the de Sitter heat bath. All curves are plotted for $P = -0.0001$ and $\Phi_+ = 0.1$	76
5.4	Specific Heat. This curve represents C_P , the specific heat of the system, as a function of the temperature. It is plotted for $P = -0.0001$ and $\Phi_+ = 0.1$	77

5.5	Total Gibbs Free Energy G_{Total}. <i>Left:</i> G_{Total} at $P = -0.0001$ where the $\{red, blue, green, purple\}$ curves correspond to the potential $\Phi_+ = \{0.1, 1, 2, 3\}$ respectively . <i>Right:</i> G_{Total} at $\Phi_+ = 0.1$ where the $\{red, blue, green, purple\}$ curves correspond to the pressure $P = \{-0.0001, -0.0003, -0.0005, -0.0008\}$ respectively	78
5.6	Canonical Gibbs Free Energy (CGFE): the green curve represents the CGFE corresponding only to the black hole, the blue curve represents the CGFE as measured at the cosmological horizon r_c , the red curve is of the CGFE of the total system <i>i.e.</i> of the black hole in a the de Sitter heat bath . All curves are plotted for $P = -0.0001$ and $Q = 1$	79

Chapter 1

Introduction

Over the past forty years a great number of studies found evidence of an important relationship between quantum theory, gravity and thermodynamics. This evidence is manifest in the behaviour of black holes and their connections to quantum physics.

Black holes, however, are peculiar objects. Classically, it is easy to compare them to ‘monstrous’ sponges: they swallow everything, not even light can escape them, but emit nothing. Yet from the perspective of an observer outside the horizon, when taking quantum mechanical effects into account, they seem strangely ordinary: they obey, like any regular matter system, a set of thermodynamics laws [1] governed by an entropy S , a temperature T and an energy E proportional respectively to the horizon’s area A , its surface gravity κ , and its mass M .

The progress made in understanding the precise way black hole thermodynamics works generated a whole new set of techniques for analysing the behaviour of black holes. Some of those techniques came from better understanding the classical theory of general relativity; others are rooted to how quantum field theory behaves on a black hole background. Other studies led to one of the most puzzling dilemmas in physics: *how the process of black hole radiation results in a loss of information*. In other words, physical information can permanently be lost in a black hole, which contradicts a fundamental concept of quantum theory: Unitarity [2, 3]. The latter implies that information is conserved in the sense that the value of a wave function, whose evolution is determined by a unitary operator, of a physical system at one point in time should be enough to determine its value at any other point in time. This is known as the *information paradox* [4]. This problem has yet to be resolved [5, 6, 7]. It was proved that black hole entropy is the Noether charge associated with diffeomorphism symmetry [8] and that gravitational laws appear to have

a deep connection with thermodynamics laws [9, 10]. Additionally, it was found that the negative cosmological constant induces a black hole phase behaviour [11], later leading to exploiting black holes as holographic systems dual to systems in conformal field theories [12, 13, 14], quantum chromodynamics [15], and condensed matter physics [16, 17].

In recent years, the subject of black hole thermodynamics rose to the spotlight with the reconsideration of the role of the cosmological constant, Λ , leading to the introduction of *pressure*, and thus a new notion of *volume for a black hole*. Black hole phase behaviour, similar to that of everyday physical systems, was unveiled. Some manifestations included triple point phase behaviour analogous to that in water, while others exhibited Van der Waals fluid-type phase transitions. Subsequent work indicated that black holes could be treated as heat engines. This subfield has come to be known as *black hole chemistry* [18, 19].

In this context, our knowledge of the thermodynamic behaviour of asymptotically de Sitter (dS) black holes, for which $\Lambda > 0$, is significantly more sparse [20, 21, 22, 23, 24, 25, 26] than our knowledge of their AdS cousins. Yet their importance to cosmology and to a posited duality between gravity in de Sitter space and conformal field theory [27] make them important objects of investigation. However this is a complex problem, since the absence of a Killing vector that is everywhere timelike outside the black hole horizon renders a good notion of the asymptotic mass questionable. Furthermore, the presence of both a black hole and a cosmological horizon yields two distinct temperatures, suggesting that the system is in a non-equilibrium state.

The thermodynamics of black holes in asymptotically de Sitter spacetime will be the general topic of this thesis. The purpose of this chapter is to provide a general introduction and summarize some key concepts, some of which will be thoroughly studied in later chapters. As some of the work done employs Lovelock theory of gravity, I start this chapter by briefly introducing these theories and their importance to gravitational physics. Furthermore, all of the work done in this thesis concerns asymptotically de Sitter spacetimes, the main reason why I will give an overview of the geometry of de Sitter spacetime and discuss some of its key concepts with regards to black holes and cosmology. I will then give an outline to the approaches taken in this thesis.

1.1 A Gravity Overview: from Einstein to Lovelock

One of the most inspiring scientific accomplishments in the 20th century was Einstein's theory of general relativity [28]. It was a result of the urgent need to harmonize the relation between Newton's laws of gravitational interaction and the theory of special relativity

[29]. It was simultaneously, yet independently, studied by both Albert Einstein and David Hilbert; hence the name of its Einstein-Hilbert action.

The Einstein-Hilbert (EH) action of a spacetime with cosmological constant¹ Λ coupled to matter reads

$$\mathcal{I}_{d=4} = \frac{1}{16\pi G} \int d^4x \sqrt{-g} (R - 2\Lambda) + \mathcal{I}_{mat} . \quad (1.1)$$

It gives rise to the field equations

$$\mathcal{G}_{\mu\nu}(g_{\alpha\beta}, g_{\alpha\beta;\gamma}, g_{\alpha\beta;\gamma\lambda}) = 8\pi T_{\mu\nu} , \quad (1.2)$$

where the tensor on the left hand side, namely the Einstein tensor, is symmetric and conserved

$$\mathcal{G}^{\mu\nu}{}_{;\nu} = 0 . \quad (1.3)$$

However, the right hand side tensor, namely the stress-energy tensor, is symmetric.

In his famous work in 1971, Lovelock [31] generalized Einstein theory of relativity in higher dimensions. He obtained the most general formal expression of $\mathcal{G}^{\mu\nu}$ in terms of powers of the the Riemann curvature tensor while maintaining its symmetric and conserved properties. Miraculously, this tensor is quasi-linear in the second derivatives of the metric without any higher derivatives. Additionally, in four dimensions (or less), these field equations coincide with the Einstein field equations

$$R_{\mu\nu} - \frac{1}{2}g_{\mu\nu}R + \Lambda g_{\mu\nu} = 8\pi G T_{\mu\nu} , \quad (1.4)$$

with the constant of proportionality being carefully chosen to reproduce the Newtonian limit.

The phenomenological relevance of the Lovelock class of gravity theories is debatable as they only exist in higher dimensions. However they provide an intriguing framework from the theoretical perspective for multiple reasons: as the higher dimensional “siblings” to Einstein’s general relativity “family”, they permit the exploration in higher dimensions of very interesting objects such as Black holes , gravitational collapse and even cosmology. Lovelock gravity theories provide many useful and unique perspectives for studying black holes: their formation, their existence, their thermodynamics, and much more.

¹The cosmological constant was first introduced by Einstein [30] to describe a stationary universe. Thereafter, he described it as his “greatest blunder” when the expansion of the universe was proven with the observation of the Hubble redshift. The concept of the cosmological constant was later revived when numerous observations, such as the discovery of the cosmic acceleration, proved that it is greater than zero.

Lovelock theories of gravity are the most general gravitational theories in higher-dimensional spacetimes that have field equations of second order. The action for Lovelock gravity in d dimensions can be written in terms of bulk and boundary terms² as

$$\mathcal{I} = \frac{1}{16\pi G} \sum_{k=0}^{k_{\max}} \frac{c_k}{d-2k} \left(\int_{\mathcal{M}} \mathcal{L}_k - \int_{\partial\mathcal{M}} \mathcal{Q}_k \right), \quad (1.5)$$

where the $\{c_k\}$ are coupling constants,

$$\mathcal{L}_k = \epsilon_{a_1 \dots a_d} R^{a_1 a_2} \wedge \dots \wedge R^{a_{2k-1} a_{2k}} \wedge e^{a_{2k+1}} \wedge \dots \wedge e^{a_d}, \quad (1.6)$$

with \wedge the standard wedge product for differential forms and

$$\mathcal{Q}_k = k \int_0^1 d\xi \epsilon_{a_1 \dots a_d} \theta^{a_1 a_2} \wedge \mathfrak{F}^{a_3 a_4} \wedge \dots \wedge \mathfrak{F}^{a_{2k-1} a_{2k}} \wedge e^{a_{2k+1}} \wedge \dots \wedge e^{a_d}. \quad (1.7)$$

Here $e^a = e^a{}_\mu dx^\mu$ is the vielbein 1-form, $R^{ab} = d\omega^{ab} + \omega^a{}_c \wedge \omega^{cb}$ is the curvature 2-form (ω^{ab} being the torsionless Levi-Civita spin connection), and $\mathfrak{F}^{ab} = R^{ab} + (\xi^2 - 1)\theta^a{}_c \wedge \theta^{cb}$ with θ^{ab} being the second fundamental form related to the extrinsic curvature via $\theta^{ab} = (n^a K^b{}_c - n^b K^a{}_c)e^c$ and ξ is the parameter of integration of ranging between 0 and 1 [33].

Note that G is the Newton constant in d spacetime dimensions and $\{c_k\}$ is a set of coupling constants with length dimensions $\ell^{2(k-1)}$, ℓ being a length scale related to the cosmological constant, with k being a positive integer given by

$$k \leq k_{\max} = \left\lfloor \frac{d-1}{2} \right\rfloor. \quad (1.8)$$

The zeroth, first, second and third terms in (1.5) correspond, respectively, to the cosmological term, the Einstein-Hilbert action, the Gauss-Bonnet gravity and the third order (cubic) Lovelock gravity. The coupling constants are chosen so that $c_0 = \ell^{-2}$ and $c_1 = 1$ correspond to the usual normalization of the zeroth and first terms with the cosmological constant costumed to satisfy $2\Lambda = -(d-1)(d-2)/\ell^2$. Λ is also easily incorporated with either a negative ($c_0 = -\ell^{-2}$), a vanishing ($c_0 = 0$) or a positive ($c_0 = \ell^{-2}$). The Gauss Bonnet term governed by $c_2 = \lambda\ell^2$ gives rise to the first non-trivial Lovelock term that contributes just for $d > 4$ with λ being the Gauss-Bonnet coupling constant.

A simple example is the cubic Lovelock theory . Its action is

$$\mathcal{I} = \frac{1}{16\pi G} \int d^d x \sqrt{-g} \left[R - 2\Lambda + \frac{(d-5)!}{(d-3)!} \lambda \ell^2 \mathcal{L}_2 + \frac{(d-7)!}{(d-3)!} \frac{\mu}{3} \ell^4 \mathcal{L}_3 \right], \quad (1.9)$$

²Here I follow the notation of [32] for consistency with the work done in chapter 4

where the quadratic lagrangian, defined only for $d > 4$, and the cubic lagrangian, defined only for $d > 6$, are

$$\mathcal{L}_2 = R^2 - 4R_{\mu\nu}R^{\mu\nu} + R_{\mu\nu\rho\sigma}R^{\mu\nu\rho\sigma} , \quad (1.10)$$

$$\begin{aligned} \mathcal{L}_3 = & R^3 + 3RR^{\mu\nu\alpha\beta}R_{\alpha\beta\mu\nu} - 12RR^{\mu\nu}R_{\mu\nu} + 24R^{\mu\nu\alpha\beta}R_{\alpha\mu}R_{\beta\nu} + 16R^{\mu\nu}R_{\nu\alpha}R_{\mu}^{\alpha} \\ & + 24R^{\mu\nu\alpha\beta}R_{\alpha\beta\nu\rho}R_{\mu}^{\rho} + 8R^{\mu\nu}_{\alpha\rho}R^{\alpha\beta}_{\nu\sigma}R^{\rho\sigma}_{\mu\beta} + 2R_{\alpha\beta\rho\sigma}R^{\mu\nu\alpha\beta}R^{\rho\sigma}_{\mu\nu} . \end{aligned} \quad (1.11)$$

In some parts of this thesis I will make use of these phenomenal gravity theories mainly in the context of de Sitter spacetime. I shall introduce this framework in the next section.

1.2 A promenade in de Sitter Land

Usually in general relativity, one doesn't need to (and maybe even can't) define manifolds and curvature by embedding them in higher dimensional spacetime, but rather simply define them intrinsically. However, de Sitter spacetime, a maximally symmetric spacetime of constant positive cosmological constant, can intuitively and easily be embedded. Its embedding can be presented as follows: a d dimensional de Sitter spacetime is equivalent to an hyperbola embedded in a $d + 1$ dimensional Minkowski spacetime. Its embedding space metric reads

$$ds_{embedded}^2 = -dX_0^2 + dX_1^2 + \dots + dX_d^2. \quad (1.12)$$

One can simply view de Sitter space of length ℓ as a hypersurface defined by

$$X_{\mu}X^{\mu} = \ell^2. \quad (1.13)$$

The induced metric of this surface can be written as

$$ds^2 = -\left(1 - \frac{r^2}{\ell^2}\right) dt^2 + \frac{dr^2}{\left(1 - \frac{r^2}{\ell^2}\right)} + r^2 d\Omega_{d-2}^2, \quad (1.14)$$

when using the following coordinates:

$$X_0 = \sqrt{\ell^2 - r^2} \sinh\left(\frac{t}{\ell}\right), \quad X_1 = \sqrt{\ell^2 - r^2} \cosh\left(\frac{t}{\ell}\right), \quad X_j = r\hat{\mu}_j. \quad (1.15)$$

Note that $d\Omega_{d-2}^2$ denotes the line element on a $(d - 2)$ -dimensional sphere and $\hat{\mu}_j$, while satisfying $\sum_j \hat{\mu}_j^2 = 1$, represents the angular coordinates of the sphere such that, for example,

$$\hat{\mu}_1 = \sin\theta \sin\phi_1 \sin\phi_2 \dots \sin\phi_{d-3}, \quad \hat{\mu}_2 = \sin\theta \sin\phi_1 \sin\phi_2 \dots \cos\phi_{d-3}. \quad (1.16)$$

Recently, de Sitter spacetime became of high interest to the study of our universe. First, as a spacetime having positive cosmological constant, de Sitter space is of great importance to cosmology. For example, its importance is manifested in the early universe during cosmic inflation as many inflationary models are approximately de Sitter space. In other words, it is simpler to conduct some analysis on the early universe’s inflation era in de Sitter space rather than a more realistic inflationary universe. Second, given the proposal for holographic duality between de Sitter space and conformal field theory has been suggested [27], there is further reason to study black hole thermodynamics in de Sitter (dS) spacetime. This proposal “conjectured that a fully quantum theory, including gravity, in pure de Sitter space with a fixed cosmological constant has a certain dual representation as a conformally invariant Euclidean field theory on the boundary of de Sitter space” [34].

Motivated by the above, I shall study the thermodynamics of black holes in asymptotically de Sitter spacetime. These black holes, however, are burdened with problems that are absent for their AdS cousins: first, an asymptotically de Sitter black hole has two-horizons, an event horizon and a cosmological horizon, which created a non-equilibrium state for any observer living between the horizons. Second, concept of mass for this system is somewhat *blurry* due to the lack of a global timelike Killing vector outside the black hole. Third, isolated de Sitter black holes evaporate due to Hawking radiation which makes them, unlike their AdS cousins where reflecting boundary conditions at ∞ ensure thermal stability, thermally “unstable”. These are the main reason why de Sitter spacetime remains not well understood despite its resemblance to our universe.

In this thesis I shall present an ensemble of studies to this end that are outlined as follows:

In chapter 2, I review some of the recent developments of black hole thermodynamics in the phase space where the cosmological constant is regarded as a thermodynamic variable equivalent to pressure, also known as the *extended thermodynamic phase space*. I start by giving an overview on the standard approaches to study the thermodynamics of black holes. Then I review the black hole thermodynamics in extended thermodynamic phase space and discuss the “thermodynamic volume” . The latter is the thermodynamic conjugate to the pressure. This discussion will be followed by an introduction to the reverse isoperimetric inequality and its importance. Furthermore, I will summarize the developments of black hole thermodynamics in extended phase space. I will then conclude by discussing the of black holes in de Sitter space and comment on the approaches proposed to understand black holes in this context.

In chapter 3, I study the thermodynamic volume of cosmological horizons in the context of Eguchi-Henson (EH) solitons.. I start by introduce the EH Solitons in odd dimensions.

Then I briefly discuss general considerations of their thermodynamics. Next, I make use of the first law and Smarr relation to compute the mass and thermodynamic volume of these solutions inside and outside the cosmological horizon of dS space . Finally, I show that explicit expressions for the two parameters can be found in general odd dimensions.

In chapter 4, I study thermalon mediated phase transitions in Gauss-Bonnet gravity. I start by briefly reviewing the basics and the essentials of the thermalon mechanism in Lovelock gravity. Then I specialize to the case of Gauss-Bonnet gravity where I study the stability, extended phase space thermodynamics, and phase structure of the thermalons. When considering the phase behaviour of these systems, I employ the extended thermodynamic phase space formalism to exhaustively study how these transitions depend on the pressure (cosmological constant). In the context of AdS \rightarrow dS + black hole thermalon mediated phase transitions I recover the results of [35]. Furthermore, by analyzing the behaviour of the free energy near the Nariai limit, I find that for a fixed value of the Gauss-Bonnet coupling, there is a minimum pressure below which thermalon mediated phase transitions are not possible. I find that in the case where the pressure is vanishing, a phase transition between thermal AdS space and an asymptotically flat geometry with a black hole is possible for any range of temperature. In the last section we comment on the similarities and differences between the thermalon mediated phase transition and the Hawking-Page transition in the regime of positive pressures.

In chapter 5, I study the thermodynamics of charged de Sitter hairy black holes. I start by briefly reviewing the basics of conformally coupling scalar fields to gravity and their resultant hairy black holes solutions. Then I specialize to the case of charged hairy black holes in de Sitter spacetime. When considering the phase behaviour of these systems, I employ the extended thermodynamic phase space formalism to study how their thermodynamic parameters behave at constant pressure (cosmological constant) and at constant chemical potential. Furthermore, in a search of possible phase transitions, I study the behaviour of the free energy in different ensembles. I find that a system of a charged hairy black hole in de Sitter will undergo a Reverse Hawking-Page phase transition if studied in the grand-canonical ensemble, but will not undergo any phase transitions if studied in the canonical ensemble. The latter is due to a violation of the conservation of charge.

I will conclude my work in Chapter 6 where I will summarize the work conducted in this thesis and suggest few approaches to better understand asymptotically de Sitter black holes. This chapter will be followed by an ensemble of appendices of relevant mathematical derivations.

Chapter 2

Black Hole Chemistry in a Nutshell

Understanding the relationship between thermodynamics, gravitation and quantum theory has been a subject of great interest in last fifty years due to the rising evidence suggesting that such a relationship indeed exists. This evidence is embedded in the relation between black holes and quantum physics, the subject known as black hole thermodynamics. Classically, this relationship is counter-intuitive [36] due to the black hole's classical nature: it absorbs all forms of matter but emits nothing. Hence it has no entropy or temperature and it is only defined by its mass, angular momentum and the charge if possible [37]. However the explorations of quantum field theory in curved spacetime affirmed this relationship through a series of famous results: the first result, found by Bekenstein, introduced the idea that the area of a black hole corresponds to its entropy[38]. This relationship was then confirmed by Hawking's result that the black hole's surface gravity corresponds to its temperature [39]. These results opened the door to a new way of understanding black holes as objects that, similar to black bodies, emit radiation. And so was born the sub-discipline of black hole thermodynamics.

2.1 Standard Black Hole Thermodynamics: Overview

Hawking's area theorem [40] states that the area of the event horizon of a black hole can never decrease. This was the first indication that black holes, then known only as classical solutions to Einstein's equations, can manifest thermodynamic behaviour¹. Thereafter

¹Hawking's proof applies to black hole spacetimes that satisfy the following assumptions:

- The spacetime on and outside the future event horizon is a regular predictable space.

Bekenstein noticed the similarity between this area law and the second law of thermodynamics. Pursuing this thought, he proposed [41] that each black hole should be assigned an entropy proportional to the area of its event horizon. Following this analogy further, Bardeen, Carter, and Hawking formulated their now famous account the “four laws of *black hole mechanics*” [1] under the assumption that the event horizon of the black hole is a Killing horizon². The four laws are:

1. The surface gravity κ of a stationary black hole is constant over the event horizon.
2. As the system including a black hole shifts from one stationary state to another, the mass of the system changes as follows

$$\delta M = \frac{\kappa}{8\pi G} \delta A + \Omega \delta J + \Phi \delta Q, \quad (2.1)$$

where κ is the black hole’s surface gravity, A is the area of the event horizon, J its angular momentum, Q its the electric charge, $\Omega = \Omega_+ - \Omega_\infty$ its angular velocity and $\Phi = \Phi_+ - \Phi_\infty$ its electric potential. Here Φ_+ and Φ_∞ correspond respectively to the potential at the event horizon and the potential at infinity. The quantity Ω_∞ corresponds to the angular velocity of the (possibly) rotating frame at infinity.

3. In a classical process $\delta A \geq 0$, i.e. the area A of a black hole’s event horizon does not decrease.
4. It is impossible to create an extremal black hole, i.e. reduce the surface gravity κ to zero, in a finite number of steps.

In the presence of a Killing horizon, the surface gravity κ reads

$$\xi^a \nabla_a \xi^b = \kappa \xi^b, \quad (2.2)$$

for a suitably normalized Killing vector ξ^a that generates the horizon. The surface gravity can be thought of as the force exerted at infinity that is required to suspend an object of unit mass at the horizon of a static black hole [42] (for example the Schwarzschild black hole).

• The stress-energy tensor satisfies the null energy condition, $T_{ab} k^a k^b \geq 0$, for arbitrary null vector k^a .

²This a null hypersurface generated by a corresponding Killing vector field

From the classical perspective, these black hole laws present a simple analogy between black hole mechanics and ordinary thermodynamics, where the first law of ordinary thermodynamics³ reads

$$\delta U = T\delta S - P\delta V + \sum_i \mu_i \delta N_i + \Phi\delta Q. \quad (2.3)$$

This analogy relates the surface gravity κ to temperature and the event horizon area to the entropy of the black hole. In fact classical black holes, just like sponges, never emit anything and they have zero temperature.

In 1974, Hawking carried out the original formalism developed by Parker [43] for computing particle production in curved spacetimes. He discovered that when taking into account the quantum mechanical effects [39] of scalar fields, a black hole emits radiation at a characteristic temperature

$$k_B T = \frac{\hbar\kappa}{2\pi c}, \quad (2.4)$$

where k_B is Boltzmann's constant, c is the speed of light, and \hbar is Planck's constant. The comparison between the $T\delta S$ term in the first law of thermodynamics with the $\kappa\delta A$ term for black holes, later confirmed by Gibbons using the Euclidean path integral approach [44], suggests that the entropy is directly related to the area by

$$S = \frac{Ac^3}{4\hbar G}. \quad (2.5)$$

The presence of \hbar accentuates the quantum mechanical nature of black holes. They are no longer classical solutions – instead they are physical objects that have thermodynamic properties.

All the above introduces an explicit first law of black hole thermodynamics that, when setting⁴ $G = c = k_B = 1$ reads:

$$\delta M = T\delta S + \Omega\delta J + \Phi\delta Q, \quad (2.6)$$

for a black hole of mass M , charge Q , and angular momentum J . Keeping this in mind, I shall henceforth suppress the explicit appearance of these quantities, restoring them on an as-needed basis.

³ In the first law of *ordinary* thermodynamics, δN_i is the changing number of particles of a given species and μ_i is its corresponding chemical potential. Similarly the term $\Phi\delta Q$ presents the variable electrostatic energy.

⁴ This convention implies that \hbar has units of [length]² and that, in d dimensions, the gravitational constant G_d has units of [length] ^{$d-4$} .

The thermodynamic parameters, as simple as they seem, communicate the behaviour of the black hole. They are related by *Smarr* relation[45], which (in four dimensions) reads

$$M = 2(TS + \Omega J) + \Phi Q . \quad (2.7)$$

It displays the relationship between the extensive (M, J, Q) and intensive (T, Ω, Φ) thermodynamic variables.

2.2 Thermodynamics with Λ

When analyzing the first law (2.6), one cannot help but wonder about the pressure-volume term $P\delta V$. As there has been no mention of pressure or volume that could be associated with a black hole, this term remained poorly understood. Several years ago a new idea was proposed. It suggested that the pressure of a black hole could be associated with the *negative* cosmological constant Λ . In other words a black hole in a negative cosmological constant environment has corresponding positive pressure that is equal in magnitude to the negative energy density of the environment. This set up describes an asymptotically anti de Sitter black hole ⁵.

In d spacetime dimensions, given the AdS length ℓ , the corresponding negative cosmological constant reads

$$\Lambda = -\frac{(d-1)(d-2)}{2\ell^2} < 0 . \quad (2.8)$$

Proposed by Teitelboim and Brown [46, 47], the idea of considering Λ as dynamical variable was adopted, which incorporated formally[48] a Pressure-Volume term into the first law of black hole mechanics ⁶, and further explored from several perspectives afterwards [49, 50].

Remaining unchanged, the area of the black hole event horizon is $A = 4S$ where S is its entropy and the temperature is $T = \kappa/2\pi$ with κ its surface gravity.

The generalization of black hole mechanics when including a non zero cosmological constant, $\Lambda \neq 0$, set a solid foundation for association of the pressure with Λ and its thermodynamic conjugate with volume [51]. A simple derivation, fully described in Appendix A, leads to the generalized first law of black hole mechanics:

$$\delta M = T\delta S + V\delta P + \Omega\delta J + \Phi\delta Q . \quad (2.9)$$

⁵This class of black holes is a solution to the Einstein equations $R_{ab} - \frac{1}{2}g_{ab}R + \Lambda g_{ab} = 8\pi T_{ab}$, where T_{ab} is the matter stress-energy tensor.

⁶Here, no interpretation of the conjugate variable to the cosmological constant was considered.

Interpreting P as the thermodynamic pressure and V as its thermodynamic conjugate [52, 53], they both read

$$P = -\frac{\Lambda}{8\pi} = \frac{(d-1)(d-2)}{16\pi l^2} \quad (2.10)$$

and

$$V \equiv \left(\frac{\partial M}{\partial P} \right)_{S,Q,J} . \quad (2.11)$$

The interpretation of this *thermodynamic volume* will be carried out in the next section. Note that M is the conserved charge associated with the time-translation Killing vector of the spacetime and J is the conserved charge associated with a rotational Killing vector of the spacetime.

Comparing (2.9) with (2.3), it is logical to think of interpreting M as a gravitational version of chemical *enthalpy* [51]. In other words, no longer being interpreted as the internal energy, the mass can be thought of as the total energy of the system including both its internal energy E and the energy PV required to displace the vacuum energy of the spacetime. Relating the two quantities through a Legendre transformation the mass reads

$$M = E + PV . \quad (2.12)$$

Jokingly, one could regard this as being the amount of energy needed to create a black hole and place it in its environment ruled by a negative cosmological constant. If only I had that *superpower*.

By including Λ , a fundamental constant of the theory, as a thermodynamic variable, the *generalized* first law of black hole thermodynamics recovers the $V\delta P$ term in ordinary thermodynamics and reads [51, 53, 54, 55]

$$\delta M = T\delta S + \sum_j^N \Omega^i \delta J^i + V\delta P + \sum_j \Phi^j \delta Q^j , \quad (2.13)$$

where the $\Phi^j = \Phi_+^j - \Phi_\infty^j$ are the conjugate potentials of the electric and magnetic charges of the $U(1)$ symmetry group. They permit a non-trivial potential on the horizon Φ_+^j and another at infinity Φ_∞^j . the quantities Ω_∞^i , arising from $\Omega^i = \Omega_+^i - \Omega_\infty^i$, allow for the possibility of a rotating frame at infinity [56]. Here, the subscript “+” corresponds to the event horizon.

Taking into consideration the crucial PV term, the *generalized* Smarr formula to AdS spacetimes in d -dimensions now reads

$$\frac{d-3}{d-2}M = TS + \sum_i \Omega^i J^i - \frac{2}{d-2}PV + \frac{d-3}{d-2} \sum_j \Phi^j Q^j . \quad (2.14)$$

2.3 Black Hole Volume Dilemma

Understanding the geometry of horizons and their general properties remains incomplete. A study, inspired by cosmic censorship ⁷ and Thorne’s hoop conjecture ⁸ [57], describes the relation between the area of the horizon (an intrinsic horizon property) and dynamical quantities such as the angular momentum or the total energy of the black hole, giving rise to the “Penrose (isoperimetric) inequalities”. As this work is done in extended phase space, it is inevitable to define the thermodynamic volume as a new *intrinsic* quantity associated with the (black hole) horizon.

This section is dedicated to study the physical meaning and characteristic properties of the thermodynamic volume and to clarify the meaning and use of the reverse isoperimetric inequality.

2.3.1 Thermodynamic Volume

The thermodynamic volume of a black hole, derived entirely from thermodynamic arguments rather than geometric ones, has dimensions of $[\text{Length}]^{d-1}$. In other words, it is a “spatial” volume that characterizes a black hole in a d dimensional spacetime.

For example, in asymptotically AdS black hole spacetime, the thermodynamic volume is the thermodynamic conjugate to pressure P defined in (2.11) by

$$V \equiv \left(\frac{\partial M}{\partial P} \right)_{S,Q,J,\dots} . \quad (2.15)$$

At first, Kastor, Traschen and Ray [51] interpreted the thermodynamic volume as a “..... finite, effective volume for the region outside the AdS black hole horizon”. However it was clarified later that it is different than the naive geometric volume [52] for most black holes [53]. Hence it remained a *thermodynamic* volume. For example, for a four-dimensional Schwarzschild (charged) AdS solution, the thermodynamic volume (2.15) reads

$$V = \frac{4}{3} \pi r_+^3 , \quad (2.16)$$

⁷Introduced by Penrose in 1969, the “weak” cosmic censorship states that there are no naked singularities in the universe other than the big bang singularity

⁸Introduced by Thorne in 1971, this conjecture states that horizons form when and only when a mass M gets compacted onto a region whose circumference in every direction is $C \leq 4\pi M$

where r_+ is the black hole horizon radius, a result that is identical for the case of a Euclidean ball of the same radius.

The simplicity of the thermodynamic volume is too good to be true. When including any additional thermodynamic parameters such as angular momentum or charge, this quantity becomes very complicated. However, many results have been found over the years for this thermodynamic quantity in a variety of black holes for which the thermodynamics has now been well established. These include charged black holes of various supergravities [53], higher-dimensional rotating black holes [53], superentropic black holes [58, 59], ‘ultraspinning black rings’ obtained in the blackfold approximation [55, 60] and accelerated black holes [61, 62].

As an example, the metric corresponding to d -dimensional Kerr-AdS black hole spacetimes [63, 64] reads ⁹

$$\begin{aligned}
ds^2 = & -\frac{W\rho^2}{l^2}d\tau^2 + \frac{2m}{U}\left(Wd\tau - \sum_{i=1}^N \frac{a_i\mu_i^2 d\varphi_i}{\Xi_i}\right)^2 + \frac{Udr^2}{F-2m} \\
& + \sum_{i=1}^N \frac{r^2 + a_i^2}{\Xi_i} \mu_i^2 d\varphi_i^2 + \sum_{i=1}^{N+\varepsilon} \frac{r^2 + a_i^2}{\Xi_i} d\mu_i^2 - \frac{1}{W\rho^2} \left(\sum_{i=1}^{N+\varepsilon} \frac{r^2 + a_i^2}{\Xi_i} \mu_i d\mu_i\right)^2, \quad (2.17)
\end{aligned}$$

where $\rho^2 = r^2 + l^2$, $d = 2N + 1 + \varepsilon$ and

$$\begin{aligned}
W &= \sum_{i=1}^{N+\varepsilon} \frac{\mu_i^2}{\Xi_i}, \quad U = r^\varepsilon \sum_{i=1}^{N+\varepsilon} \frac{\mu_i^2}{r^2 + a_i^2} \prod_j^N (r^2 + a_j^2), \\
F &= r^{\varepsilon-2} \frac{\rho^2}{l^2} \prod_{i=1}^N (r^2 + a_i^2), \quad \Xi_i = 1 - \frac{a_i^2}{l^2}. \quad (2.18)
\end{aligned}$$

Gibbons was the first to compute the thermodynamic parameter of Kerr-AdS black holes in general dimensions [56]. The mass M , the angular velocities Ω_i and the angular momenta J_i are given by

$$M = \frac{m\omega_{d-2}}{4\pi(\prod_j \Xi_j)} \left(\sum_{i=1}^N \frac{1}{\Xi_i} - \frac{1-\varepsilon}{2}\right), \quad J_i = \frac{a_i m \omega_{d-2}}{4\pi \Xi_i (\prod_j \Xi_j)}, \quad \Omega_i = \frac{a_i(1 + \frac{r_+^2}{l^2})}{r_+^2 + a_i^2}. \quad (2.19)$$

⁹The metric is written in Boyer–Lindquist coordinates

Thus the corresponding temperature T and entropy S read

$$\begin{aligned} T &= \frac{1}{2\pi} \left[r_+ \left(\frac{r_+^2}{l^2} + 1 \right) \sum_{i=1}^N \frac{1}{a_i^2 + r_+^2} - \frac{1}{r_+} \left(\frac{1}{2} - \frac{r_+^2}{2l^2} \right)^\varepsilon \right], \\ S &= \frac{A}{4} = \frac{\omega_{d-2}}{r_+^{1-\varepsilon}} \prod_{i=1}^N \frac{a_i^2 + r_+^2}{4\Xi_i}, \end{aligned} \quad (2.20)$$

where ω_d is given by (2.24). Using all of the above, the thermodynamic volume, previously defined via (2.15), then reads [53]

$$V = \frac{r_+ A}{d-1} \left(1 + \frac{1 + r_+^2/l^2}{(d-2)r_+^2} \sum_i \frac{a_i^2}{\Xi_i} \right) = \frac{r_+ A}{d-1} + \frac{8\pi}{(d-1)(d-2)} \sum_i a_i J_i. \quad (2.21)$$

Note that J_i are the associated angular momenta, a_i are various (up to $[(d-1)/2]$) rotation parameters, and A is the horizon area given by

$$A = \frac{\omega_{d-2}}{r_+^{1-\varepsilon}} \prod \frac{a_i^2 + r_+^2}{\Xi_i}, \quad \Xi_i = 1 - \frac{a_i^2}{l^2}. \quad (2.22)$$

The latter simply proves that a volume V of simplistic form and with intuitive geometrical meaning doesn't hold. It is only reasonable to wonder if there are any properties that the volume V (2.15) obeys and are related in any way with the volume of the black hole.

A famous characteristic property for the volume of a connected domain in Euclidean space is that it obeys an isoperimetric inequality. The next section investigates this property in context of black holes.

2.3.2 Reverse Isoperimetric Inequality

For a closed surface of enclosed volume V and surface area A in Euclidean space \mathbb{E}^{d-1} , the isoperimetric inequality states that the ratio

$$\mathcal{R} = \left(\frac{(d-1)V}{\omega_{d-2}} \right)^{\frac{1}{d-1}} \left(\frac{\omega_{d-2}}{A} \right)^{\frac{1}{d-2}} \quad (2.23)$$

always satisfies $\mathcal{R} \leq 1$ where the volume of the unit d -sphere reads

$$\omega_d = \frac{2\pi^{\frac{d+1}{2}}}{\Gamma\left(\frac{d+1}{2}\right)}. \quad (2.24)$$

Note that $\mathcal{R} = 1$ holds if and only if the domain is a standard round ball.

The applicability of the isoperimetric inequality was first considered by the authors of [53] for a variety of static and rotating black holes. They conjectured, using the thermodynamic volume and the area of horizon cross sections, that \mathcal{R} doesn't obey the isotropic inequality $\mathcal{R} \leq 1$ but rather its reverse. Hence the name *reverse isoperimetric inequality*

$$\mathcal{R} \geq 1. \quad (2.25)$$

This reverse inequality was conjectured to hold for any asymptotically AdS black hole of horizon area A and thermodynamic volume V . At fixed thermodynamic volume the entropy of the black hole is maximized for the Schwarzschild-AdS spacetime¹⁰, or in other words, the bound is saturated for this class of solutions.

To test this conjecture (2.25), one can take the example of Kerr-AdS black holes. The first step is to introduce a new parameter

$$z = \frac{1 + r_+^2/l^2}{r_+^2} \sum_i \frac{a_i^2}{\Xi_i}. \quad (2.26)$$

Following the authors' path in [53], one can use (2.21), (2.22) and the arithmetic/geometric (AG) inequality $(\prod_i x_i)^{1/N} \leq (1/N) \sum_i x_i$ to get

$$\begin{aligned} \mathcal{R}^{d-1} &= \left[1 + \frac{z}{d-2}\right] \left[\prod_i \frac{r_+^2 + a_i^2}{r_+^2 \Xi_i}\right]^{-\frac{1}{d-2}} \geq \left[1 + \frac{z}{d-2}\right] \left[\frac{2}{d-2} \left(\sum_i \frac{1}{\Xi_i} + \sum_i \frac{a_i^2}{r_+^2 \Xi_i}\right)\right]^{-1/2} \\ &= \left[1 + \frac{z}{d-2}\right] \left[1 + \frac{2z}{d-2}\right]^{-1/2} \equiv G(z). \end{aligned} \quad (2.27)$$

It is then easy to employ $G(0) = 1$ and $d \log G(z)/dz \geq 0$ to see that the reverse isoperimetric inequality (2.25) holds.

This conjecture has been proven valid for a large ensemble of charged and/or rotating spherical black holes [53], as well as ultraspinning black rings with toroidal horizon topology [55]. For other classes of more complicated black holes, (2.25) was confirmed numerically. However a class of black holes was subsequently found that violates this conjecture [58, 65], necessitating further investigation of the role and meaning of the volume [25]. The relationship of V to other proposed notions of volume [60, 66] is an ongoing subject of investigation.

This concludes the basic methods formulated to investigate and understand the thermodynamics of black holes. The next section will discuss the implications of introducing new thermodynamic parameters for the critical behaviour of black holes.

¹⁰The same inequality can be extended to all black holes, where ω_d is replaced by the corresponding unit volume of the space transverse to the event horizon.

2.4 Black Hole Chemistry

Having thermodynamic volume and pressure in hand permits the study of black hole thermodynamics in the context of extended thermodynamic phase space. This is known as *Black Hole Chemistry* [18]. Looking into black holes from this lens, it is inevitable to see the remarkable resemblance between a set of “everyday” thermodynamic phenomena, such as Van der Waals behaviour, solid/liquid phase transitions, triple points, reentrant phase transitions, etc. and the thermodynamic behaviour of black holes. This section summarizes these similarities using the following methodology. First, one starts by studying the thermodynamics of charged and/or rotating AdS black holes in a canonical (fixed Q or J) ensemble, relating the “fluid’ thermodynamics by comparing the corresponding physical quantity (for example the thermodynamic volume and the physical volume of the fluid etc.). In this set up, the thermodynamic potential and the local thermodynamic stability of a black hole correspond respectively to the Gibbs free energy G and the positivity of the specific heat C_P given by

$$G = M - TS = G(P, T, J_1, \dots, J_N, Q_1, \dots, Q_n) \quad (2.28)$$

and

$$C_P \equiv C_{P, J_1, \dots, J_N, Q_1, \dots, Q_n} = T \left(\frac{\partial S}{\partial T} \right)_{P, J_1, \dots, J_N, Q_1, \dots, Q_n}. \quad (2.29)$$

The goal of this section is to review the famous results of this machinery and build the foundation for the accomplishments discussed later in this thesis.

2.4.1 Hawking-Page Phase Transition

This section discusses the first and simplest black hole phase transition. Consider a four-dimensional spherically symmetric ansatz

$$ds^2 = -f dt^2 + \frac{dr^2}{f} + r^2 d\Omega_k^2, \quad (2.30)$$

with a metric function

$$f = k - \frac{2M}{r} + \frac{r^2}{l^2}, \quad (2.31)$$

where k is $\{+1, 0, -1\}$ corresponding respectively to $\{\text{spherical, planar, hyperbolic}\}$ horizon geometries. The thermodynamic quantities for this Schwarzschild-AdS black hole read

$$M = \frac{r_+ A_k}{8} \left(k + \frac{r_+^2}{l^2} \right), \quad S = \frac{\pi A_k}{4} r_+^2, \quad T = \frac{kl^2 + 3r_+^2}{4\pi l^2 r_+}, \quad P = \frac{3}{8\pi l^2}, \quad V = \frac{\pi A_k}{3} r_+^3, \quad (2.32)$$

where the area of the constant-curvature space is given by¹¹ πA_k .

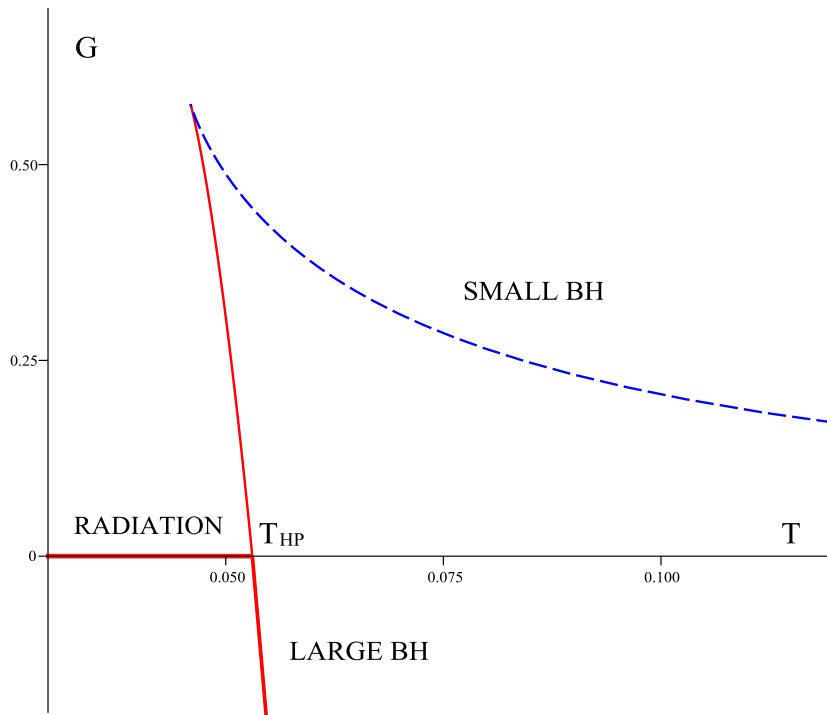


Figure 2.1: **Hawking–Page phase transition.** A plot of the Gibbs free energy of a Schwarzschild-AdS black hole as a function of temperature for fixed pressure $P = 1/(96\pi)$.

Using those key thermodynamic parameters in the spherical case, for which $k = 1$, the Gibbs free energy is computed and displayed in Figure 2.1: at $T = T_{\text{HP}} = 1/(\pi l)^{-1}$ a discontinuity in the first derivative of the Gibbs free energy, indicating a first order phase transition between a radiation state and a black hole state, now known as a Hawking-Page phase transition [11]. By analysing the specific heat, as indicated in the mechanism described at the beginning of this section, the upper branch, describing a small black hole with horizon $r_+ < l/\sqrt{3}$, is thermodynamically unstable due to the negativity of its specific heat C_P . However the lower branch, corresponding to the large black hole, has positive specific heat. Hence it is the stable branch. In addition, the large black hole has

¹¹The simplest way to think of A_k is for the following cases: for a sphere, $A_{k=1} = 4$; for a torus, $A_{k=0} = XY$, with X and Y being the sides of the torus. Unfortunately, there's no simple example for $A_{k=-1}$.

negative Gibbs free energy, for $T > T_{\text{HP}}$ or $r_+ > r_{\text{HP}} = l$, which makes it the most preferred thermodynamic state for the system at a given temperature.

A simple observation that can be made is that, for $G = 0$, a coexistence line between thermal radiation and the large black hole phase can be deduced. Relating temperature to pressure in this case, this coexistence line reads

$$P|_{\text{coexistence}} = \frac{3\pi}{8}T^2. \quad (2.33)$$

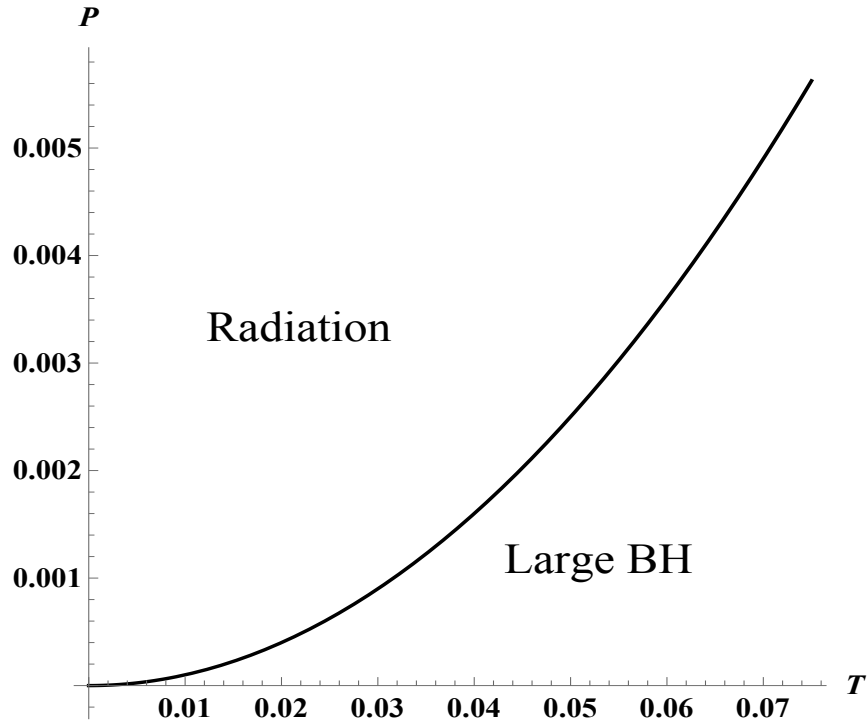


Figure 2.2: **The Hawking-Page phase transition coexistence diagram:** A plot displaying a $P - T$ coexistence line of the thermal radiation/large black hole state.

Figure 2.2 displays this coexistence line of radiation/black hole phases. It shows the resemblance to the solid/liquid phase transition with thermal radiation being analogous to the solid and the large black hole being analogous to the liquid [18].

2.4.2 Other AdS black hole phase transitions

In this sub-section I briefly review some of the interesting phase transitions of anti de Sitter black holes.

2.4.2.1 Van der Waals phase transitions

Van de Waals -like phase transitions were first seen when analysing the thermodynamics of charged black holes [67, 68].

For $d = 4$, consider the ansatz

$$ds^2 = -f(r)dt^2 + \frac{dr^2}{f(r)} + r^2d\Omega^2, \quad (2.34)$$

for which the metric function reads

$$f = 1 - \frac{2M}{r} + \frac{Q^2}{r^2} + \frac{r^2}{l^2}, \quad (2.35)$$

providing an exact solution to the Einstein–Maxwell–AdS equations.

The corresponding thermodynamic quantities for this Reissner–Nordstrom black hole are [69, 68]

$$T = \frac{l^2(r_+^2 - Q^2) + 3r_+^4}{4\pi r_+^3 l^2}, \quad S = \pi r_+^2, \quad V = \frac{4}{3}\pi r_+^3, \quad \Phi = \frac{Q}{r_+}, \quad (2.36)$$

with pressure remaining unchanged from the case of Schwarzschild-AdS black hole.

Using these thermodynamic variables, the Gibbs free energy within the canonical ensemble is

$$G = M - TS = \frac{l^2 r_+^2 - r_+^4 + 3Q^2 l^2}{4l^2 r_+}. \quad (2.37)$$

Plotted as a function of temperature T , this parameter exhibits a first order phase transition between a *small* and a *large* black hole [67, 70, 71, 72, 73]. This phase transition, shown in Figure 2.3, resembles in many ways the van de Waals phase transition between a liquid state and the gas state of a non-ideal fluid, also known as swallowtail behaviour. A brief review of the Van der Waals fluids is available in appendix B.

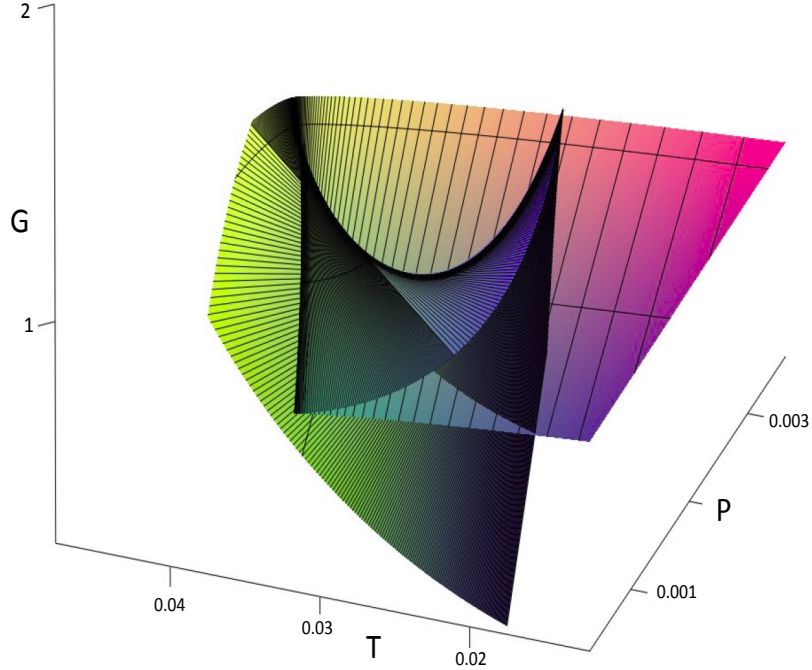


Figure 2.3: **Swallowtail behaviour of RN–AdS black hole** A plot of the Gibbs free energy of a Reissner–Nordstrom–AdS black hole at a fixed charge $Q = 1$.

The swallowtail appears only when $P < P_c$, where P_c is the pressure at critical point¹². The latter is characterized by the following thermodynamic parameters that, for a Reissner–Nordstrom black hole, read

$$P_c = \frac{1}{96\pi Q^2}, \quad v_c = 2\sqrt{6}Q, \quad T_c = \frac{\sqrt{6}}{18\pi Q}. \quad (2.38)$$

¹²As shown in the $P - T$ phase diagram in Figure 2.4, the critical point terminates the coexistence line where the phase transition is of second order. In the RN-AdS black hole case, it is characterized by standard mean theory exponents $\{\alpha, \beta, \gamma, \delta\}$ [68] where

$$\alpha = 0, \quad \beta = \frac{1}{2}, \quad \gamma = 1, \quad \delta = 3.$$

These exponents are interpreted as follows: α dictates the behaviour of the specific heat for a constant volume, β determines the behaviour of the difference of volume between the large and small black hole states, γ governs the behaviour of the isothermal compressibility and δ controls the behaviour of $|P - P_c| \propto |V - V_c|^\delta$ on the critical isotherm

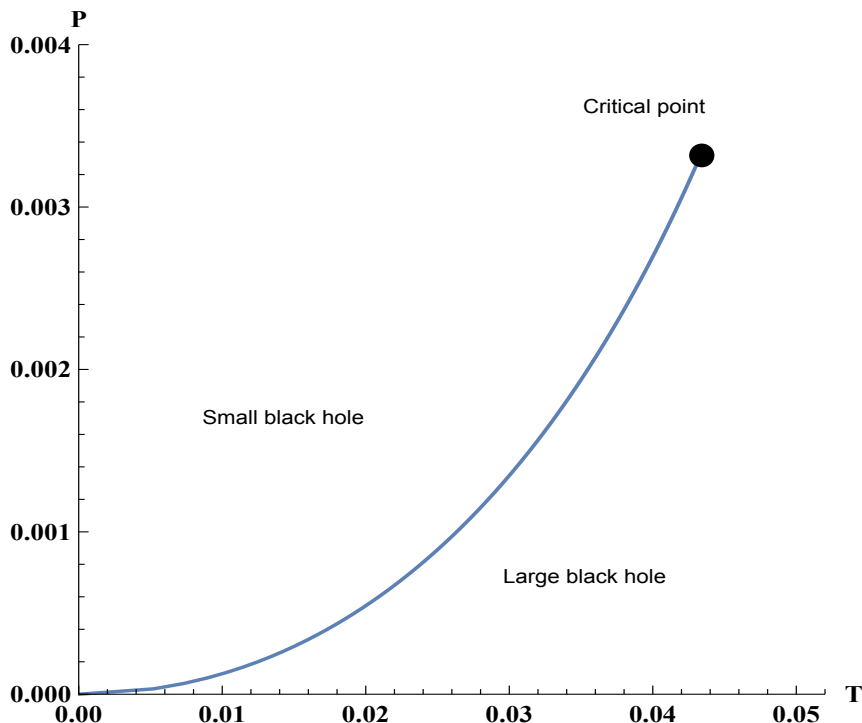


Figure 2.4: **Coexistence line of RN–AdS black hole** A plot of the $P–T$ phase diagram illustrating the small/large black hole phase transition.

At this “special” point, the phase transition becomes second order. The swallowtail only appears for pressures strictly less than the critical pressure. When looking into the coexistence diagram, resultant equation of state is

$$P = \frac{T}{v} - \frac{1}{2\pi v^2} + \frac{2Q^2}{\pi v^4}. \quad (2.39)$$

The second order phase transition at the critical point can easily be seen, as displayed in coexistence line Figure 2.4. Surprisingly, identical to a Van der Waals fluid, the critical ratio for a Reisner–Nordstom–AdS black hole $P_c v_c / T_c = 3/8$ remains the same¹³.

¹³The ratio is independent of the black hole charge Q due to dimensional arguments. However this independence vanishes for $d > 4$ [74].

2.4.2.2 Reentrant phase transitions

Another interesting black hole phase transition is a reentrant phase transition. This was first seen for a four dimensional black hole in the context of Born-Infeld theory [74]. Thereafter, this behaviour was found in singly spinning Kerr-AdS black holes in higher dimensions [75], subject of discussion of this sub-section. This phenomenon was seen in further studies of some classes of black holes in higher dimensions [76, 55, 77] and also in higher curvatures [78, 79, 80, 81, 65]

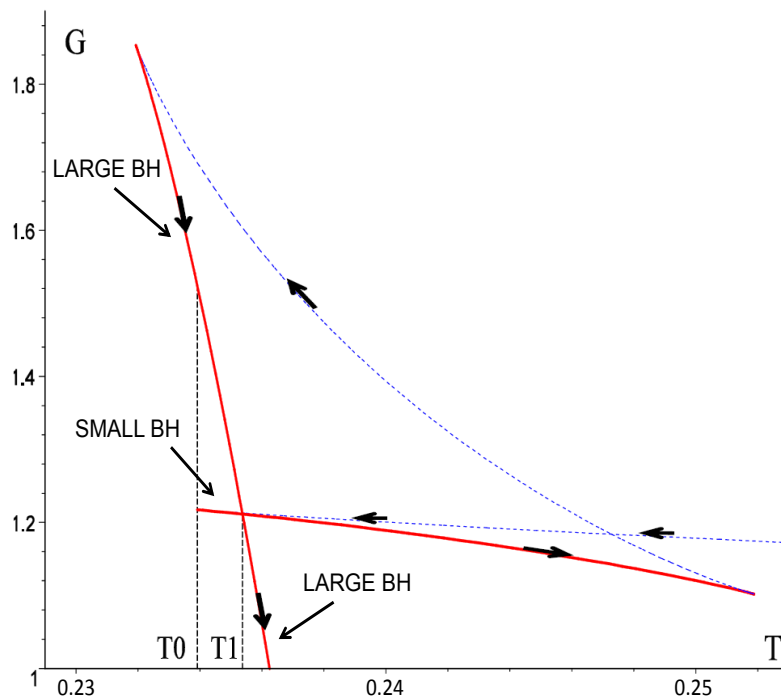


Figure 2.5: **Reentrant phase transition diagram** A plot of the Gibbs free energy of a singly spinning Kerr-AdS black hole in $d = 6$. The arrows in this figure indicate the increasing size of the event horizon r_+ .

Investigating its Gibbs free energy, shown in Figure 2.5, a singly spinning Kerr-AdS black hole in 6 dimensions illustrates a phenomenal behaviour: as temperature decreases, the system is at a stable state of large black hole until it reaches $T = T_1$ where a first order phase transition occurs making a transition from a large to a small black hole state.

Continuing to decrease the temperature the Gibbs free energy curve becomes discontinuous at $T = T_0$. At this point another zeroth order phase transition occurs passing from a small to a large black hole as the temperature continues to decrease. To recapitulate, as temperature continues to decrease, a reentrant large/small/large black hole phase transition occurs.

This phase transition is similar to the water/nicotine reentrant phase transition : the first phase transition of it kind to ever be observed. It was discovered in 1904 by Hudson [82]. The transition for the water/nicotine mixture is as follows. Water and the nicotine begin in a mixed state at high temperature. As temperature decreases, the two substances separate at some *medium* temperature. This separated state remains upon further decreasing the temperature until at some *low* temperature another phase transition occurs, taking the system back to its original mixed state. In making a comparison with the reentrant phase transition of the singly spinning Kerr–AdS black hole, the large black hole corresponds to the mixed state and the small black hole to the water/nicotine state.

Further investigation of the singly-spinning Kerr-AdS black hole revealed that for a region of parameters $P - T$, there are no black holes as seen in Figure 2.6. There’s also a large black hole region and a small black hole region. The large/small black hole coexistence line is divided into two pieces: the first, shown in *black* in the figure, corresponds to the first order phase transition and eventually terminates at a critical point. The second, shown in *red* in the figure, displays the zeroth-order phase transition.

2.4.2.3 Triple points: a solid/liquid/gas phase transition

When studying doubly spinning Kerr–AdS black holes at six dimensions, another interesting phase transition relating black hole thermodynamics to everyday physics was unveiled : the triple point [76]. This phase transition is famously observed for water, having a phase transition between solid, liquid and gas state. As shown in Figure 2.7, for an appropriate angular momenta ratio, the black hole transitions between three states: large, intermediate and a small black hole. The three states meet at a triple point where the three of them coexist. The main difference with the solid/liquid/gas phase transition is that the coexistence line between small/intermediate black hole, unlike the solid/liquid line, doesn’t reach infinity, but rather reaches a critical point, identical to the liquid/gas critical point. Other classes of black hole in higher order gravity theories exhibit this same phase transition behaviour [79, 78, 80].

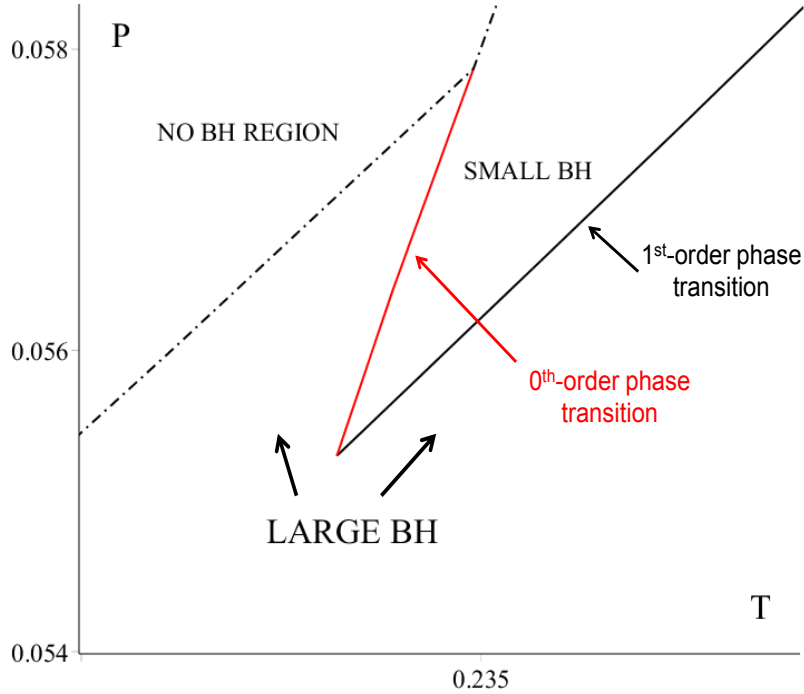


Figure 2.6: **Coexistence line of singly spinning Kerr-AdS black hole** A plot of the $P - T$ phase diagram of a singly spinning rotating black hole.

2.4.3 Thermodynamics of asymptotically de Sitter black holes

As they are much more complex systems, asymptotically de Sitter (dS) black holes were not well explored thermodynamically for two basic reasons. First, having two horizons, an event horizon that corresponds to the black hole and a cosmological horizon that corresponds to the “boundary” beyond which information can’t be retrieved, means that the system is not in thermodynamic equilibrium. In other words, an observer located between the event and the cosmological horizons is in a thermodynamic system characterized by two temperatures; hence they are in a non-equilibrium state. Second, at sufficiently large distances, outside the cosmological horizon, there is no timelike Killing vector. This prevents a clear meaning of asymptotic mass.

Due to these difficulties, despite their importance to cosmology, there have been only few investigations of the thermodynamics black holes with variable Λ in cosmological contexts

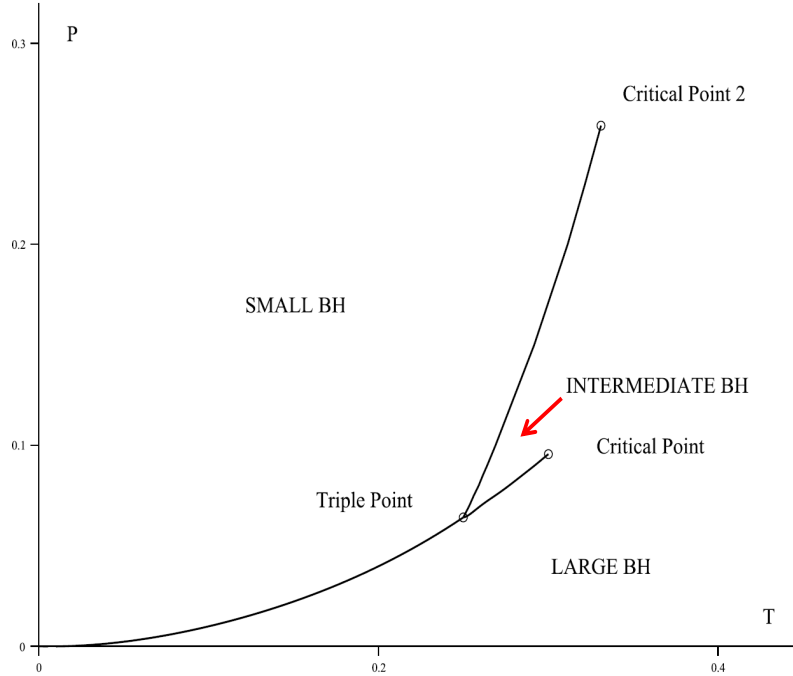


Figure 2.7: **Coexistence line of doubly spinning Kerr-AdS black hole** A plot of the $P - T$ phase diagram in $d = 6$ for a doubly-spinning Kerr-AdS black hole at fixed angular momenta ratio $J_2/J_1 = 0.05$. The diagram displays a triple-critical point where the three states could coexist.

[22, 23, 24, 83]. This section will review the few interesting results of black hole chemistry in de Sitter spacetime.

2.4.3.1 Multiple Horizons: First laws and Smarr Formulae

An interesting method of how to study the thermodynamics of black holes with multi-horizons environments is to formulate multiple independent thermodynamic first laws, one for each horizon. For example, in d -dimensions, a general rotating de Sitter black hole with multiple $U(1)$ charges usually admits three real and positive horizons that are solutions to the horizon condition ¹⁴. They are as follows:

¹⁴For example, for a metric (2.30), the horizon condition is when $f = 0$

- The *cosmological* horizon r_c corresponds to the largest positive root.
- The *black hole* outer horizon r_b is located at the second largest positive root
- The *inner* horizon r_i is located at to the third largest positive root if it exists.

Recapitulating the argumets from Appendix A for $\Lambda > 0$ [54], the first laws corresponding to the different horizons read

$$\delta M = T_b \delta S_b + \sum_k \Omega_b^k \delta J^k + \sum_j \Phi_b^j \delta Q^j + V_b \delta P, \quad (2.40)$$

$$\delta M = -T_c \delta S_c + \sum_k \Omega_c^k \delta J^k + \sum_j \Phi_c^j \delta Q^j + V_c \delta P, \quad (2.41)$$

$$\delta M = -T_i \delta S_i + \sum_k \Omega_i^k \delta J^k + \sum_j \Phi_i^j \delta Q^j + V_i \delta P. \quad (2.42)$$

Here, M is a quantity that is *equivalent* to the *ADM mass* in the asymptotically AdS and flat cases¹⁵. However, the temperatures of the different horizons T_b , T_c and T_i are each proportional to its corresponding surface gravity and each of them is positive. Note that S_b , S_c and S_i are the horizons' entropies, the Ω 's are their corresponding angular velocities, the Φ 's correspond to their electric potentials. The Q 's stand for the charges for each, the J 's denote the angular momenta, and the quantity P is the “pressure”. The latter relates to the positive cosmological constant Λ via the same equation (2.10) used in the AdS case

$$P = -\frac{\Lambda}{8\pi} = -\frac{(d-1)(d-2)}{16\pi l^2} < 0. \quad (2.43)$$

As P is negative in this set up, it is perhaps reasonable to think of it as “tension” instead of pressure. However, in this thesis, I will continue to refer to it as pressure. The thermodynamic conjugates to the pressure corresponding to the three horizons are defined by

$$V_c = \left(\frac{\partial M}{\partial P} \right)_{S_c, J^1, Q^1 \dots}, \quad V_b = \left(\frac{\partial M}{\partial P} \right)_{S_b, J^1, Q^1 \dots}, \quad V_i = \left(\frac{\partial M}{\partial P} \right)_{S_i, J^1, Q^1 \dots}. \quad (2.44)$$

For an observer situated between two of the horizons, for example the cosmological and the event horizons, it is only reasonable to introduce a subtracted first law that can describe the situation yielding

$$0 = T_b \delta S_b + T_c \delta S_c + \sum_i (\Omega_b^i - \Omega_c^i) \delta J^i + \sum_j (\Phi_b^j - \Phi_c^j) \delta Q^j - V \delta P, \quad (2.45)$$

¹⁵Au-contre to those cases, this quantity, M , is conserved in space rather than in time in the de Sitter case. This is due to that fact that the Killing field ∂_t in the region near infinity is spacelike [84].

with

$$V = V_c - V_b \geq 0. \quad (2.46)$$

Here, V is the net volume of the *observable* universe, which can be the naive geometric volume for ordinary cases [54].

Each corresponding Smarr relation for each of the three horizons, derived from the corresponding first laws (2.40)–(2.42) via the dimensional scaling argument [51], reads

$$\frac{d-3}{d-2}M = T_b S_b + \frac{d-3}{d-2} \sum_j \Phi_b^j Q^j + \sum_k \Omega_b^k J^k - \frac{2}{d-2} V_b P, \quad (2.47)$$

$$\frac{d-3}{d-2}M = -T_c S_c + \frac{d-3}{d-2} \sum_j \Phi_c^j Q^j + \sum_k \Omega_c^k J^k - \frac{2}{d-2} V_c P, \quad (2.48)$$

$$\frac{d-3}{d-2}M = -T_i S_i + \frac{d-3}{d-2} \sum_j \Phi_i^j Q^j + \sum_k \Omega_i^k J^k - \frac{2}{d-2} V_i P. \quad (2.49)$$

2.4.3.2 Multiple Horizons: Effective thermodynamics

Using the first laws and the Smarr formulae presented in the previous section, a few proposals were presented to address the thermodynamic non-equilibrium. A discussion of some of these proposals will take place in this section.

The simplest of these proposals is to study the thermodynamics of the three dS horizons [25] independently. In other words, one can treat each horizon as a thermodynamic system that is described by its own temperature and has its own thermodynamic behaviour. In this case, the behaviour of all horizons is captured by a single thermodynamic potential. The latter is in a way equivalent to the Gibbs free energy of asymptotically AdS black holes with a negative pressure¹⁶ and temperatures¹⁷. Hence if any phase transition is observed for any of the horizons, it is interpreted to be a phase transition for the asymptotically de Sitter black hole. Following this logic, a reentrant phase transition [25], similar to the AdS case, was found for a doubly spinning rotating de Sitter black hole in six dimensions.

Another slightly more complicated approach is to focus on an observer standing somewhere between the black hole and the cosmological horizons. The temperature of the system is posited to correspond to an “*effective temperature*” T_{eff} that the observer, in an

¹⁶As mentioned earlier, the negativity of the pressure is caused by the *positive* cosmological constant.

¹⁷The only negative temperatures are the ones corresponding to the inner horizon and the cosmological horizon.

“observable” part of the universe anywhere between the two horizons, sees. This temperature is not universal. This justifies the need for a new *effective thermodynamic first law*. Multiple versions of this effective method have been considered, each based on a different interpretation of the mass parameter M and each introducing a different T_{eff} .

First introduced by Urano et al. [85] and further analysed in [86, 87, 88, 89, 90, 91], the first version of the effective method suggested that the parameter of mass M is regarded as the system’s *internal energy* E . The other thermodynamic parameters of the system are determined as follows: the effective volume V is equal to the volume of the observable universe¹⁸ and reads

$$S = S_b + S_c, \quad V = V_c - V_b, \quad E = M. \quad (2.50)$$

The entropy, however, is a ‘*total entropy*’ S ., and it is the sum of the entropies the black hole horizon and the cosmological horizon [92, 93]. Using (2.40) and (2.41), the effective first law reads

$$\delta E = T_{\text{eff}}\delta S - P_{\text{eff}}\delta V + \sum_i \Omega_{\text{eff}}^i \delta J^i + \sum_j \Phi_{\text{eff}}^j \delta Q^j. \quad (2.51)$$

Here, Ω_{eff}^i and Φ_{eff}^j are respectively the thermodynamic conjugates of J^i and Q^j . For the case Schwarzschild dS black holes, this method leads to a phase transition analogous to the Hawking-Page phase transition seen for Schwarzschild AdS black holes.

The second version of this approach treats the mass parameter M as the *gravitational enthalpy* [94]. This analogy is the same as for the AdS case. Hence, the effective thermodynamic first law is given by

$$\delta H = T_{\text{eff}}\delta S + V_{\text{eff}}\delta \mathcal{P} + \sum_i \Omega_{\text{eff}}^i \delta J^i + \sum_j \Phi_{\text{eff}}^j \delta Q^j, \quad (2.52)$$

with $H = -M$, $\mathcal{P} = -P$ and $V = V_c - V_b$. Here, the actual volume of the system is V_{eff} . Similar to the previous version of this effective approach, an effective first law (2.52) is deduced from (2.40) and (2.41). As the entropy S of the effective system is simply given by the sum of the entropies $S = S_c + S_b$ [94], the effective temperature reads

$$T_{\text{eff}} = \left(\frac{1}{T_c} - \frac{1}{T_b} \right)^{-1}. \quad (2.53)$$

This temperature is not necessarily always positive which can lead to unphysical behaviour for the system. An improvised solution to this issue is to define the effective entropy as

¹⁸Here, the observable universe corresponds to the region of the universe between the black hole horizon and the cosmological horizon

$S = S_c - S_b \geq 0$.¹⁹ Then, the thermodynamic quantities computed using the effective first law (2.52) read

$$\begin{aligned} T_{\text{eff}} &= \left(\frac{1}{T_c} + \frac{1}{T_b} \right)^{-1} \geq 0, & V_{\text{eff}} &= T_{\text{eff}} \left(\frac{V_c}{T_c} + \frac{V_b}{T_b} \right) \geq 0, \\ \Omega_{\text{eff}}^i &= -T_{\text{eff}} \left(\frac{\Omega_b^i}{T_b} + \frac{\Omega_c^i}{T_c} \right), & \Phi_{\text{eff}}^j &= -T_{\text{eff}} \left(\frac{\Phi_b^j}{T_b} + \frac{\Phi_c^j}{T_c} \right). \end{aligned} \quad (2.54)$$

Despite the attempts to establish a general approach to understand the thermodynamics of asymptotically de Sitter black holes, none of the previously discussed could fully describe dS black hole thermodynamics independently of whether or not the cosmological constant is permitted to vary. The two-horizon problem (i.e. existence of two horizons) prevents the spacetime from being in thermal equilibrium state, requiring either adopting an effective temperature approach or considering each horizon as a separate thermodynamic system, as discussed above. However, isolated de Sitter black holes evaporate due to Hawking radiation, unlike their AdS cousins where reflecting boundary conditions at ∞ ensure thermal stability, making dS black hole thermally “unstable”. In section 5 of this thesis, a new approach will be thoroughly discussed to this end and overcome some of these issues.

The following chapters of this manuscript are dedicated to study the thermodynamics of asymptotically de Sitter of black holes. I shall take two foundational paths to this end: The first path will shed the light on the thermodynamic volume, previously introduced, in the context of cosmological horizons. This notion is not at all understood as, whenever studied, is accompanied by the presence of the event horizon. I shall present an approach to study the thermodynamic volume of cosmological horizons in isolation. The second path will focus on the studying black hole phase transitions in the context of de Sitter space for thermalons and for hairy black holes.

¹⁹This method would ensure the positivity of both effective temperature T_{eff} and effective volume V_{eff}

Part I

Cosmological Horizons

Chapter 3

Thermodynamic Volume of Cosmological Solitons

The presence of both a black hole horizon and a cosmological horizon yields two distinct temperatures, suggesting that the system is in a non-equilibrium state. This in turn leads to some ambiguity in interpreting the thermodynamic volume, since distinct volumes can be associated with each horizon. In all known examples the *reverse* isoperimetric inequality $\mathcal{R} \geq 1$ holds separately for each; however if the volume is taken to be the naive geometric volume in between these horizons then the isoperimetric inequality $\mathcal{R} \leq 1$ holds [54].

It would be preferable to study the ‘chemistry’ of cosmological horizons in isolation. For this one needs a class of solutions that are not of constant curvature and that have only a cosmological horizon. Fortunately a broad class of such solutions exists: Eguchi-Hanson de Sitter solitons [95].

The Eguchi-Hanson (EH) metric is a self-dual solution of the four-dimensional vacuum Euclidean Einstein equations [96]. It has odd-dimensional generalizations that were discovered few years ago [95] in Einstein gravity with a cosmological constant. They are referred to as the Eguchi-Hanson solitons. For $\Lambda < 0$ they are horizonless solutions that in five dimensions are asymptotic to AdS_5/Z_p ($p \geq 3$) and have Lorentzian signature, yielding a non-simply connected background manifold for the CFT boundary theory [97]. Solutions in higher dimensions have a more complicated asymptotic geometry. For $\Lambda > 0$ these solutions in any odd dimension have a single cosmological horizon, by which I mean that they have a Killing vector $\partial/\partial t$ that becomes spacelike at sufficiently large distance from the origin. Upon taking the mass to be the conserved quantity associated with this Killing vector at future infinity, and computing it using the counterterm method [84], these

solutions all satisfy a *maximal mass conjecture* [98], whose implication is that they all have mass less than that of pure de Sitter spacetime with the same asymptotics.

In this chapter I will study the Eguchi-Hanson de Sitter (EHdS) solitons in the context of extended phase space thermodynamics. In this framework where $\Lambda > 0$, as discussed in section 2.4.3.1, the cosmological constant is considered a thermodynamic variable equivalent to the pressure in the first law (2.43) and reads

$$P = -\frac{\Lambda}{8\pi G}. \quad (3.1)$$

The thermodynamic conjugate to the pressure is the volume V and is defined from geometric arguments [54]. It ensures the validity of the extended first law (2.40)

$$\delta M + T\delta S - V\delta P = 0, \quad (3.2)$$

and (consistent with Eulerian scaling) renders the Smarr formula (2.47) valid

$$(D-2)M + (D-1)TS + 2VP = 0, \quad (3.3)$$

where $d = (D+1)$ is the spacetime dimension.

Motivated by the above, I use the Eguchi-Hanson solitons in de Sitter space to investigate their thermodynamics and cosmological volume in the context of extended phase space. The particular advantage afforded by these solutions is that, unlike the situation with de Sitter black holes, thermodynamic equilibrium is satisfied. I find explicit expressions for the thermodynamic volume inside and outside the cosmological horizon. For the inner case, the reverse isoperimetric inequality is satisfied only for a small range of $a > \sqrt{3/4}\ell$ when a regularity condition for the soliton is not satisfied. For the outer case, an important role is played by a Casimir-like term that appears as an arbitrary constant in the first law and Smarr relation. I compare my results to those obtained using the counterterm method [95] and I find that they match. Note that for this case the mass is always smaller than maximal mass given by the Casimir term and that the thermodynamic volume is always positive if the regularity condition is applied.

The outline of this chapter is as follows: in the next section I introduce the EH Solitons in odd dimensions. General considerations of their thermodynamics will be discussed in section 3.2. The first law and Smarr relation will be used to compute the mass and thermodynamic volume of these solutions inside and outside the cosmological horizon of dS space. I will show that explicit expressions for the two parameters can be found in general odd dimensions. A briefly summarize the results in a the discussion section.

3.1 EHdS solitons

EHdS solitons [95, 97] in general odd $(D+1)$ dimensions are exact solutions to the Einstein equations with $\Lambda > 0$, and have metrics, derived in Appendix C, of the form

$$ds^2 = -g(r)dt^2 + \left(\frac{2r}{D}\right)^2 f(r) \left[d\psi + \sum_{i=1}^k \cos(\theta_i) d\phi_i \right]^2 + \frac{dr^2}{g(r)f(r)} + \frac{r^2}{D} \sum_{i=1}^k d\Sigma_{2(i)}^2 \quad (3.4)$$

in $D = 2k + 2$ dimensions, where the metric functions are given by

$$g(r) = 1 - \frac{r^2}{\ell^2}, \quad f(r) = 1 - \left(\frac{a}{r}\right)^D, \quad (3.5)$$

with

$$d\Sigma_{2(i)}^2 = d\theta_i^2 + \sin^2(\theta_i) d\phi_i^2, \quad (3.6)$$

and

$$\Lambda = +\frac{D(D-1)}{2\ell^2}, \quad (3.7)$$

parametrizing the positive cosmological constant.

The radial coordinate is given by $r \geq a$; for $r < a$ the metric changes signature, indicative of its solitonic character. There is a cosmological horizon at $r = \ell$. Constant (t, r) sections consist of the fibration of a circle over a product of k 2-spheres. Generalizations to Gauss-Bonnet gravity [99] and to spacetimes with more general base spaces [100] exist but I will not consider these solutions here.

For $\ell \rightarrow \infty$, the metric (3.4) becomes

$$ds^2 = \left(\frac{2r}{D}\right)^2 \left(1 - \left(\frac{a}{r}\right)^D\right) \left[d\psi + \sum_{i=1}^k \cos(\theta_i) d\phi_i \right]^2 + \frac{dr^2}{1 - \left(\frac{a}{r}\right)^D} + \frac{r^2}{D} \sum_{i=1}^k d\Sigma_{2(i)}^2, \quad (3.8)$$

for a constant t hypersurface. This class of metrics can be regarded as d -dimensional generalizations of the original [96] $D = 4$ Eguchi-Hanson metric.

In general, the metric (3.4) will not be regular unless some conditions are imposed to eliminate the singularities. Noting that a constant (t, r) section has the form

$$ds^2 = F(r) \left[d\psi + \sum_{i=1}^k \cos(\theta_i) d\phi_i \right]^2 + \frac{dr^2}{G(r)}, \quad (3.9)$$

where $F(r) = \left(\frac{2r}{D}\right)^2 f(r)$ and $G(r) = f(r)g(r)$, regularity requires the absence of conical singularities. This implies that the periodicity of ψ at infinity must be an integer multiple of its periodicity as $r \rightarrow a$. Consequently

$$\frac{4\pi}{\sqrt{|F'G'|}} \Big|_{r=a} = \frac{4\pi}{p}, \quad (3.10)$$

where p is an integer. Note that $r = r_+$ is the simultaneous root of F and G and that $F'_+ G'_+ = 4 \left(1 - \frac{a^2}{\ell^2}\right)$.

The implications of the regularity condition vary depending on the following three cases: $a^2 < \ell^2$, $a^2 > \ell^2$ and $a^2 = \ell^2$. If $a^2 < \ell^2$, the regularity condition yields $p = 1$ and thus $a^2 = \frac{3}{4}\ell^2$. If $a^2 > \ell^2$, when $\ell < r < a$, the metric has closed timelike curves. If $a = \ell$ the metric is not static for $r > a$. I will not consider these latter two cases in this work.

In the sequel I shall investigate the thermodynamic behaviour of the metric (3.4) for general values of $a < \ell$, imposing the regularity condition $a^2 = \frac{3}{4}\ell^2$ at the end of the calculation. This will allow us to explore the thermodynamics of a cosmological horizon in thermodynamic equilibrium under rather general conditions without any complicating features due to the presence of a black hole.

3.2 Soliton Thermodynamics

Since the Killing vector $\partial/\partial t$ is not everywhere timelike, I cannot compute the mass M of the soliton unambiguously. As a consequence I cannot directly compute the thermodynamic volume $V = \frac{\partial M}{\partial P}$ without additional assumptions. I shall assume the validity of the first law (3.2) and the Smarr relation (3.3) to compute their mass and the volume. This approach is analogous to that taken for asymptotically Lifshitz black holes [101], for which computation of the mass is also fraught with ambiguity in certain cases. I shall then relate our computation of the mass to that obtained in other procedures.

In $(D+1)$ spacetime dimensions, the entropy of the EHdS soliton follows from the area law

$$S = K \ell^{(D-1)} \sqrt{1 - \left(\frac{a}{\ell}\right)^D}, \quad (3.11)$$

with standard arguments implying the temperature at the cosmological horizon is

$$T = \frac{\sqrt{1 - \left(\frac{a}{\ell}\right)^D}}{2\pi\ell}, \quad (3.12)$$

where $K = \frac{1}{2p} \left(\frac{4\pi}{D}\right)^{\frac{D}{2}}$ is one-quarter of the area of the cosmological horizon when $a = 0$.

Before proceeding, it is worth noting that (3.2) and (3.3) determine the mass and volume for any solution to the field equations only up to an additive term that depends on ℓ . Using (3.1) and (3.7) it is straightforward to compute this contribution

$$M_{\Delta} = \alpha_D \ell^{D-2}, \quad V_{\Delta} = \frac{|\Lambda| 8\pi(D-2)}{\Lambda D(D-1)} \alpha_D \ell^D, \quad (3.13)$$

for both the AdS and dS cases, where α_D is an arbitrary constant. Note that the respective contributions to the mass and volume have opposite signs in the AdS case but the same sign in the de Sitter case.

These additional terms depend only on ℓ , suggesting they be considered as Casimir¹ contributions to the mass and volume. However this interpretation is fraught with problems in the AdS case for several reasons. First, they are present in any spacetime dimension, whereas Casimir contributions to the mass occur only for odd spacetime dimensions (even d), and so this interpretation is inapplicable for odd D . Second, they alternate in sign: for $D = 4, 6, 8$ it has been shown that $\alpha_D = 3\pi/32, -5\pi^2/128, 35\pi^3/3072$ respectively [103]. This necessarily yields a negative contribution to the volume for $D = 4n$ where n is an integer, and these contributions can make the overall volume of a sufficiently small Schwarzschild Anti de Sitter black hole negative. Finally, there is no sensible $\Lambda \rightarrow 0$ (or $\ell \rightarrow \infty$) limit of these contributions unless $\alpha_D = 0$. For these reasons the constant α_D is generally set to zero for asymptotically AdS solutions.

However in the de Sitter case, (3.2) and (3.3) imply that M_{Δ} and V_{Δ} have the same sign, and it is not clear that such contributions should be set to zero. For the soliton solutions that are considered here, D is always even and so it is reasonable to expect a Casimir contribution to the cosmological volume. Indeed I shall see that a variety of interpretations for this additional term exist, and I shall explore a number of distinct possibilities.

I solve the first law and Smarr relation for the conserved mass and the cosmological volume of EHdS solitons in both cases: inside and outside the cosmological horizon. On dimensional grounds I expand the mass M and the cosmological volume V_c in powers of a and ℓ

$$M = \sum_{k=0}^{\frac{D}{2}} m_k a^{D-2k} \ell^{2k-2}, \quad (3.14)$$

¹ This comes from the suggestive argument in [102] that the AdS/CFT correspondence predicts the existence of extra light states. This means that the boundary energy of pure AdS_5 is identical to the Casimir energy of $N = 4$ super $U(N)$ Yang-Mills theory on S^3 .

and

$$V = \sum_{k=0}^{\frac{D}{2}} v_k a^{D-2k} \ell^{2k}, \quad (3.15)$$

which are the most general expansions admitting a solution that satisfies both (3.2) and (3.3). In fact it is more than needed – noting that the ℓ -dependent term in the mass is divergent in the limit $\Lambda \rightarrow 0$ suggests that I should consider excluding it. However since there is no soliton in this limit, this term was retained. I shall investigate the implications of identifying it with the Casimir energy [84] in the dS/CFT correspondence conjecture [27].

3.2.1 Inside the cosmological horizon

The Smarr relation (3.3) and the first law (3.2) are valid for a black hole horizon. For a cosmological horizon these equations are modified in (2.41), (2.48) to read [54]

$$\delta M_{in} + T dS - V_{in} \delta P = 0, \quad (3.16)$$

$$(D-2)M_{in} + (D-1)TS + 2V_{in}P = 0, \quad (3.17)$$

from the perspective of an observer in a region where $\partial/\partial t$ is timelike, and where the plus signs in the second terms of these equations arises because the surface gravity of the de Sitter horizon is negative, while the corresponding temperature $T > 0$ since it is proportional to the magnitude of the surface gravity.

Using (3.11) and (3.12), I found that most terms in both (3.14) and (3.15) vanish and obtain

$$M_{in} = \frac{K a^D}{4\pi \ell^2} + m_{\frac{D}{2}} \ell^{D-2}, \quad V_{in} = \frac{-2K}{D-1} a^D + \left(\frac{8(D-2)}{D(D-1)} \pi m_{\frac{D}{2}} + \frac{4K}{D} \right) \ell^D, \quad (3.18)$$

for the mass and volume respectively, where I have relabeled $\alpha_D \rightarrow m_{\frac{D}{2}}$.

If one imposes the requirement that the mass remain finite as $\Lambda \rightarrow 0$, then $m_{\frac{D}{2}} = 0$ and

$$M_{in} = \frac{\left(\frac{4\pi}{D}\right)^{\frac{D}{2}} a^D}{8p\pi \ell^2} \xrightarrow{\Lambda \rightarrow 0} M_{sol} = \frac{1}{8\pi} \left(\frac{3\pi}{D}\right)^{D/2} \ell^{D-2}, \quad (3.19)$$

$$V_{in} = \frac{2\left(\frac{4\pi}{D}\right)^{\frac{D}{2}}}{pD} \ell^D \left(1 - \frac{D}{2(D-1)} \frac{a^D}{\ell^D}\right) \xrightarrow{\Lambda \rightarrow 0} V_{sol} = \frac{2\ell^D \left(\frac{4\pi}{D}\right)^{\frac{D}{2}}}{D} \left(1 - \frac{D}{2(D-1)} \left(\frac{3}{4}\right)^{\frac{D}{2}}\right), \quad (3.20)$$

where the latter relations follow from imposing the regularity condition (3.10).

Suspending the regularity condition, it becomes clear that for any value of $a < \ell$ the mass M_{in} and cosmological volume V_{in} in (3.18) are both positive for vanishing $m_{\frac{D}{2}}$. However the volume V_{in} does not vanish in the $\Lambda \rightarrow 0$ limit, and so one might consider a variety of choices of $m_{\frac{D}{2}}$ that will yield various desired outcomes. These I depict in tables 1 and 2. In table 1 I have not imposed the regularity condition (3.10), and indicate the choices of $m_{\frac{D}{2}}$ such that the rows correspond to finite mass as $\ell \rightarrow \infty$ (case 1), vanishing mass (case 2), vanishing volume (case 3), and requiring the volume to depend only on the soliton parameter a (case 4). In table 2 the regularity condition is imposed, the rows in this table corresponding to those in table 1 for the respective choices of $m_{\frac{D}{2}}$.

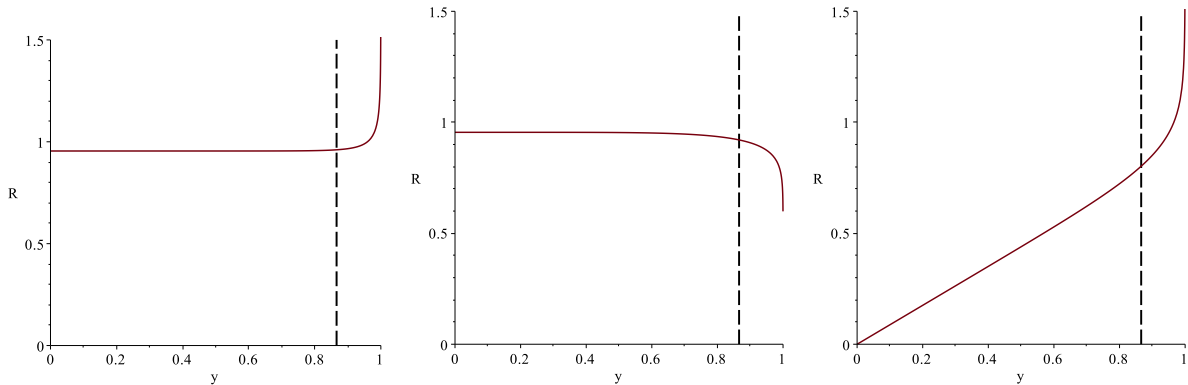


Figure 3.1: Plots of the isoperimetric ratio \mathcal{R} (for a representative dimension $D = 6$) as a function of the parameter $y = \frac{a}{\ell}$. The plots, from left to right, correspond respectively to case 1, case 2, and case 4 discussed in Table 3.1. The dashed line corresponds to the regularity condition $y = \sqrt{3/4}$.

Since the soliton is not a black hole, the premises of the Reverse Isoperimetric Inequality Conjecture [53] does not apply. In a $d = D + 1$ dimensions, the isoperimetric factor reads

$$\mathcal{R} = \left(\frac{(d-1)V}{\omega_{d-2}} \right)^{\frac{1}{d-1}} \left(\frac{\omega_{d-2}}{A} \right)^{\frac{1}{d-2}} = \left(\frac{DV}{\omega_{D-1}} \right)^{\frac{1}{D}} \left(\frac{\omega_{D-1}}{A} \right)^{\frac{1}{D-1}}. \quad (3.21)$$

However the parameter \mathcal{R} provides a useful measure of the relationship between volume and entropy, and so I indicate in each table a computation of the isoperimetric ratio \mathcal{R} in (3.21). I find that \mathcal{R} is always less than unity if the regularity condition is imposed, as indicated in table 2 and illustrated in figures 3.1 and 3.2. If the regularity condition is not

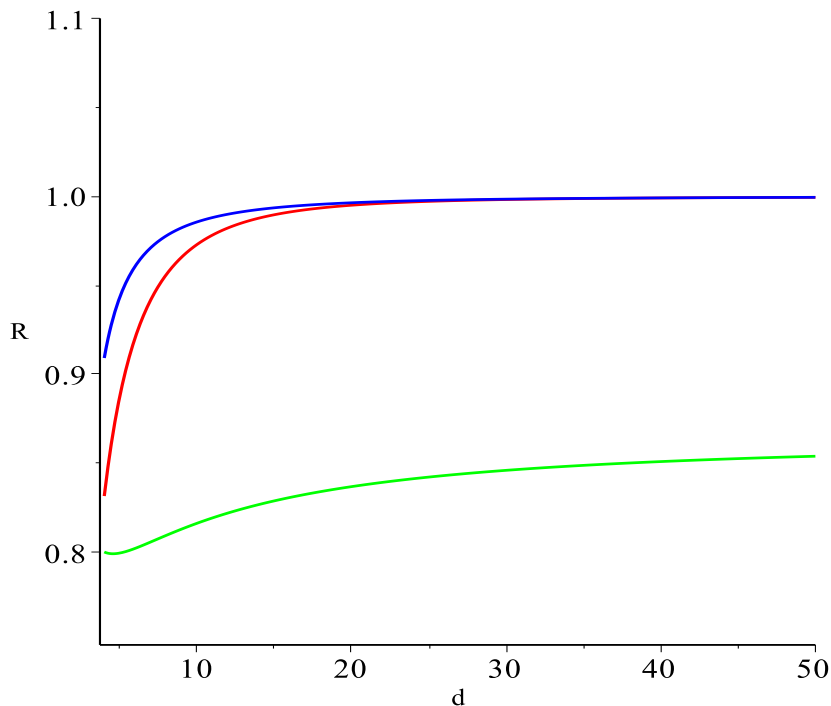


Figure 3.2: A plot of the isoperimetric factor \mathcal{R} for the cases 1, 2 and 4 of the cosmological volume as a function of the spatial dimension D when the regularity condition is imposed (see Table 3.2). The first case is (blue), the second is in (red) and the fourth is in (green).

imposed then for a small range of values of $a > \sqrt{3/4}\ell$ one can obtain $\mathcal{R} > 1$, as shown in figure 3.1.

3.2.2 Outside the cosmological horizon

In this section I consider the thermodynamics of EH-dS solitons outside of the cosmological horizon, where $r > \ell$. This problem (without taking thermodynamic volume into account) has been previously considered in the context of the proposed dS/CFT correspondence [27], which entails computing quantities at past/future infinity. As its name indicates, this method suggests an information correlation regarding Euclidean CFT of asymptotically de Sitter (a)dS spacetimes. Some calculation for conserved charges for pure and asymptotically de Sitter were performed inside the cosmological horizon where the Killing vector

	$m_{\frac{D}{2}}$	M_{in}	V_{in}	$\mathcal{R}(y = \frac{a}{\ell})$
Case 1: Finite M_{in} as $\ell \rightarrow \infty$	0	$\frac{K a^D}{4\pi \ell^2}$	$\frac{-2K}{D-1} a^D + \frac{4K \ell^D}{D}$	$(4 - \frac{2D}{D-1} y^D)^{\frac{1}{D}} \left(\frac{1}{4\sqrt{1-y^D}} \right)^{\frac{1}{D-1}}$
Case 2: Vanishing Mass	$\frac{-K}{4\pi} \left(\frac{a}{\ell} \right)^D$	0	$\frac{4K}{D} (\ell^D - a^D)$	$(4 - 4y^D)^{\frac{1}{D}} \left(\frac{1}{4\sqrt{1-y^D}} \right)^{\frac{1}{D-1}}$
Case 3: Vanishing Volume	$\frac{K}{2\pi} \frac{D-1}{D-2} + \frac{KD}{4\pi(D-2)} \left(\frac{a}{\ell} \right)^D$	$\frac{K}{2\pi} \frac{(D-1)}{(D-2)} \left(\frac{a^D}{\ell^2} - \ell^{D-2} \right)$	0	0
Case 4: V_{in} as function of a	$\frac{-K}{2\pi} \frac{D-1}{D-2}$	$\frac{-K}{4\pi} \frac{(2(D-1)) \ell^{D-2} - a^D}{(D-2)}$	$\frac{-2K}{D-1} a^D$	$y \left(\frac{2D}{D-1} \right)^{\frac{1}{D}} \left(\frac{1}{4\sqrt{1-y^D}} \right)^{\frac{1}{D-1}}$

Table 3.1: General results

	$m_{\frac{D}{2}}$	M_{sol}	V_{sol}	$\mathcal{R} (D = 6)$
Case 1: Finite M_m as $\ell \rightarrow \infty$	0	$\frac{1}{8\pi} \left(\frac{3\pi}{D}\right)^{\frac{D}{2}} \ell^{D-2}$	$\left[-\frac{1}{D-1} \left(\frac{3\pi}{D}\right)^{\frac{D}{2}} + \frac{1}{8D} \left(\frac{4\pi}{D}\right)^{\frac{D}{2}} \right] \ell^D$	0.96073
Case 2: Vanishing Mass	$-\frac{1}{8\pi} \left(\frac{3\pi}{D}\right)^{\frac{D}{2}}$	0	$-\frac{1}{8D} \left(\frac{4\pi}{D}\right)^{\frac{D}{2}} \left(1 - \left(\frac{3}{4}\right)^{\frac{D}{2}}\right) \ell^D$	0.92058
Case 3: Vanishing Volume	$\frac{1}{4\pi(D-2)} \left(\frac{4\pi}{D}\right)^{\frac{D}{2}} \left[D - 1 + \frac{D}{2} \left(\frac{3}{4}\right)^{\frac{D}{2}} \right]$	$\frac{1}{4\pi} \frac{D-1}{D-2} \left(\frac{4\pi}{D}\right)^{\frac{D}{2}} \left[\left(\frac{3}{4}\right)^{\frac{D}{2}} - 1 \right] \ell^{D-2}$	0	0
Case 4: V_m as fonction of a	$-\frac{1}{4\pi} \frac{D-1}{D-2} \left(\frac{4\pi}{D}\right)^{\frac{D}{2}}$	$-\frac{1}{8\pi} \left(\frac{4\pi}{D}\right)^{\frac{D}{2}} \left[2 \frac{D-1}{D-2} - \left(\frac{3}{4}\right)^{\frac{D}{2}} \right] \ell^{D-2}$	$-\frac{1}{D-1} \left(\frac{3\pi}{D}\right)^{\frac{D}{2}} \ell^D$	0.80220

Table 3.2: Results with the regularity condition $y^2 = \frac{3}{4}$ imposed

$\xi = \partial/\partial t$ is timelike [104].

Nevertheless outside the horizon, the spacetime boundaries at past/future infinity are Euclidean surfaces. So one can use a different set of coordinates [98] to turn the timelike Killing vector to a spacelike Killing vector. Hence its associated conserved charge can be calculated using the relationship

$$\mathfrak{M} = \mathfrak{Q}_\xi = \oint_\Sigma D^{D-1} S^a \xi^b T_{ab}^{\text{eff}}, \quad (3.22)$$

where T_{ab}^{eff} is stress-energy on the boundary Σ of the manifold, determined from varying the Einstein-dS action with counter-terms. Full expansions for this quantity have been previously computed [84]. Using (3.22) the maximal mass conjecture — *any asymptotically dS spacetime with mass greater than dS has a cosmological singularity* — was proposed [98]. A straightforward evaluation of (3.22) at future infinity for the Schwarzschild de Sitter solution whose metric functions in the ansatz (3.4) are $g(r) = 1 - r^2/\ell^2 - 2m/r^2$, $f(r) = 1$ for $D = 4$ yields $\mathfrak{M} = -m$ [105], which is sign-reversed from the quantity employed in (3.16) and (3.17). This is a general property of computing the mass outside of a cosmological horizon using (3.22) [105].

Hence in order to apply this approach, one can make use of the Smarr relation (3.17) and the first law (3.16) with $M \rightarrow -M$ to solve for the outer mass and the cosmological volume. The net effect of this is to recover the relations (3.3) and (3.2) but with $V \rightarrow -V$:

$$\delta M_{out} - T dS + V_{out} \delta P = 0, \quad (3.23)$$

$$(D-2)M_{out} - (D-1)TS - 2V_{out}P = 0, \quad (3.24)$$

and I shall solve these for M_{out} and V_{out} using (3.11) and (3.12).

The calculation is very similar to the inside case yielding

$$M_{out} = -\frac{K a^D}{4\pi\ell^2} + m_{\frac{D}{2}} \ell^{D-2}, \quad (3.25)$$

and

$$V_{out} = -\frac{2K}{D-1} a^D - \left(\frac{8(D-2)}{D(D-1)} \pi m_{\frac{D}{2}} - \frac{4K}{D} \right) \ell^D, \quad (3.26)$$

as the general solutions to (3.3) and (3.2). One can see that in general the contribution proportional to $m_{\frac{D}{2}}$ is now of opposite sign for the mass and volume.

One can compare these results in $D = 4$ to a direct computation of the mass. The EHdS metric reads in this case

$$ds^2 = -g(r)dt^2 + \frac{r^2}{p^2}f(r) \left[d\Psi + \frac{p}{2} \cos \theta d\Phi \right]^2 + \frac{1}{f(r)g(r)}dr^2 + \frac{r^2}{4}d\Omega_2^2, \quad (3.27)$$

where the counter-term method [84] yields

$$\mathfrak{M} = \frac{\pi(3\ell^4 - 4a^4)}{32p\ell^2}, \quad (3.28)$$

for the conserved mass using (3.22) [95]. The action can likewise be directly computed in this approach and is

$$I = \frac{\beta\pi(4a^4 - 5\ell^4)}{32p\ell^2}, \quad (3.29)$$

yielding the entropy

$$S = \frac{\beta\pi(\ell^4 - a^4)}{4p\ell^2}, \quad (3.30)$$

via the Gibbs-Duhem relation $S = \beta M - I$, where

$$\beta = \frac{2\pi\ell^3}{\sqrt{\ell^4 - a^4}}, \quad (3.31)$$

is the period of the Euclidean time τ that ensures regularity in the (τ, r) section of the Euclidean solution. Note that the regularity condition has not been applied.

Clearly for $D = 4$, $\beta = 1/T$ from (3.12), and the entropy (3.30) agrees with (3.11). Requiring that these quantities along with the mass (3.28) satisfy both the first law (3.2) and Smarr relation (3.3) yields

$$V_{out} = \frac{\pi^2}{24p} (9\ell^4 - 8a^4), \quad (3.32)$$

for the thermodynamic volume of the EHdS soliton, where from (3.1) the pressure is

$$P = -\frac{\Lambda}{8\pi G} = -\frac{3}{4\pi\ell^2}. \quad (3.33)$$

By imposing the regularity condition $p = 1$, I obtain

$$M_{out} = \frac{3\pi\ell^2}{128}, \quad V_{out} = \frac{3\pi^2\ell^2}{16}, \quad (3.34)$$

Dimension	$m_{\frac{D}{2}}$	M_{out}	V_{out}
$D = 4$	$\frac{3\pi}{32}$	$\frac{3\pi}{128}\ell^2$	$\frac{3\pi^2}{16}\ell^4$
$D = 6$	$\frac{5\pi^2}{128}$	$\frac{3\pi^2}{128}\ell^2$	$\frac{13\pi^3}{405}\ell^6$
$D = 8$	$\frac{35\pi^3}{3072}$	$\frac{877\pi^3}{98304}\ell^2$	$\frac{87\pi^4}{28672}\ell^8$

Table 3.3: Mass and Volume computed outside the cosmological horizon. The constant $m_{\frac{D}{2}}$ is chosen to yield the mass of de Sitter spacetime when $a = 0$.

which is in agreement with both the mass (3.25) and the cosmological volume (3.26) if I set $m_2 = \frac{3\pi}{32}$ (and noting that $K = \pi^2/2p$ for $D = 4$). Note from (3.34) that $M_{out} < M_{dS} = \frac{3\pi\ell^2}{32}$, in accord with the maximal mass conjecture [98, 105, 106], and that this yields a positive thermodynamic volume. If one chooses $M_{out} = M_{dS}$, then $m_2 = \frac{21\pi}{128}$, and the volume is still positive. A negative volume requires $m_2 > \frac{15\pi}{64}$, which then yields $M_{out} = \frac{21\pi\ell^2}{128} > M_{dS}$, in violation of the conjecture.

Similar arguments for $D > 4$ can be made. It is always possible to choose the constant $m_{\frac{D}{2}}$ to yield $M_{out} = M_{dS}$ when $a = 0$, and it is clear from (3.34) that the maximal mass conjecture will necessarily be satisfied. As shown in table 3.3, one finds for all values that have been calculated for M_{dS} [84] that the volume $V_{out} > 0$. I expect that this is a general feature for any (odd) dimension.

3.3 Discussion

In this work, general expressions for the thermodynamic volume inside and outside the cosmological horizon for EH solitons in any odd dimension were found. These quantities are calculable and well-defined regardless of whether or not the regularity condition for the soliton is satisfied. They illustrate that cosmological volume is a well-defined concept, and that cosmological horizons indeed have meaningful thermodynamic properties.

For observers within the cosmological horizon, the mass and volume can be defined using the first law and Smarr relations. I have shown that for this case that the reverse isoperimetric inequality [53] is not satisfied for general values of the soliton parameter a

(including the value satisfying the regularity condition), though it is satisfied for a narrow range of values of this parameter. This situation stands in contrast to that for the class of Kerr de Sitter spacetimes, for which $\mathcal{R} \geq 1$ holds for cosmological horizons [54]. That \mathcal{R} is less than unity even when the soliton regularity condition is satisfied hints at a relationship between the degrees of freedom of cosmological horizons and their entropy that is distinct from that of black holes.

For the outer case I exploited the definition (3.22) of conserved mass to obtain the unique result (3.32) for the cosmological volume in 5 dimensions (or alternatively (3.34) when the regularity condition holds). The mass M_{out} satisfies the maximal mass conjecture and the volume is positive. By computing M_{out} to yield the mass (3.22) for de Sitter space when $a = 0$, I find that the associated cosmological volume is always positive in all dimensions for which (3.22) has been computed. I expect this to be a general feature for all spacetimes satisfying the maximal mass conjecture.

The thermodynamics of these objects remains to be explored. The equation of state for the (non-regular) soliton will, from (3.12), be a highly non-linear relationship between the pressure, volume, and temperature, and whether or not any interesting phase behaviour can result remains to be determined. Generalizations of these solutions to Lovelock gravity exist [99], and it is quite possible that these objects may also exhibit interesting thermodynamic behaviour.

Part II

Black Hole Chemistry in de Sitter Spacetime

Chapter 4

Thermalons

Phase transitions in gravitational physics have been a subject of interest for the last few decades. More than 35 years ago, Coleman and de Luccia discussed *gravitational instantons*, showing that coupling a scalar field to a dynamical metric can lead to phase transitions between two competing vacua with different cosmological constants [107, 108]. These transitions proceed via the nucleation of expanding bubbles of true vacuum within the false vacuum when the free energy of the true vacuum becomes smaller than that of the false vacuum. Mechanisms of this kind have been utilized in various proposed solutions to the cosmological constant problem [109, 47]. Another classic example of a gravitational phase transition is the *Hawking-Page transition* [11], which has significance in various proposed gauge/gravity dualities. This phenomenon is a first order phase transition between thermal Anti de Sitter (AdS) space and the Schwarzschild-AdS black hole, with the latter becoming thermodynamically preferred (i.e. lower in free energy) above a certain critical temperature.

A number of recent studies have focused on *thermalon mediated phase transitions* in higher curvature gravity [32, 35, 110]. These phase transitions proceed via the nucleation of spherical shells, called *thermalons*, that separate spacetime into two regions described by different branches of the solution, hosting a black hole in the interior. Above a certain critical temperature the thermalon configuration is thermodynamically preferred to finite temperature AdS space. The thermalon, once formed, is dynamically unstable and expands to fill all space in finite time, effectively changing the asymptotic structure of the spacetime. In a study focusing on a fixed value of the cosmological constant, it has been shown [35, 111] that thermal AdS space can undergo a thermalon-mediated phase transition to an asymptotically dS black hole geometry—in some sense a generalized version of the Hawking-Page transition.

In this chapter, I will be studying thermalon mediated phase transitions in the context of extended phase space thermodynamics. In this framework, the relationship between the cosmological constant and the thermodynamic pressure is

$$P = -\frac{\Lambda}{8\pi G} = -2\Lambda, \quad (4.1)$$

where the last equality follows since I employ the normalization $16\pi G = 1$ for consistency with ref.[32]. The corresponding conjugate quantity is the thermodynamic volume which is defined to ensure the validity of the extended first law (2.13) a result which follows from geometric arguments [51], and which renders the Smarr relation (2.14) consistent with Eulerian scaling. A natural consequence of the extended phase space paradigm is that it allows us to understand mass as the gravitational analogue of the enthalpy of a black hole rather than the total energy of the system, which has far-reaching consequences. My motivation for using this framework comes from the fact that it is particularly well suited for an exhaustive study of the thermodynamic phase space as discussed in chapter 2. As a result, I will be able to explore the properties of these phase transitions as the pressure varies.

The organization of this chapter is as follows: In the next section I briefly review the basics and the essentials of the thermalon mechanism in Lovelock gravity. In section 4.2 I specialize to the case of Gauss-Bonnet gravity where I study the stability, extended phase space thermodynamics, and phase structure of the thermalons. When considering the phase behaviour of these systems, I employ the extended thermodynamic phase space formalism to exhaustively study how these transitions depend on the pressure (cosmological constant). In the context of AdS \rightarrow dS + black hole thermalon mediated phase transitions I recover the results of [35]. Furthermore, by analysing the behaviour of the free energy near the Nariai limit, I find that for a fixed value of the Gauss-Bonnet coupling, there is a minimum pressure below which thermalon mediated phase transitions are not possible. I find that in the case where the pressure is vanishing, a phase transition between thermal AdS space and an asymptotically flat geometry with a black hole is possible for any range of temperature. In the last section I comment on the similarities and differences between the thermalon mediated phase transition and the Hawking-Page transition in the regime of positive pressures.

4.1 Thermalons in Lovelock gravity

It is generally expected that in any attempt to perturbatively quantize gravity one will find that the standard Einstein-Hilbert action is modified by the addition of higher curvature

terms. Natural candidates for the higher curvature corrections are provided by Lovelock gravities, which are the unique theories that give rise to generally covariant field equations containing at most second order derivatives of the metric [112].

One can obtain spherically symmetric solutions to the field equations of this theory, described via the boundary and bulk action in (1.5), of the form

$$ds^2 = -f(r)dt^2 + \frac{dr^2}{f(r)} + r^2 d\Omega_{(\sigma)d-2}^2, \quad (4.2)$$

with $d\Omega_{(\sigma)d-2}^2$ denoting the line element on a $(d-2)$ -dimensional compact space of constant curvature ($\sigma = 1, 0, -1$ denoting spherical, flat and hyperbolic topologies, respectively). Making use of the notation $g = (\sigma - f)/r^2$, the field equations are solved provided, the characteristic polynomial satisfies

$$\Upsilon[g] = \sum_{k=0}^K c_k g^k = \frac{M}{r^{d-1}}, \quad (4.3)$$

where M is a constant of integration identified as the mass parameter¹ of the solution. Note that here I have suppressed, for convenience, a factor proportional to the volume of the unit radius manifold whose metric is given by $d\Omega_{(\sigma)d-2}^2$.

This chapter is concerned with *thermalon-mediated phase transitions*. These transitions proceed via the production of a thermodynamically favoured but dynamically unstable spherical shell, called the thermalon, which divides spacetime into two regions. The case of interest is when the spacetime metric is continuous but not differentiable at the junction, a condition which, in Einstein gravity, would require the junction shell to possess stress-energy but does not have such a requirement in higher curvature gravity—one can think of the higher curvature terms themselves as providing the matter source. Since the thermalon is dynamically unstable, once formed it expands rapidly, reaching spatial infinity in finite time and therefore changing the asymptotic structure of the spacetime. In this way, the thermalon can be considered to mediate a phase transition between two vacua with different asymptotic structure.

I now turn our attention to a brief recapitulation of the junction conditions and thermalon properties as discussed in [32]. Here I am interested in the case where a timelike junction surface separates an inner region and an outer region, which is denoted with a “−” and “+”, respectively. In particular, I will be interested in the scenario where the

¹Here, the mass is related to the standard definition via $\tilde{M} = \frac{16\pi G}{(d-2)\Sigma_d^{(\sigma)}} M$.

metric function describing the inner geometry, $f_-(r)$, is different from the metric function describing the outer geometry, $f_+(r)$. To this end, I decompose the spacetime manifold: $\mathcal{M} = \mathcal{M}_- \cup (\Sigma \times \xi) \cup \mathcal{M}_+$ where Σ is the junction hypersurface and $\xi \in [0, 1]$ is a real parameter used to interpolate both regions.

Since the thermalon is a finite temperature instanton ², I take the Euclidean metric to be

$$ds^2 = f_{\pm}(r)dt^2 + \frac{dr^2}{f_{\pm}(r)} + r^2 d\Omega_{(\sigma)d-2}^2, \quad (4.4)$$

and describe the junction with the parametric equations

$$r = a(\tau), \quad t_{\pm} = T_{\pm}(\tau), \quad (4.5)$$

and induced metric

$$ds^2 = d\tau^2 + a(\tau)^2 d\Omega_{(\sigma)d-2}^2. \quad (4.6)$$

Note that writing the hypersurface metric in the form of (4.6) assumes that the condition

$$f_{\pm} \dot{T}_{\pm}^2 + \frac{\dot{a}^2}{f_{\pm}(a)} = 1 \quad (4.7)$$

is satisfied for all τ (a dot representing a τ derivative). In the case of the thermalon, which is characterized by the static configuration $\dot{a} = \ddot{a} = 0$, i.e. $a(\tau) = a_*$, this condition amounts to the physical statement that the temperature of the bubble is the same as seen from both sides

$$\sqrt{f_-(a_*)} \beta_- = \sqrt{f_+(a_*)} \beta_+ = \beta_0, \quad (4.8)$$

where β_- is the inverse Hawking temperature of the inner black hole and β_+ is the inverse temperature seen by an observer at infinity.

As discussed in detail in [32], the junction conditions for this set up (without matter) amount to the continuity of the canonical momenta across the hypersurface Σ

$$\pi_{ab}^+ = \pi_{ab}^-, \quad (4.9)$$

where the canonical momenta are computed via the variation of the boundary terms at the junction surface [114]

$$\delta \mathcal{I}_{\partial} = - \int_{\partial \mathcal{M}} d^{d-1} x \pi^{ab} \delta h_{ab}. \quad (4.10)$$

²Instantons are particle-like solutions to the equations of motion of classical field theories in Euclidean space [113]. It carries out a description of quantum tunneling.

However, for the case just described, the canonical momenta have only diagonal components, which are themselves all related by the constraint

$$\frac{d}{d\tau} (a^{d-2} \pi_{\tau\tau}^{\pm}) = (d-2)a^2 \dot{a} \pi_{\varphi_i \varphi_i}^{\pm}, \quad (4.11)$$

where φ_i represent the angular coordinates on Σ . Due to the Bianchi identity, only the $\tau\tau$ component of the canonical momenta matters. A detailed calculation of $\pi_{\tau\tau}^{\pm}$ is provided in Appendix D.

In the following section I shall specialize to the case of Gauss-Bonnet (GB) gravity.

4.2 Gauss-Bonnet case

Gauss-Bonnet gravity is the simplest extension of the Einstein-Hilbert action to include higher curvature Lovelock terms (1.5). In the following I shall adopt for the normalization of the Lovelock couplings as discussed in the introduction

$$c_0 = \frac{-2\Lambda_d}{(d-1)(d-2)} = -2\Lambda, \quad c_1 = 1, \quad c_2 = \lambda. \quad (4.12)$$

Note that here our definitions differ from those in refs. [32, 35, 110] in two ways. First, I have not assumed a particular sign for the cosmological term and I have written it in terms of the radius of curvature, L . This decision is simply for convenience when I will later identify the cosmological constant as a pressure. Note also here our introduction of the terminology “ Λ_d ” where the dimension-dependent factors have been absorbed to make a more convenient shorthand. Secondly, I have not rescaled the GB coupling by a power of Λ to make it dimensionless, since doing so would introduce extra and unnecessary factors of the pressure, thereby complicating the analysis.

The characteristic polynomial (4.3) now reads

$$\Upsilon[g_{\pm}] = -2\Lambda + g_{\pm} + \lambda g_{\pm}^2 = \frac{M_{\pm}}{r^{d-1}}. \quad (4.13)$$

Explicitly solving this for $g_{\pm}(r)$ yields

$$g_{\pm}(r) = -\frac{1}{2\lambda} \left[1 \pm \sqrt{1 + 4\lambda \left(2\Lambda + \frac{M_{\pm}}{r^{d-1}} \right)} \right], \quad (4.14)$$

and so

$$f_{\pm}(r) = \sigma + \frac{r^2}{2\lambda} \left[1 \pm \sqrt{1 + 4\lambda \left(2\Lambda + \frac{M_{\pm}}{r^{d-1}} \right)} \right]. \quad (4.15)$$

A point of particular interest is that for each branch of the solution there is an *effective cosmological constant* given by

$$\Lambda_{\pm}^{\text{eff}} = -\frac{1 \pm \sqrt{1 + 8\lambda\Lambda}}{2\lambda}, \quad (4.16)$$

and so the two branches describe two asymptotically distinct solutions. The effective cosmological constants are generally different, being equal only when $\lambda = -1/(8\Lambda)$, a case that corresponds to Chern-Simons theory [115].

Expressing the junction condition $\tilde{\Pi} = 0$ in the more convenient form $\dot{a}^2 - 2V(a) = 0$ yields

$$V(a) = \frac{a^{d+1}}{24\lambda(M_+ - M_-)} \left[g_+(3 + 2\lambda g_+)^2 - g_-(3 + 2\lambda g_-)^2 \right] + \frac{\sigma}{2}, \quad (4.17)$$

for the thermalon potential. Making use of (4.13), I can put V into a more useful form by reducing the order in g_{\pm} . The result is

$$V(a) = \frac{a^{d+1}}{24\lambda(M_+ - M_-)} \left[(1 + 8\lambda\Lambda)g + (2 + \lambda g) \frac{4M}{a^{d-1}} \right] \Big|_{-}^{+} + \frac{\sigma}{2}. \quad (4.18)$$

Note that in the above, the factor $1 + 8\lambda\Lambda$ can be written as

$$1 + 8\lambda\Lambda = \lambda^2 (\Lambda_-^{\text{eff}} - \Lambda_+^{\text{eff}})^2, \quad (4.19)$$

where the term in parentheses could be interpreted as proportional to the difference between “effective pressures” inside and outside the bubble. Working further with this potential, I can obtain expressions for its a derivatives, the first of which reads

$$V'(a) = \frac{a^d}{24\lambda(M_+ - M_-)} \left[(d+1)(1 + 8\lambda\Lambda)g - [d - 17 + 2\lambda(d-5)g] \frac{M}{a^{d-1}} \right] \Big|_{-}^{+}. \quad (4.20)$$

In obtaining (4.20) I have utilized the characteristic polynomial and its derivative to remove expressions involving $g'_{\pm}(a)$. Expressions for higher derivatives of the potential can be obtained in the same manner, but for our analysis I shall need only the potential and its first derivative, since solving for consistent thermalon configurations amounts to the static condition $V(a_{\star}) = V'(a_{\star}) = 0$.

4.2.1 Stability

Before moving on to the analysis of the thermodynamics of these systems, I pause to comment on the stability of thermalon configurations in GB gravity. As was outlined in [32], there are two primary stability concerns: the dynamical instability of the thermalon solution and the possibility of the bubble escaping to infinity. By expanding the junction condition about the thermalon solution $a = a_*$, to leading order it takes the form (cf. eq. (4.32) from [32])

$$\frac{\dot{a}^2}{2} + \frac{1}{2}k(a - a_*)^2 = 0, \quad (4.21)$$

where k is given by

$$k = \frac{a_*^2}{2} \left(\frac{\partial \tilde{\Pi}}{\partial H} \right) \frac{\partial^2 \tilde{\Pi}}{\partial a^2} \Big|_{a=a_*}, \quad (4.22)$$

which can be thought of as an effective Hooke's constant. The sign of k determines the stability of the thermalon configuration – if it is positive, the thermalon is stable (the bubble can oscillate about $a = a_*$ or remain fixed there) while a negative value of k indicates that the thermalon is unstable (the bubble can expand, causing a phase transition).³ Since I am interested in thermalon mediated phase transitions, I am interested only in cases where $k < 0$. In the case at hand, k is proportional to the second derivative of the thermalon potential V . The particular expression for k (or, equivalently, V'') is quite messy, but I have confirmed numerically that $k < 0$ here, provided $\lambda > 0$, for all physically relevant values of Λ .

The second condition I am interested in is the possibility of the bubble escaping to infinity. To this end, it is of interest to see how the speed of the bubble (\dot{a}) behaves in the limit of large a . A consistent solution of the junction conditions in this limit yields

$$H \approx \frac{a^{d-1}}{2(M_+ - M_-)} \int_{\Lambda_-^{\text{eff}}}^{\Lambda_+^{\text{eff}}} dx \Upsilon[x], \quad (4.23)$$

where $H = (\sigma + \dot{a}^2)/a^2$ is related to the velocity of the bubble and approaches infinity as the bubble expands to infinity (for more details see Appendix D). In the case considered here this expression has the simple form

$$H \approx \frac{a^{d-1}}{2(M_+ - M_-)} \frac{(1 + 8\lambda\Lambda)^{\frac{3}{2}}}{6\lambda^2} = \frac{a^{d-1}\lambda}{12(M_+ - M_-)} (\Lambda_-^{\text{eff}} - \Lambda_+^{\text{eff}})^3. \quad (4.24)$$

³The possibility of collapsing bubbles was discussed at length in [32].

The limit $H \rightarrow \infty$ is consistent with the bubble expanding to infinity ($a \rightarrow \infty$) provided that I have $M_+ > M_-$, $\lambda > 0$ and $\Lambda > -1/(8\lambda)$. Looking at the last term I see that $H \sim \Delta P_{\text{eff}}^3$. This result fits well with our thermodynamic intuition: the bubble will be able to expand to infinity provided there is a positive difference between the effective pressures inside and outside of the bubble, which is the situation here.

4.2.2 Thermodynamic picture

In this section I wish to develop the extended phase space thermodynamics of the system under study. In particular, I am interested in the case where the outer solution describes an asymptotically AdS spacetime, while the inner solution is asymptotically dS. First, I consider the location of the bubble relative to the black hole horizon and the de Sitter horizon. Recall that the thermalon corresponds to the static solution $V(a_\star) = V'(a_\star) = 0$. I can then solve eqs. (4.17) and (4.20) to obtain M_\pm as functions of g_\pm and a_\star . By substituting these results into the characteristic polynomial (4.13) I arrive at a system of two quadratic equations which can be solved for $g_\pm(a_\star)$. The solution can be obtained analytically; however it is important to mention criteria used in determining which root is correct. First, I cannot have $g_+(a_\star) = g_-(a_\star)$, since in this case I would not be considering jump metrics and so no phase transition would occur. Second, $g_+(a_\star)$ must be strictly negative, so that the metric function $f_+(r)$ is positive and properly describes an AdS spacetime outside the bubble.

Having solved for $g_\pm(a_\star)$, an explicit expression for $M_-(a_\star, \Lambda)$ can be obtained via the characteristic polynomial (4.13). One can then compare a_\star with the event and cosmological horizon radii by solving $f_-(r_h) = f_-(r_c) = 0$ for r_h and r_c as functions of $M_-(a_\star, \Lambda)$. It is easy to find that for all well-defined parameters the thermalon radius is larger than the event horizon radius, but smaller than the radius of the cosmological horizon up until the Nariai limit, at which all three occur at the same value. The result is highlighted for the specific case $d = 5$, $\Lambda = 0.5$, $\lambda = 0.1$ and $\sigma = 1$ in Figure 4.1. One consequence of this is that the cosmological horizon is not part of the spacetime, since outside the bubble the solution is given by the AdS branch. One has, therefore, a Killing field which is timelike everywhere outside the event horizon allowing us to form a well-defined thermodynamic picture, free of the usual issues that plague dS spacetimes.

I now focus on a development of the extended first law and Smarr formulae for this set up. Since λ here is dimensionful, I must consider it as a thermodynamic variable in the first law with a conjugate potential Ψ . Recalling that the pressure is given by eq. (4.1) and using this, along with the various properties of the inner black hole solution, it is

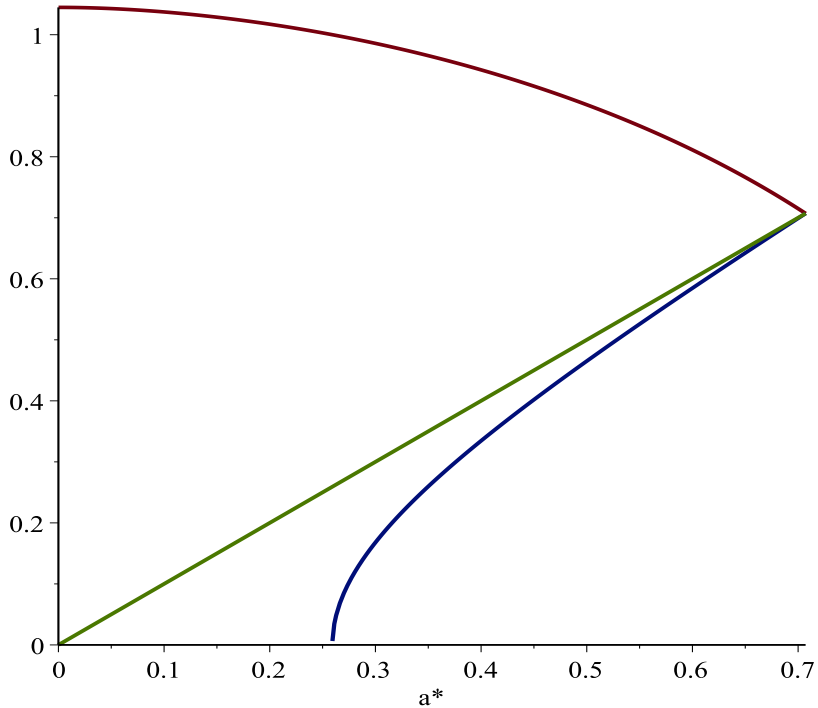


Figure 4.1: A plot of r_h (blue), r_c (red) and a_* (green) as functions of a_* for $d = 5$, $\lambda = 0.1$, $\Lambda = 0.5$, $\sigma = 1$. I see that the bubble location, a_* , is always found between the event horizon and the cosmological horizon until all three meet at the Nariai bound, $a_* = 1/\sqrt{4\Lambda}$. The plot is qualitatively the same for $d > 5$.

straightforward to show that the extended first law [54, 116]

$$dM_- = T_- dS + V_- dP + \Psi_- d\lambda, \quad (4.25)$$

is satisfied provided I identify

$$V_- = r_h^{d-1}, \quad (4.26)$$

as the thermodynamic volume⁴ and

$$\Psi_- = \sigma r_h^{d-5} \left(\sigma - \frac{8\pi r_h T_-}{d-4} \right), \quad (4.27)$$

⁴ The absence of a prefactor of the form $2\pi^2$ follows from the conventions employed throughout this work.

for the potential conjugate to λ . Note that here the Hawking temperature of the black hole is obtained in the standard way by requiring the absence of conical singularities in the Euclidean section ($t \rightarrow -it_E$)

$$T_- = \frac{f'_-(r)}{4\pi} \Big|_{r=r_h}, \quad (4.28)$$

while the entropy in this normalization is given by [32]

$$S = 4\pi r_h^{d-2} \left(\frac{1}{d-2} + \frac{2\sigma\lambda}{r_h^2(d-4)} \right). \quad (4.29)$$

These thermodynamic quantities satisfy the Smarr relation for the black hole

$$(d-3)M_- = (d-2)T_-S - 2V_-P + 2\Psi_- \lambda, \quad (4.30)$$

as derived from scaling.

I now wish to develop the first law and Smarr relation for the quantities outside the bubble. The outer first law and Smarr formula are given by

$$\begin{aligned} dM_+ &= T_+ dS + V_+ dP + \Psi_+ d\lambda, \\ (d-3)M_+ &= (d-2)T_+ S - 2V_+ P + 2\Psi_+ \lambda, \end{aligned} \quad (4.31)$$

which the thermodynamic quantities must satisfy. As mentioned earlier, when the conditions for the existence of the thermalon are enforced (i.e. $V(a_\star) = V'(a_\star) = 0$), I obtain expressions for M_+ and M_- in terms of a_\star and Λ , the latter of which equivalently means I obtain an implicit relationship between r_h , a_\star , and Λ

$$M_-(a_\star, \Lambda) = r_h^{d-1} \Upsilon \left[\frac{\sigma}{r_h^2} \right]. \quad (4.32)$$

This relationship gives us the freedom to write down thermodynamic expressions in terms of either a_\star or r_h . In the outer first law it is easier to work directly with the former, since I have explicitly $M_+(a_\star, \Lambda)$. For the temperature, from the matching condition at the bubble I know that

$$T_+ = \sqrt{\frac{f_+(a_\star)}{f_-(a_\star)}} T_-. \quad (4.33)$$

The entropy that appears in the outer first law is simply that given in (4.29) for the black hole, since the bubble does not contribute to the entropy.

It is only practical to compute the expressions of the quantities in (4.31) analytically in $d = 5$, but even then they are particularly messy—especially V_+ and Ψ_+ . For these reasons I have verified a consistent solution of (4.31) numerically. In general, V_+ is not independent of P , which is (at least in part) due to the relationship (4.32) including P as the zeroth order contribution in $\Upsilon[\sigma/r_h^2]$.

4.2.3 Criticality & phase phenomena

With the tools developed in the previous sections I am now situated to perform the extended phase space analysis for these transitions. I focus on the case $\sigma = 1$ and $d = 5$. The thermodynamically preferred state at a given temperature and pressure is that which minimizes the Gibbs free energy. In [32] the Euclidean action for the thermalon configuration was shown to be

$$\mathcal{I} = \beta_+ M_+ - S. \quad (4.34)$$

In general, the Euclidean action of the thermalon configuration is divergent; however, it can be suitably regularized by subtracting the (infinite) contribution of thermal AdS space yielding the result above. It is then the case that the Gibbs free energy is given by

$$G = M_+ - T_+ S. \quad (4.35)$$

Here I will be comparing the free energy of the thermalon configuration to that of pure AdS space, the latter being identically zero due to the fact that it was used in the background subtraction. Despite the naive impression that there are six independent parameters ($M_{\pm}, \beta_{\pm}, a_{\star}$ and P), there are in fact only two, T_+ and P , since there are four equations relating the six quantities: $V(a_{\star}) = V'(a_{\star}) = 0$, the Hawking condition for the inner black hole, and the matching of thermal circles (4.33) imposed at the junction. In general it is difficult or impossible to write M_+ and S as explicit functions of T_+ and P , therefore I studied the behaviour of G numerically.

4.2.3.1 Negative pressure: thermal AdS to dS black hole transitions

I begin by considering the situation in which the thermalon separates spacetime into regions with AdS asymptotics outside and dS asymptotics inside. I build upon the approach of [35] by performing an exhaustive analysis of the pressure parameter space.

I first consider the parameter range over which I can obtain a sensible solution of the four equations governing the thermalon. A representative plot is shown in Figure 4.2 which

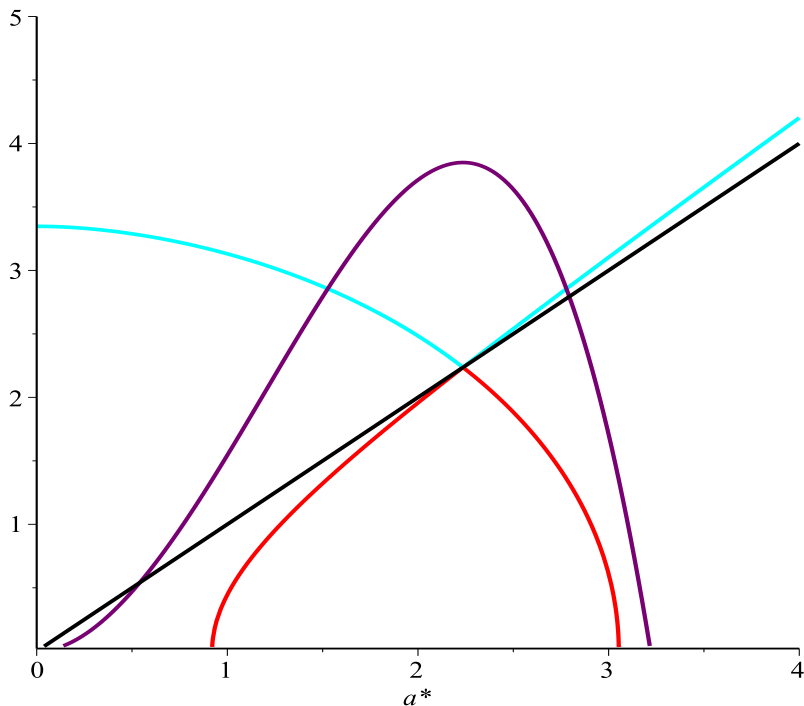


Figure 4.2: A plot displaying a_* (black), the cosmological horizon (cyan), the event horizon (red) and the mass parameter M_- (purple) as functions of a_* , in units of the Planck length. The Nariai limit corresponds to the point where the black, cyan, and red curves meet. This plot corresponds to $P = -0.1$ and $\lambda = 1.35$; plots for other parameter values are qualitatively similar.

highlights the salient features. I see that for some range of a_* there is a consistent solution where the inner de Sitter space has a cosmological horizon, an event horizon and the mass parameter M_- is positive. Outside of this region (values of a_* that lie beyond the edges of the red curve) there is no consistent solution and bubbles of these sizes cannot form. To the right of the Nariai limit, the conditions $V(a_*) = V'(a_*) = 0$ are satisfied. However in this region $\Pi^+ = -\Pi^-$, and so the junction conditions cannot be satisfied without the addition of a shell of stress-energy. Furthermore, it can be shown that $\Pi^+ < 0$ for $a_* > a_{\text{Nariai}}$, since the only zero of Π^+ occurs at the Nariai limit and its slope as a function of a is negative there. Consequently any such shell must be composed of exotic matter, since $\rho \sim \Pi^+ - \Pi^- = 2\Pi^+ < 0$.

The behaviour of the Gibbs free energy is very interesting and is influenced by both the

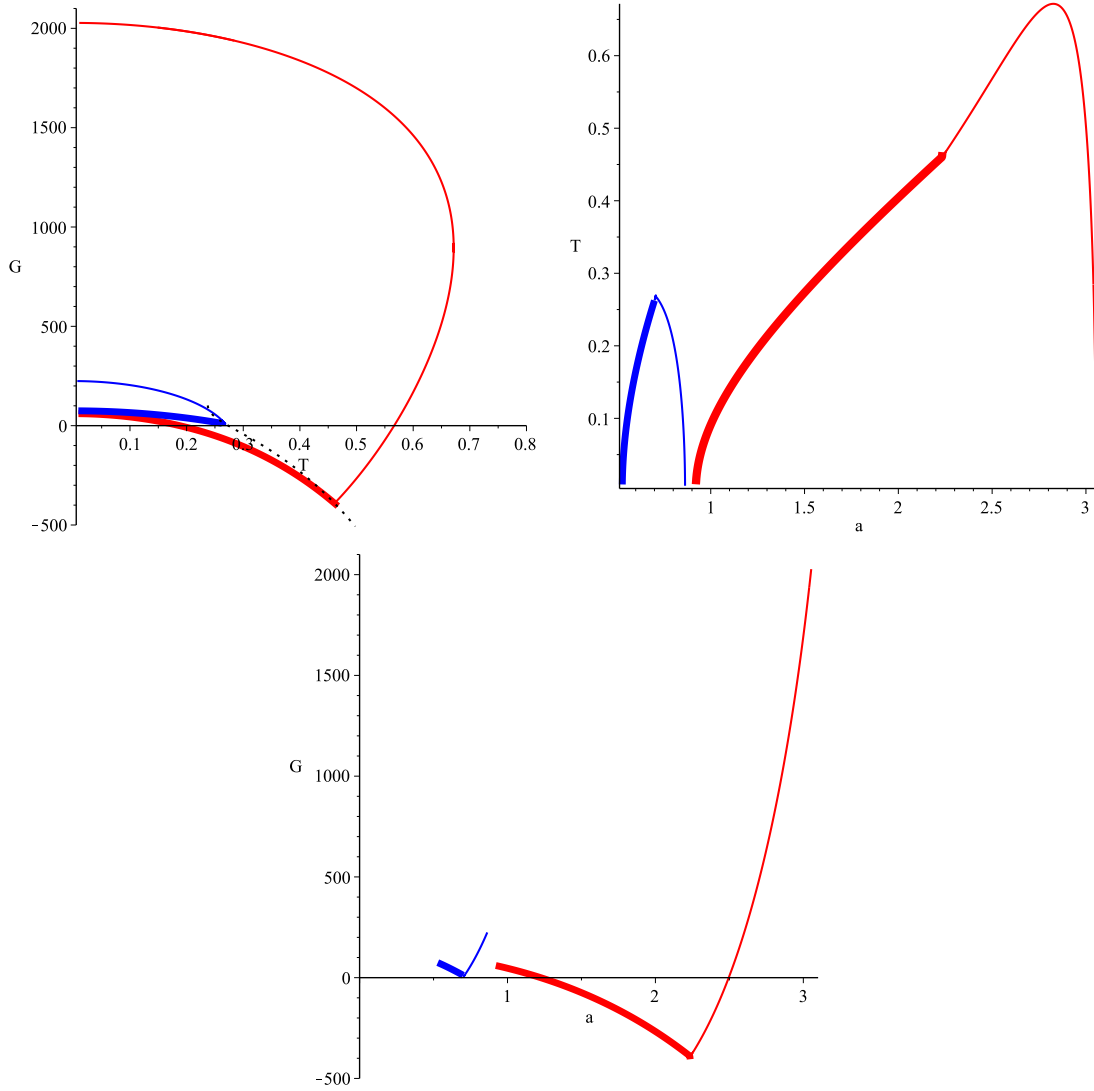


Figure 4.3: **AdS to dS transition: pressure effects:** $\lambda = 1.35$. The red curves correspond to $P = -0.1$ while the blue curves correspond to $P = -1$. *Upper left:* A plot of the free energy vs. T_+ . For $P = -0.1$ a thermalon mediated phase transition is possible over a range of temperature, while it is not possible for $P = -1$. In each case the thin upper branch is unphysical, corresponding to $\Pi^+ = -\Pi^-$. The dotted black line corresponds to the Gibbs free energy for the Nariai limit as a function of pressure. *Upper right:* A plot of the temperature, T_+ vs. a_* in both the blue and red curve, the cusp corresponds to the Nariai limit. *Bottom:* A plot showing the Gibbs free energy as a function of a_* with the cusps again corresponding to the Nariai limit. All quantities are measured in units of the Planck length. The thick lines correspond to the physical curves.

pressure and the Gauss-Bonnet coupling. First let us consider the effect the pressure has on the Gibbs free energy. Figure 4.3 shows free energy and temperature plots for $\lambda = 1.35$ with the red and blue curves corresponding to $P = -0.1$ and $P = -1$, respectively. These plots illustrate a general feature: for a given fixed λ , thermalon mediated phase transitions are possible for values of P near zero, while for P increasingly negative there is a point after which the free energy is strictly positive, and no phase transitions can occur—in Figure 4.3 this happens for pressures near $P = -1$. As the pressure becomes closer to zero, the range of temperatures over which the thermalon mediated phase transitions can occur becomes larger. This suggests the possibility of observing AdS \rightarrow Minkowski space phase transitions in the limit where $P = 0$, which I explore in the following section.

From Figure 4.3 it appears as though the free energy is double valued, with the possibility of small and large bubbles for each value of temperature. However, this is not the case. The large bubble branch turns out to be unphysical (or would require exotic matter): while it satisfies $V(a_*) = V'(a_*) = 0$ it does not satisfy $\Pi^+ = \Pi^-$. The same is true for the branches to the right of the cusp in Figure 4.4. The cusp in the Gibbs free energy vs. temperature curve corresponds to parameter values that yield the Nariai limit.

The next feature I examine is how the free energy depends on λ , with representative results shown in Figure 4.4. From these plots I see that for various ranges of temperatures the free energy is negative, indicating the possibility of thermalon mediated phase transitions. I note that the range of temperatures over which these transitions are possible increases as λ is made smaller.

I can attain further insight by considering these phase transitions in the $P - T$ -plane, as shown in Figure 4.5 for $\lambda = 0.1$. Here, the red curve marks the parameter values for which the free energy of the thermalon is identically zero. Within the region bounded by the left-most part of the red curve and the Nariai temperature (the cusp of the red curve), the free energy of the thermalon is negative and a phase transition can occur. Outside of this region, either the free energy of the thermalon is positive or no physical thermalon solution exists, and thus the thermal AdS space will not undergo a thermalon mediated phase transition. The piece of the red curve to the right of the cusp corresponds to the zeros of the unphysical (or exotic matter) branch.

I pause here to make a cautionary remark. While Figure 4.5 is similar to coexistence plots, it is important to distinguish these thermalon mediated phase transitions from the type of phase transitions I normally study using the tools of extended phase space thermodynamics. Typically one compares a number of configurations all of which are in thermal equilibrium. The key difference for the thermalon is that it is unstable—once it forms it rapidly expands to infinity, changing the asymptotics of the spacetime. Furthermore, there

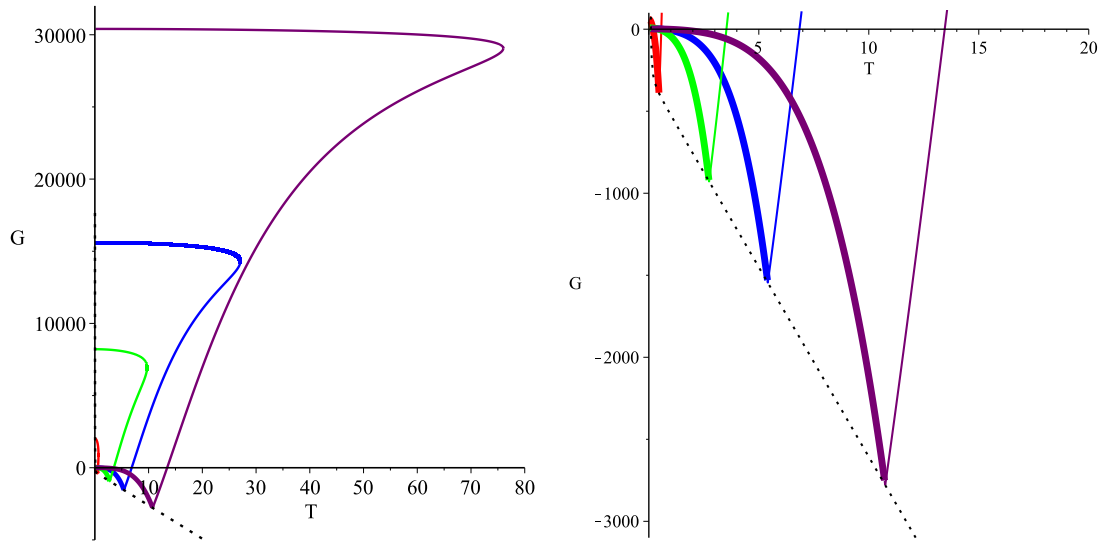


Figure 4.4: **AdS to dS transition: λ effects:** $P = -0.1$. The above plots show the free energy vs temperature (T_+) for $\lambda = 0.05, 0.1, 0.2, 1.35$ (from right to left) with the right plot being just a zoomed-in version of the left. Thermalon mediated phase transitions are possible over a wider range of temperatures for larger values of λ . The physical parts of the curves are the thick ones to the left of the cusps. The dotted black line corresponds to the Nariai limit as a function of λ . Quantities are measured in units of the Planck length.

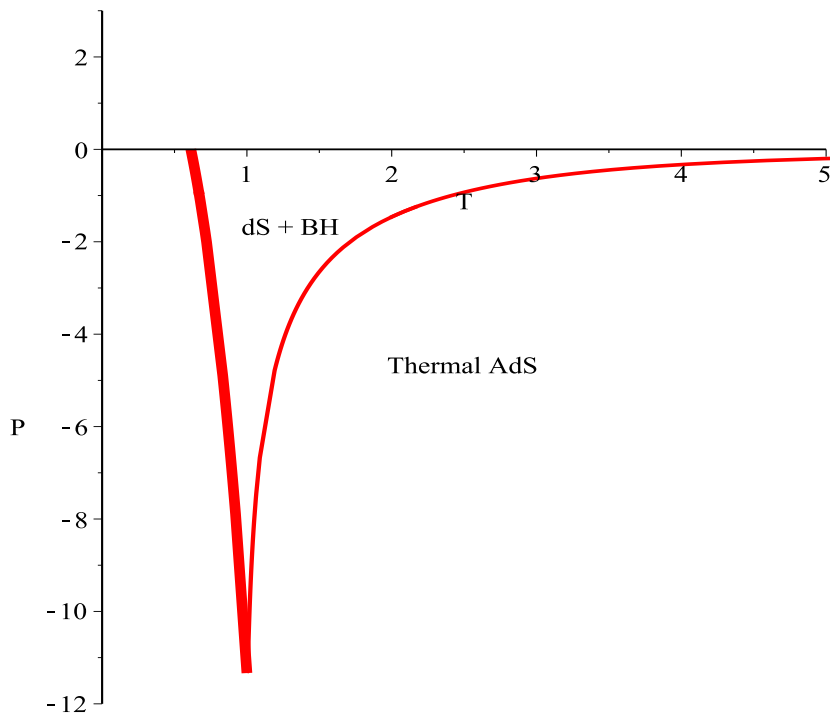


Figure 4.5: **AdS to dS transition: $P - T$ plane:** $\lambda = 0.1$. For parameter values inside the red curve a thermalon mediated phase transition is permitted, while parameters outside of this wedge correspond to thermal AdS space—no phase transition is possible. The cusp corresponds to the Nariai limit; the physical curve is the thick one at the left.

is no regular thermalon solution with dS asymptotics outside and AdS asymptotics inside. In other words, this phase transition can only proceed in the direction of thermal AdS to a de Sitter black hole; the reverse process is not possible. The consequence is this: if one wishes to read Figure 4.5 in a manner similar to how a coexistence plot would be read, it must be kept in mind that the only physical interpretations correspond to adjusting parameters so that the state of the system *enters* the region bounded by the red curve, and never exits it. In other words, it would be incorrect to say that the plot physically describes a $AdS \rightarrow dS + BH \rightarrow AdS$ re-entrant phase transition for a single spacetime. Rather, in the context of an ensemble of spacetimes, as temperature is monotonically increased, I go from stable thermal AdS, to unstable AdS in which a black hole forms in a de Sitter environment, and then back to stable thermal AdS.

Although the discussion above focused on the specific case $\lambda = 0.1$, the ideas are quite

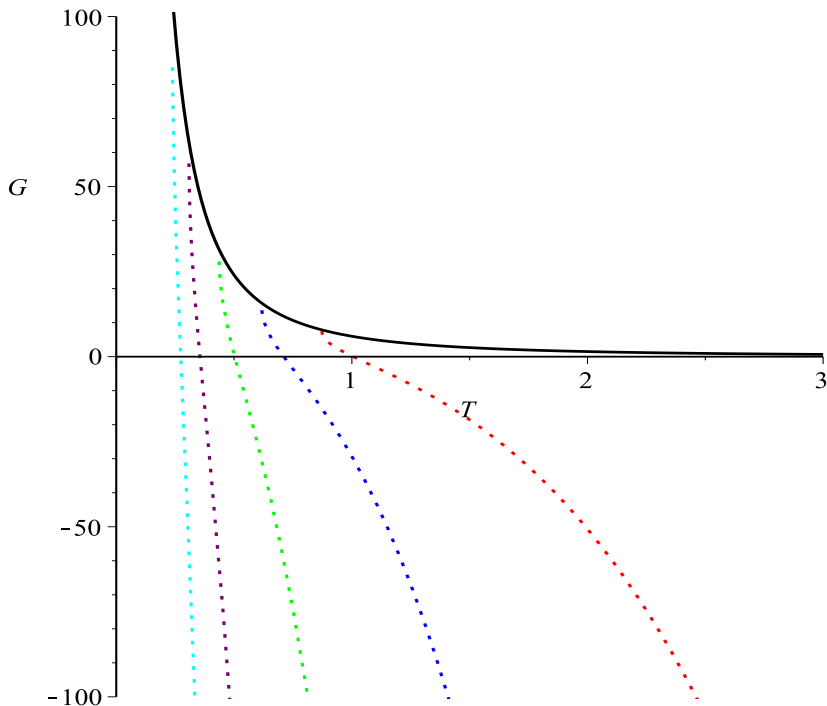


Figure 4.6: **AdS to dS transition: Nariai Gibbs free energy.** The dotted lines display the Gibbs free energy at the Nariai limit for $\lambda = 0.1, 0.2, 0.4, 0.8, 1.35$ (right to left, respectively). The solid black curve displays the locus of points corresponding the limit $P \rightarrow -\infty$ of the Nariai Gibbs free energy. The quantities are measured in units of the Planck length.

general, and results are qualitatively identical for all $\lambda > 0$, as I shall now discuss. For example, one universal feature is that, for all $\lambda > 0$, there is a pressure beyond which no phase transition will occur or alternatively, for which the Gibbs free energy is always positive. To see this, I can study the Gibbs energy in the Nariai limit which I denote $\tilde{G} = \tilde{M}_+ - \tilde{T}_+ \tilde{S}$, where the tilde represents the quantities are evaluated in this extremal limit. This will be helpful since, as I saw in the earlier discussion, the (physical) Gibbs free energy terminates at the Nariai limit, and this point corresponds to the minimum of the Gibbs free energy. Note that, even though T_- is zero in this limit, T_+ remains finite since

$$\tilde{T}_+ = \sqrt{\frac{f_+(r_h)}{f_-(r_h)}} T_-, \quad (4.36)$$

and T_- and $\sqrt{f_-(r_h)}$ approach zero at the same rate. The expression for \tilde{G} takes the form

$$\tilde{G} = \frac{192P^2\lambda^2 + 9 - 84P\lambda - (4 - 48\lambda P)\sqrt{9 - 24\lambda P}}{48\lambda P^2}, \quad (4.37)$$

and

$$\tilde{T}_+ = \frac{1}{8\pi\lambda} \sqrt{\frac{48\lambda P - 18}{P}}. \quad (4.38)$$

For a given fixed value of λ , as $P \rightarrow 0_-$, I have $\tilde{T}_+ \rightarrow \infty$ and $\tilde{G} \rightarrow -\infty$, so the Gibbs free energy will always be negative for negative pressures sufficiently close to zero. On the other hand, as $P \rightarrow -\infty$ I have

$$\tilde{T}_+ \rightarrow \frac{1}{2\pi} \sqrt{\frac{3}{\lambda}}, \quad \tilde{G} = 4\lambda + \mathcal{O}(\sqrt{T}), \quad (4.39)$$

meaning the Gibbs energy at the Nariai limit will be positive for sufficiently large negative pressures. What I glean from these two cases is that, regardless of the value of λ (so long as it is positive), the plot of $\tilde{G}(T)$ will always resemble the dotted lines of Figure 4.6: it will be positive for large negative pressures and negative for sufficiently small pressures. For the pressures that satisfy $\tilde{G} > 0$, there will be no phase transitions. In other words, for any given λ there will exist a minimum pressure P_0 such that for all $P < P_0$ the free energy of the thermalon is always positive, and no phase transitions take place.

4.2.3.2 Vanishing pressure: thermal AdS to asymptotically flat black hole transitions

The analysis above hinted towards the possibility of observing transitions between thermal AdS space and an asymptotically flat black hole when $P = 0$. The junction conditions discussed earlier are in no way changed by specializing to the specific case $P = 0$, and so I can proceed as before. Note that, for $P = 0$, the effective cosmological constants are

$$\Lambda_{\pm}^{\text{eff}} = -\frac{1 \pm 1}{2\lambda}, \quad (4.40)$$

or in other words $\Lambda_+^{\text{eff}} = -1/\lambda$ and $\Lambda_-^{\text{eff}} = 0$. The Gibbs energy remains $G = M_+ - T_+S$, and Figure 4.7 shows representative plots of G vs. T for various values of λ .

Since the “ $-$ ” branch describes an asymptotically flat black hole, I do not face the complications associated with the Nariai limit here. In Figure 4.7 this amounts to the

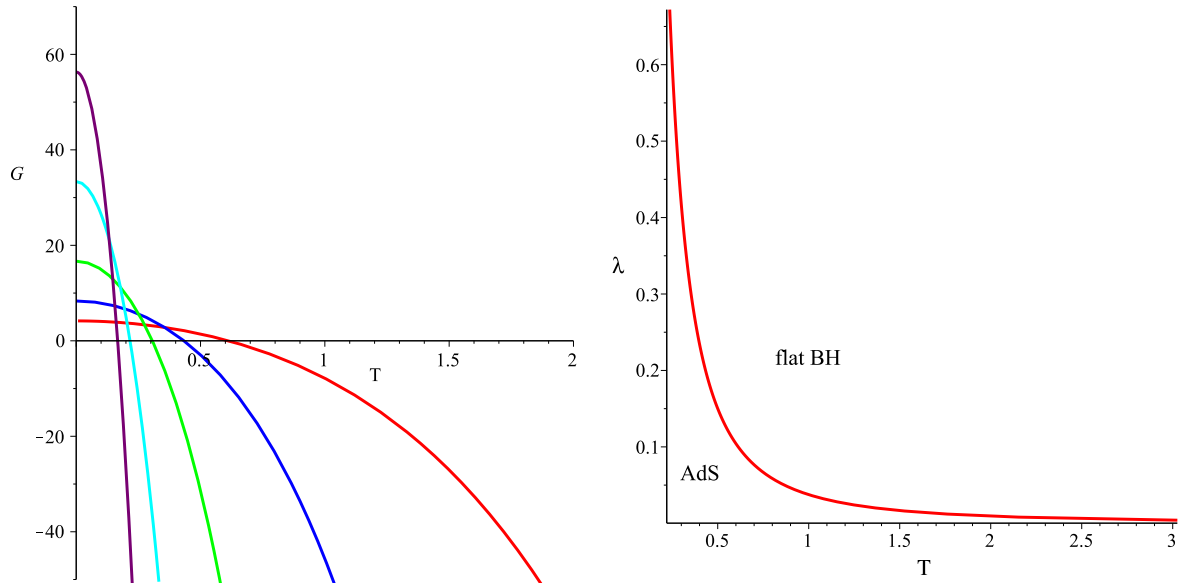


Figure 4.7: **AdS to flat space transition:** *Left:* G vs. T plot for $P = 0$ showing $\lambda = 0.1, 0.2, 0.4, 0.8, 1.35$ (bottom to top in y -intercept). For each value of λ there is a temperature above which the thermalon-mediated transition can occur. *Right:* The coexistence plot in $\lambda - T$ space for the AdS to asymptotically flat black hole transition. Below the red line, the thermodynamically preferred state is thermal AdS space, while above the red line an asymptotically black hole is thermodynamically preferred. The coexistence plot can only be read from left to right, and not from right to left, since the thermalon is dynamically unstable.

fact that the Gibbs free energy does not terminate at a particular temperature, but is well-defined for all positive temperatures. This feature is highlighted in the right plot of Figure 4.7, which shows a $\lambda - T$ coexistence plot for $P = 0$. One must keep in mind that, because the thermalon is not an equilibrium configuration, the coexistence plot can only be read from left to right—an asymptotically flat black hole will not spontaneously decay to AdS space by this mechanism. As a consequence of this, I see that regardless the value of $\lambda > 0$, there will always be a temperature above which it becomes thermodynamically favourable for the thermal AdS vacuum to decay to an asymptotically flat black hole.

One might be concerned about this transition from the point of view of energy: thermal AdS space is decaying into a spacetime containing an asymptotically flat black hole. However, it is important to keep in mind that the “true” cosmological constant, c_0 in the characteristic polynomial, is zero here. The asymptotically AdS structure of the outer branch is a result of the non-zero Gauss-Bonnet coupling, as observed in eq. (4.40). The equivalent transition could not occur in Einstein gravity.

4.2.3.3 Positive pressures: thermal AdS to AdS black hole transitions

Considering the stability constraints discussed earlier, there is a small range of positive pressures for which the thermalon mediated phase transitions can occur. Specifically, our constraints were found earlier to be $\Lambda > -1/(8\lambda)$, which in terms of pressure reads $P < 1/(4\lambda)$. For pressures in the range $0 < P < 1/(4\lambda)$ both branches of the GB solution admit AdS asymptotics, and the thermalon then describes a transition between thermal AdS space and an AdS black hole, in some ways analogous to the Hawking-Page transition. The behaviour of the free energy in this case is qualitatively identical to that shown in Figure 4.7, and so I do not replicate the plot again here. Due to the similarities, one may wonder whether there is some competition between the Hawking-Page and thermalon mechanisms.

As it turns out, such a situation does not arise. In the case of the Hawking-Page transition, one finds that an AdS black hole is thermodynamically favoured to thermal AdS space above a certain critical temperature. In order to make sense of this transition, the thermal AdS space and AdS black hole should have the same asymptotic structure, i.e. the same (effective) cosmological constant. In the case of the thermalon mediated phase transitions, one is again considering a transition between thermal AdS space and an AdS black hole; however the difference in this case is that the effective cosmological constants of the thermal AdS space and the AdS black hole *are different*.

This makes the comparison between the two transitions a questionable one for the fol-

lowing reasons. Given values for Λ and λ , these correspond to some $\Lambda_{\pm}^{\text{eff}}$. If I am interested in considering a thermalon mediated phase transition, then I consider the thermal AdS vacuum to have cosmological constant Λ_{+}^{eff} , which then decays to a black hole with cosmological constant Λ_{-}^{eff} . However, this poses a problem for the Hawking-Page transition, since for thermal AdS space with Λ and λ corresponding to Λ_{+}^{eff} , the theory does not permit a black hole solution which has the *same* cosmological constant *and* coupling constants Λ and λ . In other words, the branch of the Gauss-Bonnet solution that is asymptotically described by Λ_{+}^{eff} does not describe a black hole, and so the Hawking-Page transition would not occur for it. In order to describe a Hawking-Page transition for thermal AdS space with cosmological constant Λ_{+}^{eff} , one would have to consider a theory with different values of Λ and λ such that $\Lambda_{+}^{\text{eff}}(\Lambda, \lambda) = \Lambda_{-}^{\text{eff}}(\tilde{\Lambda}, \tilde{\lambda})$. To summarize, it does not seem sensible to talk about a comparison between the Hawking-Page and thermalon mediated phase transitions for a given theory specified by value of Λ and λ .

4.3 Discussion

I have performed an analysis of thermalon mediated phase transitions in extended thermodynamic phase space. In addition to showing the results previously studied in [32, 114, 35] are consistent with the extended phase space paradigm, I have found a number of new and interesting features of these transitions. In terms of the effect of the thermodynamic pressure, I have shown that for any given value of the Gauss-Bonnet coupling, for large enough negative pressures (i.e. large, positive cosmological constants) the phase transitions are not possible.

In addition to considering thermalon phase transitions in the case where the inner solution is de Sitter, I have also considered the possibility where the inner solution is asymptotically flat. Here I have found that thermal AdS space can undergo a thermalon mediated phase transition to an asymptotically flat black hole spacetime. In contrast to the de Sitter case, where the phase transitions are only possible over a small range of temperatures, in the asymptotically flat case, a thermalon transition is possible at arbitrarily large temperatures.

The results found in chapter indicate that asymptotically de Sitter black holes do have phase transitions, and so the next chapter will focus on establishing a complete approach that overcomes the two-horizon problem in de Sitter spacetime and successfully studies its black hole chemistry using a class of exact hairy black hole solutions to Einstein gravity with conformally coupled scalar fields.

Chapter 5

Hairy Black Holes

In this chapter we present a new approach that overcomes the two-horizon problem in de Sitter spacetime and successfully studies its black hole chemistry. By adding hair to the black hole, the thermodynamic equilibrium between the two horizons can be maintained. Other conserved quantities (such as charge) can be added to the black hole and it becomes possible to explore a range of black hole phase transitions in de Sitter spacetime. I find considerably different behaviour for charged hairy de Sitter black holes than I do for their Anti de Sitter (AdS) counterparts [117, 118, 119]. In specific terms, I find that the system can undergo a phase transition that resembles the Hawking-Page phase transition, but I do not find any swallowtail structure in the free-energy, signatory of a first order phase transition from large to small black holes. Our results are commensurate with studies of de Sitter black holes in a cavity [120, 121], though significant details differ once the thermodynamic phase space is extended to include pressure [122].

This chapter is organized as follows. In the next section I briefly review the basics of conformally coupled scalar field to gravity and their resultant hairy black holes solutions. In section 5.2 I specialize to the case of charged hairy black holes in de Sitter spacetime. When considering the phase behaviour of these systems, I employ the extended thermodynamic phase space formalism to study how their thermodynamic parameters behave at constant pressure (cosmological constant) and at constant “chemical” potential. Furthermore, in a search of possible phase transitions, I study the behaviour of the free energy in different ensembles. I find that a system of a charged hairy black hole in de Sitter will undergo a *Reverse* Hawking-Page phase transition if studied in the grand-canonical ensemble, but will not undergo any phase transitions if studied in the canonical ensemble since otherwise there would be violation of the conservation of charge.

5.1 Conformal Scalar Coupling and Hairy Black Hole Thermodynamics

Although in this chapter I am only interested in Einstein gravity, I shall set our investigation in the context of Lovelock gravity minimally coupled to a Maxwell field. The scalar hair is conformally coupled to gravity via the dimensionally extended Euler densities in terms of the rank four tensor [123]

$$S_{\mu\nu}{}^{\gamma\delta} = \phi^2 R_{\mu\nu}{}^{\gamma\delta} - 2\delta_{[\mu}^{[\gamma}\delta_{\nu]}^{\delta]}\nabla_\rho\phi\nabla^\rho\phi - 4\phi\delta_{[\mu}^{[\gamma}\nabla_{\nu]}\nabla^{\delta]}\phi + 8\delta_{[\mu}^{[\gamma}\nabla_{\nu]}\phi\nabla^{\delta]}\phi, \quad (5.1)$$

where ϕ is the scalar field. Under a conformal transformation $g_{\mu\nu} \rightarrow \Omega^2 g_{\mu\nu}$ and $\phi \rightarrow \Omega^{-1}\phi$ the tensor $S_{\mu\nu}{}^{\gamma\delta} \rightarrow \Omega^4 S_{\mu\nu}{}^{\gamma\delta}$. The action is

$$\mathcal{I} = \frac{1}{16\pi G} \int d^d x \sqrt{-g} \left(\sum_{k=0}^{k_{\max}} \mathcal{L}^{(k)} - 4\pi G F_{\mu\nu} F^{\mu\nu} \right), \quad (5.2)$$

where

$$\mathcal{L}^{(k)} = \frac{1}{2^k} \delta^{(k)} \left(a_k \prod_r^k R_{\mu_r \nu_r}^{\alpha_r \beta_r} + b_k \phi^{d-4k} \prod_r^k S_{\mu_r \nu_r}^{\alpha_r \beta_r} \right), \quad (5.3)$$

with $\delta^{(k)} = \delta_{\mu_1 \nu_1 \dots \mu_k \nu_k}^{\alpha_1 \beta_1 \dots \alpha_k \beta_k}$ the generalized Kronecker tensor, a_k and b_k are coupling constants, and $k_{\max} \leq (d-1)/2$.

The corresponding spherically symmetric topological black hole solutions to the metric of this theory are called Hairy Black Holes [118]. In a d dimensional spacetime, this metric is of the form

$$ds^2 = -f dt^2 + f^{-1} dr^2 + r^2 d\Sigma_{\sigma(d-2)}^2, \quad (5.4)$$

where $d\Sigma_{\sigma(d-2)}^2$ is the line element on a hypersurface of constant scalar curvature that corresponds to the flat, spherical and hyperbolic horizon geometries for $\sigma = 0, +1, -1$, respectively. The volume of this submanifold, $\omega_{(d-2)}^{(+1)} = 2\pi^{(d-1)/2}/\Gamma(\frac{d-1}{2})$, is simply the volume of a sphere for $\sigma = +1$. The field equations of this theory of gravity give a solution provided f solves the following polynomial equation [118]

$$\sum_{k=0}^{k_{\max}} \alpha_k \left(\frac{\sigma - f}{r^2} \right)^k = \frac{16\pi GM}{(d-2)\omega_{(d-2)}^{(\sigma)} r^{d-1}} + \frac{H}{r^d} - \frac{8\pi G}{(d-2)(d-3)} \frac{Q^2}{r^{2d-4}}, \quad (5.5)$$

where M , H and Q are the mass, hair parameter and charge respectively, and

$$\alpha_0 = \frac{a_0}{(d-1)(d-2)}, \quad \alpha_1 = a_1, \quad \alpha_k = a_k \prod_{n=3}^{2k} (d-n) \text{ for } k \geq 2. \quad (5.6)$$

For consistency with [118], I shall set $\alpha_1 = a_1 = 1$ and $a_0 = -2\Lambda < 0$ to recover general relativity at the limit $\alpha_k \rightarrow 0$ for $k > 1$ and I also set $G = 1$. I also have

$$\phi = \frac{N}{r}, \quad H = \sum_{k=0}^{k_{\max}} \frac{(d-3)!}{(d-2(k+1))!} b_k \sigma^k N^{d-2k}, \quad (5.7)$$

the respective scalar field and ‘‘hair parameter’’. To satisfy the equations of motion the integration constant N must satisfy the following constraints

$$\begin{aligned} \sum_{k=1}^{k_{\max}} k b_k \frac{(d-1)!}{(d-2k-1)!} \sigma^{k-1} N^{2-2k} &= 0, \\ \sum_{k=0}^{k_{\max}} b_k \frac{(d-1)!(d(d-1)+4k^2)}{(d-2k-1)!} \sigma^k N^{-2k} &= 0. \end{aligned} \quad (5.8)$$

Since N is the only unknown in (5.8), then one of these equations plays the role of a constraint on the permitted coupling constants .

For asymptotically de Sitter solutions $a_0 < 0$, and a black hole solution for f from (5.5) will have at least two horizons: a cosmological horizon at $r = r_c$ and a black hole horizon at $r = r_+$.

To investigate the thermodynamics of these black holes I need to compute their temperature and entropy. For the latter, as shown in [118], I use Wald’s method ¹ [8], obtaining

$$S_h = \frac{\Sigma_{d-2}^\sigma}{4G} \left[\sum_{k=1}^{k_{\max}} \frac{(d-2)k\sigma^{k-1}\alpha_k r_h^{d-2k}}{d-2k} - \frac{dH}{2\sigma(d-4)} \right], \quad (5.9)$$

where $r_h \in \{r_c, r_+\}$ is the horizon size and I have set $b_k = 0 \forall k > 2$ for simplicity. Recalling that temperature $T_h = \left| \frac{f'(r_h)}{4\pi} \right|$, it is straightforward to verify that both the

¹Wald’s method of computing entropy consists of considering the black hole entropy as the Noether charge associated with diffeomorphism invariance of the Lagrangian. This came from an attempt to understand how corrections to the area law are computed when transitioning from general relativity, where the entropy is the proportional to the area of the horizon, to higher curvature theories of gravity

(extended) first law of thermodynamics and the Smarr relation hold at both horizons [54]. For the black hole these read respectively

$$\delta M_+ = T_+ \delta S_+ + V_+ \delta P_+ + \Phi_+ \delta Q + \kappa \delta H, \quad (5.10)$$

$$(d-3)M_+ = (d-2)T_+ S_+ - 2V_+ P_+ + (d-3)\Phi_+ Q + (d-2)\kappa H, \quad (5.11)$$

where the subscript ‘+’ refers to the black hole. Similarly, but not identically, the extended first law and the Smarr relation corresponding to the cosmological horizon are respectively

$$\delta M_c = -T_c \delta S_c + V_c \delta P_c + \Phi_c \delta Q + \kappa \delta H, \quad (5.12)$$

$$(d-3)M_c = -(d-2)T_c S_c - 2V_c P_c + (d-3)\Phi_c Q + (d-2)\kappa H, \quad (5.13)$$

where the subscript ‘c’ refers to the cosmological horizon.

The idea of fixing the two-horizon problem for black holes in de Sitter space is not new. A few studies have investigated “lukewarm” black holes [124, 125, 126], which are black hole solutions in which the temperature is fixed to match that of the de Sitter background. However these solutions don’t have enough parameters to manipulate the system and see if it undergoes any phase transitions. The key feature that I will exploit in examining the thermodynamics of these black holes is that the additional degree of freedom from the hair parameter provides an additional ‘control parameter’ while still allowing us to require that the temperatures at both horizons be equal

$$T_+ = \left| \frac{f'(r_+)}{4\pi} \right| = \left| \frac{f'(r_c)}{4\pi} \right| = T_c = T, \quad (5.14)$$

equilibrating the particle flux at both horizons. This ensures thermodynamic equilibrium whilst retaining the same numbers of thermodynamic degrees of freedom present in the Reissner-Nordstrom AdS black hole. In the sequel I shall consider the thermodynamics of these charged hairy black holes in Einstein gravity.

5.2 Asymptotically de Sitter Hairy black holes

With the tools developed in the previous sections, I am now situated to perform the extended phase space analysis for these systems. As I want to see if there are any hidden phase transitions that either the black hole or the full system undergo, I will not study the thermodynamic behaviour of each and every parameter, but rather focus on analyzing the Gibbs free energy, with the equilibrium state being the global minimum of this quantity.

The latter can be considered in the grand-canonical ensemble, in which the charge is considered as variable and the potential is fixed. Alternatively I can consider the canonical ensemble in which charge is the parameter that is fixed.

In what follows I shall study asymptotically de Sitter charged hairy black holes in both the canonical and grand-canonical ensembles.

5.2.1 Setup

Naively, one would start the analysis of the chosen black holes at $d = 4$. But since I am coupling the scalar field to the Gauss-Bonnet term, the latter makes no contribution to the field equations at $d = 4$. In other words, the metric function only receives a “hairy” contribution when $d > 4$. All the expressions for the entropy in the previous section (5.9) were derived assuming $d > 4$.

Therefore I specify to $d = 5$ Einstein gravity and I set $a_0 = -2\Lambda < 0$, $a_1 = 1$, $a_{k>1} = 0$ and $G = 1$, obtaining

$$f(r) = -\frac{1}{6}r^2\Lambda + 1 - \frac{H}{r^3} - \frac{8}{3}\frac{M}{\pi r^2} + \frac{4}{3}\frac{\pi Q^2}{r^4}, \quad (5.15)$$

from (5.5). At each horizon I have

$$-\frac{1}{6}\Lambda + \frac{1}{r_h^2} - \frac{H}{r_h^5} - \frac{8}{3}\frac{M}{\pi r_h^4} + \frac{4}{3}\frac{\pi Q^2}{r_h^6} = 0, \quad (5.16)$$

and solve this polynomial equation, at both the event horizon $r_h = r_+$ and the cosmological horizon $r_h = r_c$, for the mass and the hair parameters. Both can be regarded as functions of $\{r_c, r_+, Q, \Lambda\}$ and so the metric function f now depends on these parameters. Since I am working in extended phase space, I use the relationship between the cosmological constant and the pressure $\Lambda = -8\pi P$ (which, since $P < 0$, is actually a tension) and then solve (5.14) for the cosmological horizon parameter r_c where

$$\begin{aligned} T_+ &= -\frac{1}{12}\frac{\Lambda r_+}{\pi} - \frac{4}{3}\frac{Q^2}{r_+^5} + \frac{3}{4}\frac{H}{\pi r_+^4} + \frac{4}{3}\frac{M}{\pi^2 r_+^3}, \\ T_c &= \frac{1}{12}\frac{\Lambda r_c}{\pi} + \frac{4}{3}\frac{Q^2}{r_c^5} - \frac{3}{4}\frac{H}{\pi r_c^4} - \frac{4}{3}\frac{M}{\pi^2 r_c^3}. \end{aligned} \quad (5.17)$$

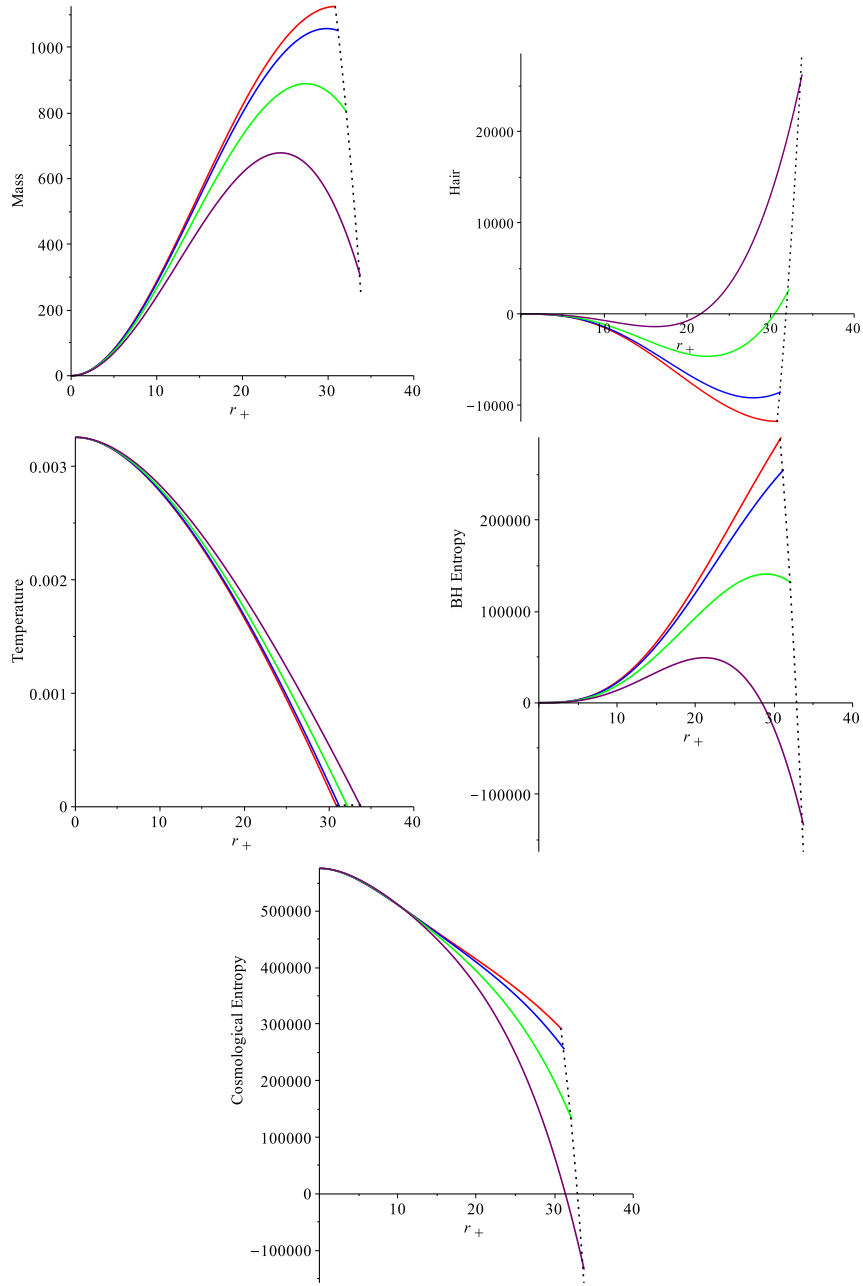


Figure 5.1: **The thermodynamic parameters of the charged hairy asymptotically de Sitter black holes:** for $P = -0.0001$. The $\{red, blue, green, purple\}$ curves correspond to the potential $\Phi_+ = \{0.1, 1, 2, 3\}$ respectively. The dotted line represents the Nariai limit.

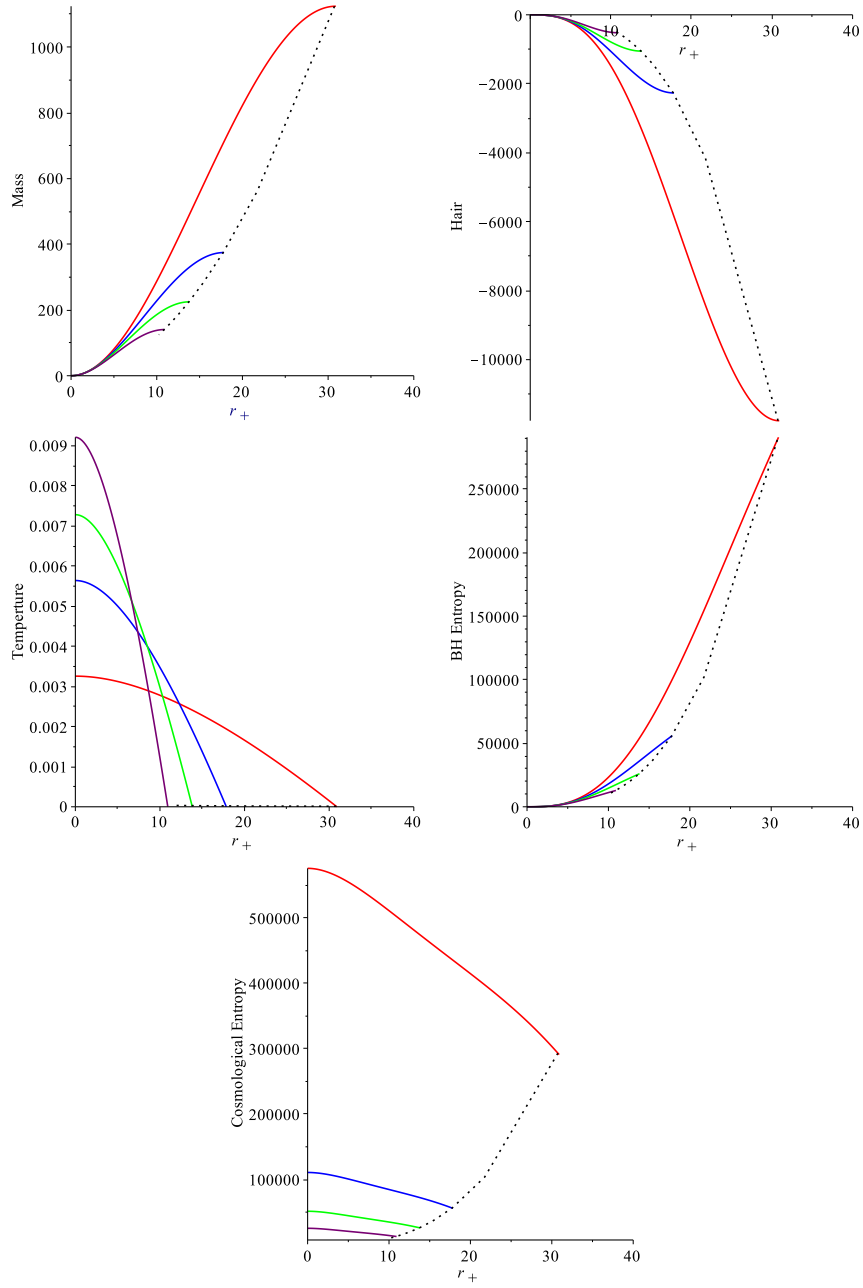


Figure 5.2: **The thermodynamic parameters of the charged hairy asymptotically de Sitter black holes for fixed potential:** the case of $\Phi_+ = 0.1$. The $\{red, blue, green, purple\}$ curves correspond respectively to the pressure $P = \{-0.0001, -0.0003, -0.0005, -0.0008\}$. The dotted line represents the Nariai limit.

The resultant equation has nine different roots but only one of them is a physical solution. The net result is that all thermodynamic parameters – mass M , entropy S , temperature T , and hair H – are now functions of $\{r_+, Q, P\}$. This makes the analysis analogous to that of charged AdS black holes [68], and our setup can be understood and studied in several ways. The most relevant involves trying to understand this system’s thermodynamics in the contexts of the canonical ensemble and the grand-canonical ensemble.

5.2.2 The Grand Canonical Ensemble: Thermodynamics with Fixed Potential

The grand canonical ensemble is defined as the process that couples the energy and charge reservoirs of the system in question while holding the temperature and the potential fixed [67, 70]. Its corresponding thermodynamic potential is the known Gibbs free energy.

The first question presented by our de Sitter black holes is that of which Gibbs free energy should I consider? There are three possibilities: that of the black hole, that of the cosmological horizon or that of the total system that includes the black hole and the cosmological horizon. These respectively read

$$\begin{aligned} G_+ &= M - TS_+ - \Phi_+Q, \\ G_c &= M - TS_c - \Phi_cQ, \\ G_{Total} &= M - T(S_+ + S_c) - (\Phi_+ - \Phi_c)Q, \end{aligned} \tag{5.18}$$

where S_+ is the entropy of the black hole and S_c is the entropy at the cosmological horizon. Note that I regard the black hole as a thermodynamic system in equilibrium with the de Sitter vacuum. I plot M , T , and S of the black hole as a function of r_+ in figures 5.1 and 5.2. I consider only those values of r_+ for which these quantities are positive, and ensure that $r_+ < r_c$, so that I do not attain the Nariai limit.

Plotting the Gibbs free energy for the different cases in figure 5.3 I see that the black hole and the cosmological horizons cannot undergo any phase transitions if isolated from each other: the *red* curve is the Gibbs free energy of the black hole when isolated from the cosmological horizon. On its own, it cannot undergo a phase transition as the curve does not cross the plane of $G_{Total} = 0$. Nonetheless, the *blue* curve that represents the free energy of the cosmological horizon does. Yet it cannot undergo a phase transition since the cosmological horizon cannot be decoupled from the black hole (i.e. I use the mass of the black hole to compute the free energy of the cosmological horizon) and so has no physical meaning; the curve is plotted for reference.

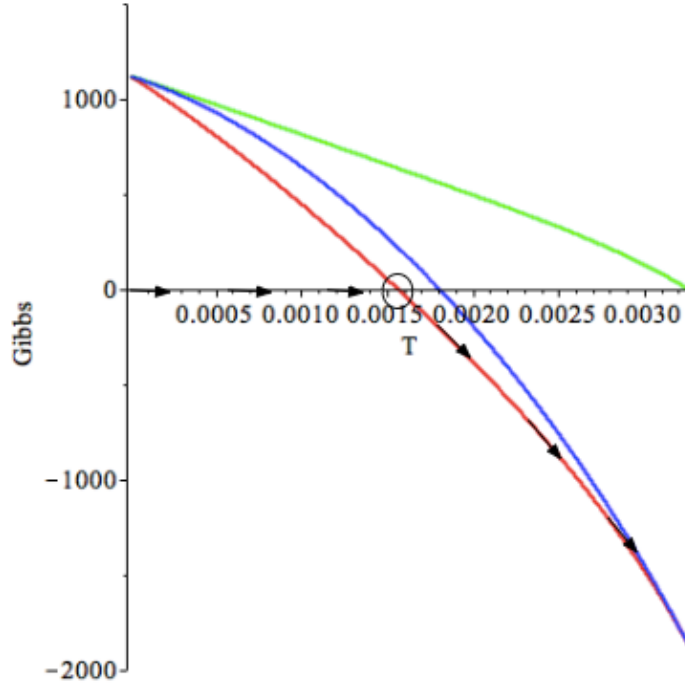


Figure 5.3: **Gibbs Free Energy with fixed potential.** The green curve represents G_+ , corresponding only to the black hole, as a function of temperature. The blue curve represents G_c as measured at the cosmological horizon r_c and the red curve is that of G_{Total} for the total system *i.e.* of the black hole in a the de Sitter heat bath. All curves are plotted for $P = -0.0001$ and $\Phi_+ = 0.1$.

However, the full system undergoes a phase transition that resembles the Hawking-Page phase transition: at low temperatures, the equilibrium state of the system is de Sitter space with scalar radiation, and not a black hole. As the temperature increases, the system can undergo a first order phase transition to a new equilibrium state of a black hole with scalar hair. The black hole would be of large size and would keep shrinking down as the system heats up. But at high temperatures, unlike the Schwarzschild black holes which have a negative specific heat and are unstable, the charged and hairy de Sitter black holes have a positive specific heat as shown in figure 5.4 and are stable – as the small (high-T) black hole radiates, the cosmological horizon will restore the particle flux to ensure equilibrium.

The arrows in the plot 5.3 indicate how the equilibrium state of the system changes from a state of scalar radiation in de Sitter spacetime to a charged hairy black hole. Along

the black hole branch the arrows correspond to decreasing values of the radius of the black hole event horizon. This is quite unlike the corresponding situation in anti de Sitter space [11], as well as for de Sitter black holes in cavities [120, 121, 122], in which large black holes are at higher temperature. I call this a *Reverse* Hawking-Page phase transition.

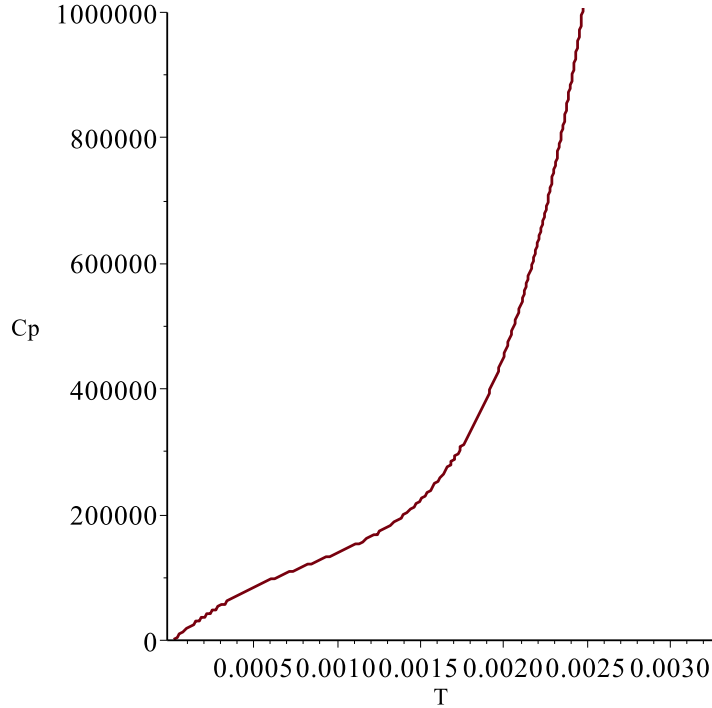


Figure 5.4: **Specific Heat.** This curve represents C_P , the specific heat of the system, as a function of the temperature. It is plotted for $P = -0.0001$ and $\Phi_+ = 0.1$.

The behaviour of the total Gibbs free energy G_{Total} for a variety of tensions and potentials, as seen in figure 5.5, shows that the system is sensitive to each. These two parameters have different effects as to the temperature at the phase transition can actually happen. The transition temperature of the system is almost indifferent to the choice of fixed potential of the system but is highly sensitive to its tension. This is understandable as the effect of the charge located at the centre of the black hole should not be significant, unlike the tension that is applied on the black hole by the de Sitter spacetime that affects the critical temperature dramatically.

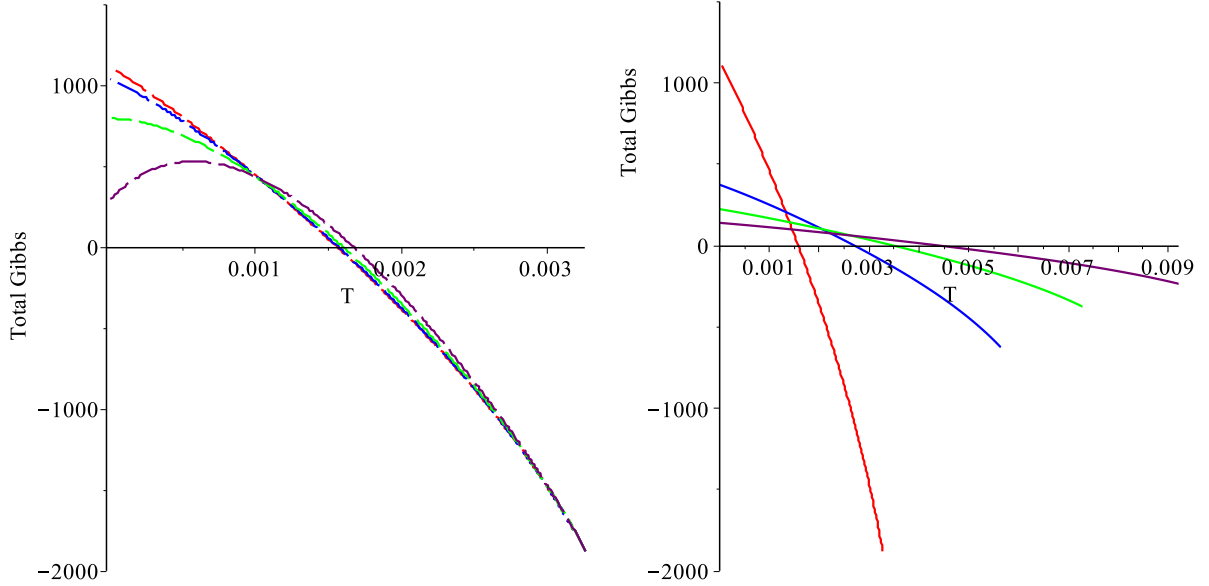


Figure 5.5: **Total Gibbs Free Energy** G_{Total} . *Left:* G_{Total} at $P = -0.0001$ where the $\{red, blue, green, purple\}$ curves correspond to the potential $\Phi_+ = \{0.1, 1, 2, 3\}$ respectively. *Right:* G_{Total} at $\Phi_+ = 0.1$ where the $\{red, blue, green, purple\}$ curves correspond to the pressure $P = \{-0.0001, -0.0003, -0.0005, -0.0008\}$ respectively.

5.2.3 Canonical Ensemble: Thermodynamics with Fixed Charge

The canonical ensemble, unlike the grand canonical ensemble, holds the charge fixed instead of the potential [67, 70]. However unlike these investigations, since the mass M as the enthalpy in the extended phase space, I consider minimization of the Gibbs free energy F and not the Helmholtz free energy. Once again I consider the multiple scenarios: the free energy of the black hole, of the cosmological horizon, and of the total system. They respectively read :

$$\begin{aligned}
 F_+ &= M - TS_+, \\
 F_c &= M - TS_+, \\
 F_{Total} &= M - T(S_+ + S_c).
 \end{aligned}
 \tag{5.19}$$

As in the previous section, I start by studying the different scenarios of different Gibbs free energies: The free energy of the black hole versus the free energy of the total system. I see in figure 5.6 the behaviour of all three is respectively analogous to that found in the

grand canonical ensemble. However due to the conservation of charge, the total system will not undergo a phase transition at $F_{Total} = 0$ – there will always be an equilibrium state consisting of a charged hairy black hole in de Sitter space. This system is always stable, as its specific heat is always positive (the plot of the specific heat for this case is similar to that in figure 5.4).

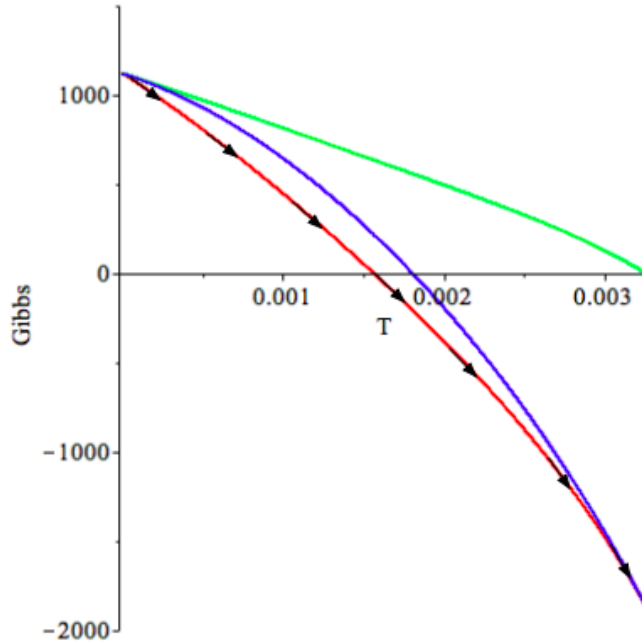


Figure 5.6: **Canonical Gibbs Free Energy (CGFE)**: the green curve represents the CGFE corresponding only to the black hole, the blue curve represents the CGFE as measured at the cosmological horizon r_c , the red curve is of the CGFE of the total system *i.e.* of the black hole in a the de Sitter heat bath . All curves are plotted for $P = -0.0001$ and $Q = 1$.

The behaviour of the total Gibbs free energy F_{Total} for a variety of tensions and charges showed similar results to 5.5. These two parameters have different effects on the free energy. But as there is no phase transition possible this sensitivity is of marginal interest.

5.3 Discussion

I have for the first time studied the thermodynamics of a black hole with two horizons with thermodynamic equilibrium imposed and with a control parameter. This study is possible because this class of black holes has an additional degree of freedom given by a hair parameter that allows us to impose thermodynamic equilibrium.

In addition of thoroughly studying the thermodynamic parameters of these black holes in de Sitter, I have analyzed the free energy of these systems in different ensembles. I have found that the system can undergo a phase transition that resembles the Hawking-Page phase transition in the grand-canonical ensemble, a result that is consistent with results previously found for de Sitter black holes isolated inside a cavity with thermodynamic equilibrium externally imposed [120]. However a key difference in our result is that at high- T the small black hole remains stable as it radiates, the cosmological horizon restoring the particle flux; for this reason I call it a “Reverse Hawking-Page” phase transition. As the black hole radiates, the hair parameter will adjust itself to preserve the thermodynamic equilibrium. I also found that these systems cannot undergo any phase transition in the canonical ensemble as such a transition violates the conservation of charge.

The situation here also stands in notable contrast to a recent study of the behaviour of charged de Sitter black holes in a cavity that takes into account pressure (tension) and volume [122]. In this case the cavity is used to ensure equilibrium, and one finds not only a standard Hawking Page transition but also a Van der Waals transition that exists only for a finite range of non-zero pressure, described by a “swallowtube” structure in a plot of free energy vs. pressure and temperature. However we find that this structure does not appear when scalar hair is used to ensure equilibrium, and only a reverse Hawking-Page transition is possible.

Mine is an exceptional setup that allows to uncover the thermodynamic properties and phase transitions that can give more insight to de Sitter space. It is certainly very important to further study these classes of black holes in higher dimensions and in other higher-curvature theories of gravity to see what other interesting phase behavior might be present.

Chapter 6

General Conclusions

The study of Black Holes as thermodynamic systems has been an increasingly active area of research in the last couple of decades. Investigations of asymptotically anti de-Sitter (AdS) black holes have been at the forefront in advancing our understanding of this subject. A key finding that has emerged from a rather large body of work is that their thermodynamic behaviour has been found to be analogous to everyday life thermodynamic systems, a subject known as Black Hole Chemistry.

However, our knowledge of the thermodynamic behaviour of asymptotically de Sitter (dS) black holes is significantly more sparse. Unfortunately this is a complex problem, since the absence of a Killing vector that is everywhere timelike outside the black hole horizon renders a good notion of the asymptotic mass questionable. Furthermore, the presence of both a black hole horizon and a cosmological horizon yields two distinct temperatures, suggesting that the system is in a non-equilibrium state. Yet their importance to cosmology and to a posited duality between gravity in de Sitter space and conformal field theory make them important objects of investigation.

In this thesis I used a variety of classes of solutions that allowed me to map out two approaches that are foundational to understanding black hole thermodynamics in de Sitter spacetime. The first approach is to understand the “thermodynamic volume” of cosmological horizons in isolation, without the additional complication of a black hole horizon. Fortunately a broad class of exact solutions having only a cosmological horizon exists: Eguchi-Hanson de Sitter solitons. I carried out the first study of thermodynamic volume associated with the cosmological horizon for Eguchi-Hanson de Sitter solitons in general dimensions. These results have shown that these quantities are calculable inside and outside the cosmological horizon in any odd dimension whether or not the regularity condition for

the soliton is imposed. This illustrates that cosmological volume is a well-defined concept, and that cosmological horizons indeed have meaningful thermodynamic properties.

The second approach entailed including black hole horizons. My first step along this path was to understand the phase transitions of thermalons – objects that describe a transition from a black hole in Anti de Sitter spacetime to one in de Sitter spacetime. This indicated that Thermalons can be understood in black holes chemistry terms and that asymptotically de Sitter black holes do have phase transitions.

I then focused on establishing a more complete approach that overcomes the two-horizon problem in de Sitter spacetime and successfully studies its black hole chemistry. Again, I exploited a class of exact hairy black hole solutions to Einstein gravity with conformally coupled scalar fields to this end . By adding hair to the black hole I found that thermodynamic equilibrium could be maintained between the two horizons. These solutions retain the same numbers of thermodynamic degrees of freedom present in the Reissner-Nordstrom AdS black hole, making it possible to explore a range of black hole phase transitions in de Sitter spacetime. I found that the this hairy charge black hole system, and the de Sitter space surrounding it, undergo a ‘Reverse’ Hawking-Page phase transition within the grand-canonical ensemble. This is the first approach that addressed the two-horizon problem whilst including all contributions of energy from every part of the system and without invoking additional artifacts such as cavities.

Many steps are yet to be taken to firmly establish black hole thermodynamics in de Sitter spacetime. I shall list several approaches to this end.

The first is to study the thermodynamics of isolated cosmological horizons. The method here will be to broaden the range of exact (and approximate) solutions having non-trivial curvature and a single cosmological horizon. This can be done by finding exact solitonic solutions to higher-curvature theories of gravity. It has been established in AdS spacetime that such higher curvature black holes exhibit a rich and interesting phase behaviour, and there is good reason to expect interesting behaviour to likewise occur in the de Sitter case. Among other things, this approach will allow to better understand the physical significance of thermodynamic volume and more generally the “chemistry” of cosmological horizons. Another study along these lines is to investigate the thermodynamic volume of de Sitter cosmological wormhole solutions [127], instead of the solitonic solutions. A study of thermodynamics of these systems is also possible as the thermodynamic equilibrium condition can be satisfied between the cosmological horizon and the wormhole throat. These studies, in combination, will provide a much better understanding of the thermodynamics of cosmological horizons.

The second direction is to broaden the class of de Sitter black holes whose temperatures

at both horizons are the same so that thermodynamic equilibrium is maintained. Again, an obvious place to look is in higher curvature theories of gravity, such as Lovelock gravity, and its more general quasi-topological counterparts. It is straightforward to add scalar hair to these solutions, whose key advantage is that the parameter space is much larger, allowing a lot more flexibility in requiring thermodynamic equilibrium between the two horizons. Some results are known for their AdS counterparts, and one can exploit this in investigating the de Sitter case to see what other interesting phase behaviour might be present. Moving beyond this, one can then consider thermodynamics of de Sitter black hole solutions with general base manifolds in Lovelock gravity. Recently constructed by Ray [128], these ‘exotic’ black hole solutions have the interesting property that their horizons do not have constant curvature. This introduces a new set of geometric and topological parameters that offer new possibilities for achieving thermodynamic equilibrium and for finding new kinds of phase transitions.

The long-run aim is to establish a general approach to de Sitter black hole thermodynamics. It is generally expected that the knowledge of black hole thermodynamics is key to understanding quantum gravity, and so it is of crucial importance to establish firm and reliable knowledge as to what happens in de Sitter space. Such a study is of more than academic interest – de Sitter spacetime is the closest model to our own accelerating universe. By studying it, the hope is to answer questions that have yet to be explored, that are relevant to the understanding of the universe, and that perhaps can be tested experimentally.

References

- [1] J. M. Bardeen, B. Carter and S. W. Hawking, *The Four laws of black hole mechanics*, *Commun. Math. Phys.* **31** (1973) 161–170.
- [2] S. B. Giddings, *The Black hole information paradox*, in *Particles, strings and cosmology. Proceedings, 19th Johns Hopkins Workshop and 5th PASCOS Interdisciplinary Symposium, Baltimore, USA, March 22-25, 1995*, pp. 415–428, 1995. [hep-th/9508151](#).
- [3] S. D. Mathur, *The Information paradox: A Pedagogical introduction*, *Class. Quant. Grav.* **26** (2009) 224001, [[0909.1038](#)].
- [4] S. W. Hawking, *Breakdown of predictability in gravitational collapse*, *Phys. Rev. D* **14** (Nov, 1976) 2460–2473.
- [5] S. D. Mathur, *The Fuzzball proposal for black holes: An Elementary review*, *Fortsch. Phys.* **53** (2005) 793–827, [[hep-th/0502050](#)].
- [6] A. Almheiri, D. Marolf, J. Polchinski and J. Sully, *Black Holes: Complementarity or Firewalls?*, *JHEP* **02** (2013) 062, [[1207.3123](#)].
- [7] S. W. Hawking, M. J. Perry and A. Strominger, *Soft Hair on Black Holes*, *Phys. Rev. Lett.* **116** (2016) 231301, [[1601.00921](#)].
- [8] R. M. Wald, *Black hole entropy is the Noether charge*, *Phys. Rev.* **D48** (1993) R3427–R3431, [[gr-qc/9307038](#)].
- [9] T. Jacobson, *Thermodynamics of space-time: The Einstein equation of state*, *Phys. Rev. Lett.* **75** (1995) 1260–1263, [[gr-qc/9504004](#)].
- [10] T. Padmanabhan, *Thermodynamical Aspects of Gravity: New insights*, *Rept. Prog. Phys.* **73** (2010) 046901, [[0911.5004](#)].

- [11] S. Hawking and D. Page, *Thermodynamics of Black Holes in anti-De Sitter Space*, *Commun.Math.Phys.* **87** (1983) 577.
- [12] J. M. Maldacena, *The Large N limit of superconformal field theories and supergravity*, *Int. J. Theor. Phys.* **38** (1999) 1113–1133, [[hep-th/9711200](#)].
- [13] E. Witten, *Anti-de Sitter space and holography*, *Adv. Theor. Math. Phys.* **2** (1998) 253–291, [[hep-th/9802150](#)].
- [14] E. Witten, *Anti-de Sitter space, thermal phase transition, and confinement in gauge theories*, *Adv. Theor. Math. Phys.* **2** (1998) 505–532, [[hep-th/9803131](#)].
- [15] P. Kovtun, D. T. Son and A. O. Starinets, *Viscosity in strongly interacting quantum field theories from black hole physics*, *Phys. Rev. Lett.* **94** (2005) 111601, [[hep-th/0405231](#)].
- [16] S. A. Hartnoll, P. K. Kovtun, M. Muller and S. Sachdev, *Theory of the Nernst effect near quantum phase transitions in condensed matter, and in dyonic black holes*, *Phys. Rev.* **B76** (2007) 144502, [[0706.3215](#)].
- [17] S. A. Hartnoll, C. P. Herzog and G. T. Horowitz, *Building a Holographic Superconductor*, *Phys. Rev. Lett.* **101** (2008) 031601, [[0803.3295](#)].
- [18] D. Kubiznak and R. B. Mann, *Black hole chemistry*, *Can. J. Phys.* **93** (2015) 999–1002, [[1404.2126](#)].
- [19] R. B. Mann, *The Chemistry of Black Holes*, *Springer Proc. Phys.* **170** (2016) 197–205.
- [20] L. J. Romans, *Supersymmetric, cold and lukewarm black holes in cosmological einstein-maxwell theory*, *Nucl.Phys. B* **383** (1992) 395–415, [[hep-th/9203018](#)].
- [21] R. B. Mann and S. F. Ross, *Cosmological production of charged black holes pairs*, *Phys. Rev. D* **52** (1995) 2254, [[gr-qc/9504015](#)].
- [22] G.-Q. Li, *Effects of dark energy on PV criticality of charged AdS black holes*, *Phys. Lett.* **B735** (2014) 256–260, [[1407.0011](#)].
- [23] D. W. Tian and I. Booth, *Friedmann equations from nonequilibrium thermodynamics of the Universe: A unified formulation for modified gravity*, *Phys. Rev.* **D90** (2014) 104042, [[1409.4278](#)].

- [24] M. Azreg-Aiou, *Charged de Sitter-like black holes: quintessence-dependent enthalpy and new extreme solutions*, *Eur. Phys. J. C* **75** (2015) 34, [[1410.1737](#)].
- [25] D. Kubiznak and F. Simovic, *Thermodynamics of horizons: de Sitter black holes and reentrant phase transitions*, *Class. Quant. Grav.* **33** (2016) 245001, [[1507.08630](#)].
- [26] L. C. Zhang and R. Zhao, *The critical phenomena of Schwarzschild-de Sitter black hole*, *Europhys. Lett.* **113** (2016) 10008.
- [27] A. Strominger, *The dS / CFT correspondence*, *JHEP* **10** (2001) 034, [[hep-th/0106113](#)].
- [28] A. Einstein, *Die grundlage der allgemeinen relativittstheorie*, *Annalen der Physik* **354** 769–822, [<https://onlinelibrary.wiley.com/doi/pdf/10.1002/andp.19163540702>].
- [29] A. Einstein, *Zur elektrodynamik bewegter krper*, *Annalen der Physik* **322** 891–921, [<https://onlinelibrary.wiley.com/doi/pdf/10.1002/andp.19053221004>].
- [30] A. Einstein, *Cosmological Considerations in the General Theory of Relativity*, *Sitzungsber. Preuss. Akad. Wiss. Berlin (Math. Phys.)* **1917** (1917) 142–152.
- [31] D. Lovelock, *The einstein tensor and its generalizations*, *Journal of Mathematical Physics* **12** (1971) 498–501.
- [32] X. O. Camanho, J. D. Edelstein, G. Giribet and A. Gomberoff, *Generalized phase transitions in Lovelock gravity*, *Phys.Rev.* **D90** (2014) 064028, [[1311.6768](#)].
- [33] R. C. Myers, *Higher-derivative gravity, surface terms, and string theory*, *Phys. Rev. D* **36** (Jul, 1987) 392–396.
- [34] A. Strominger, *Inflation and the dS / CFT correspondence*, *JHEP* **11** (2001) 049, [[hep-th/0110087](#)].
- [35] X. O. Camanho, J. D. Edelstein, A. Gomberoff and J. A. Sierra-Garca, *On AdS to dS transitions in higher-curvature gravity*, *JHEP* **10** (2015) 179, [[1504.04496](#)].
- [36] J. Bardeen, B. Carter and S. Hawking, *The Four laws of black hole mechanics*, *Commun.Math.Phys.* **31** (1973) 161–170.

- [37] W. Israel, *Event horizons in static electrovac space-times*, *Commun. Math. Phys.* **8** (1968) 245–260.
- [38] J. D. Bekenstein, *Black holes and entropy*, *Phys. Rev. D* **7** (Apr, 1973) 2333–2346.
- [39] S. W. Hawking, *Particle Creation by Black Holes*, *Commun. Math. Phys.* **43** (1975) 199–220.
- [40] S. W. Hawking, *Black holes in general relativity*, *Commun. Math. Phys.* **25** (1972) 152–166.
- [41] J. D. Bekenstein, *Black holes and entropy*, *Phys. Rev.* **D7** (1973) 2333–2346.
- [42] R. M. Wald, *General relativity*. Chicago Univ. Press, Chicago, IL, 1984.
- [43] L. Parker, *Quantized fields and particle creation in expanding universes. 1.*, *Phys. Rev.* **183** (1969) 1057–1068.
- [44] G. W. Gibbons and S. W. Hawking, *Cosmological Event Horizons, Thermodynamics, and Particle Creation*, *Phys. Rev.* **D15** (1977) 2738–2751.
- [45] L. Smarr, *Mass formula for Kerr black holes*, *Phys. Rev. Lett.* **30** (1973) 71–73.
- [46] C. Teitelboim, *THE COSMOLOGICAL CONSTANT AS A THERMODYNAMIC BLACK HOLE PARAMETER*, *Phys. Lett.* **158B** (1985) 293–297.
- [47] J. D. Brown and C. Teitelboim, *Neutralization of the Cosmological Constant by Membrane Creation*, *Nucl.Phys.* **B297** (1988) 787–836.
- [48] J. D. E. Creighton and R. B. Mann, *Quasilocal thermodynamics of dilaton gravity coupled to gauge fields*, *Phys. Rev.* **D52** (1995) 4569–4587, [[gr-qc/9505007](#)].
- [49] M. M. Caldarelli, G. Cognola and D. Klemm, *Thermodynamics of Kerr-Newman-AdS black holes and conformal field theories*, *Class. Quant. Grav.* **17** (2000) 399–420, [[hep-th/9908022](#)].
- [50] T. Padmanabhan, *Classical and quantum thermodynamics of horizons in spherically symmetric space-times*, *Class. Quant. Grav.* **19** (2002) 5387–5408, [[gr-qc/0204019](#)].
- [51] D. Kastor, S. Ray and J. Traschen, *Enthalpy and the Mechanics of AdS Black Holes*, *Class. Quant. Grav.* **26** (2009) 195011, [[0904.2765](#)].

- [52] B. P. Dolan, *The cosmological constant and the black hole equation of state*, *Class. Quant. Grav.* **28** (2011) 125020, [[1008.5023](#)].
- [53] M. Cvetič, G. Gibbons, D. Kubiznak and C. Pope, *Black Hole Enthalpy and an Entropy Inequality for the Thermodynamic Volume*, *Phys. Rev.* **D84** (2011) 024037, [[1012.2888](#)].
- [54] B. P. Dolan, D. Kastor, D. Kubiznak, R. B. Mann and J. Traschen, *Thermodynamic Volumes and Isoperimetric Inequalities for de Sitter Black Holes*, *Phys. Rev.* **D87** (2013) 104017, [[1301.5926](#)].
- [55] N. Altamirano, D. Kubiznak, R. B. Mann and Z. Sherkatghanad, *Thermodynamics of rotating black holes and black rings: phase transitions and thermodynamic volume*, *Galaxies* **2** (2014) 89–159, [[1401.2586](#)].
- [56] G. W. Gibbons, M. J. Perry and C. N. Pope, *The First law of thermodynamics for Kerr-anti-de Sitter black holes*, *Class. Quant. Grav.* **22** (2005) 1503–1526, [[hep-th/0408217](#)].
- [57] G. W. Gibbons, *What is the Shape of a Black Hole?*, *AIP Conf. Proc.* **1460** (2012) 90–100, [[1201.2340](#)].
- [58] R. A. Hennigar, D. Kubiznak and R. B. Mann, *Entropy Inequality Violations from Ultraspinning Black Holes*, *Phys. Rev. Lett.* **115** (2015) 031101, [[1411.4309](#)].
- [59] R. A. Hennigar, D. Kubiznak, R. B. Mann and N. Musoke, *Ultraspinning limits and super-entropic black holes*, *JHEP* **06** (2015) 096, [[1504.07529](#)].
- [60] J. Armas, N. A. Obers and M. Sanchioni, *Gravitational Tension, Spacetime Pressure and Black Hole Volume*, [[1512.09106](#)].
- [61] M. Appels, R. Gregory and D. Kubiznak, *Thermodynamics of Accelerating Black Holes*, *Phys. Rev. Lett.* **117** (2016) 131303, [[1604.08812](#)].
- [62] H. Liu and X.-h. Meng, *PV criticality in the extended phasespace of charged accelerating AdS black holes*, *Mod. Phys. Lett.* **A31** (2016) 1650199, [[1607.00496](#)].
- [63] G. Gibbons, H. Lu, D. N. Page and C. Pope, *The General Kerr-de Sitter metrics in all dimensions*, *J. Geom. Phys.* **53** (2005) 49–73, [[hep-th/0404008](#)].

- [64] G. W. Gibbons, H. Lu, D. N. Page and C. N. Pope, *Rotating black holes in higher dimensions with a cosmological constant*, *Phys. Rev. Lett.* **93** (2004) 171102, [[hep-th/0409155](#)].
- [65] R. A. Hennigar and R. B. Mann, *Reentrant phase transitions and van der Waals behaviour for hairy black holes*, [1509.06798](#).
- [66] J. Couch, W. Fischler and P. H. Nguyen, *Noether charge, black hole volume and complexity*, [1610.02038](#).
- [67] A. Chamblin, R. Emparan, C. V. Johnson and R. C. Myers, *Charged AdS black holes and catastrophic holography*, *Phys. Rev.* **D60** (1999) 064018, [[hep-th/9902170](#)].
- [68] D. Kubiznak and R. B. Mann, *P-V criticality of charged AdS black holes*, *JHEP* **1207** (2012) 033, [[1205.0559](#)].
- [69] B. P. Dolan, *Pressure and volume in the first law of black hole thermodynamics*, *Class.Quant.Grav.* **28** (2011) 235017, [[1106.6260](#)].
- [70] A. Chamblin, R. Emparan, C. V. Johnson and R. C. Myers, *Holography, thermodynamics and fluctuations of charged AdS black holes*, *Phys. Rev.* **D60** (1999) 104026, [[hep-th/9904197](#)].
- [71] X. N. Wu, *Multicritical phenomena of Reissner-Nordstrom anti-de Sitter black holes*, *Phys. Rev.* **D62** (2000) 124023.
- [72] M. Cvetič and S. S. Gubser, *Phases of R charged black holes, spinning branes and strongly coupled gauge theories*, *JHEP* **04** (1999) 024, [[hep-th/9902195](#)].
- [73] M. Cvetič and S. S. Gubser, *Thermodynamic stability and phases of general spinning branes*, *JHEP* **07** (1999) 010, [[hep-th/9903132](#)].
- [74] S. Gunasekaran, R. B. Mann and D. Kubiznak, *Extended phase space thermodynamics for charged and rotating black holes and Born-Infeld vacuum polarization*, *JHEP* **1211** (2012) 110, [[1208.6251](#)].
- [75] N. Altamirano, D. Kubiznak and R. B. Mann, *Reentrant Phase Transitions in Rotating AdS Black Holes*, *Phys.Rev.* **D88** (2013) 101502, [[1306.5756](#)].

- [76] N. Altamirano, D. Kubiznak, R. B. Mann and Z. Sherkatghanad, *Kerr-AdS analogue of triple point and solid/liquid/gas phase transition*, *Class.Quant.Grav.* **31** (2014) 042001, [[1308.2672](#)].
- [77] S.-W. Wei, P. Cheng and Y.-X. Liu, *Analytical and exact critical phenomena of d-dimensional singly spinning Kerr-AdS black holes*, *Phys. Rev.* **D93** (2016) 084015, [[1510.00085](#)].
- [78] A. M. Frassino, D. Kubiznak, R. B. Mann and F. Simovic, *Multiple Reentrant Phase Transitions and Triple Points in Lovelock Thermodynamics*, *JHEP* **09** (2014) 080, [[1406.7015](#)].
- [79] S.-W. Wei and Y.-X. Liu, *Triple points and phase diagrams in the extended phase space of charged Gauss-Bonnet black holes in AdS space*, *Phys. Rev.* **D90** (2014) 044057, [[1402.2837](#)].
- [80] R. A. Hennigar, W. G. Brenna and R. B. Mann, *Pv criticality in quasitopological gravity*, *JHEP* **07** (2015) 077, [[1505.05517](#)].
- [81] Z. Sherkatghanad, B. Mirza, Z. Mirzaiyan and S. A. Hosseini Mansoori, *Critical behaviors and phase transitions of black holes in higher order gravities and extended phase spaces*, *Int. J. Mod. Phys.* **D26** (2016) 1750017, [[1412.5028](#)].
- [82] C. Hudson *Z. Phys. Chem.* **47** (1904) 113.
- [83] D. Kastor, S. Ray and J. Traschen, *Genuine Cosmic Hair*, *Class. Quant. Grav.* **34** (2017) 045003, [[1608.04641](#)].
- [84] A. Ghezelbash and R. B. Mann, *Action, mass and entropy of Schwarzschild-de Sitter black holes and the de Sitter / CFT correspondence*, *JHEP* **0201** (2002) 005, [[hep-th/0111217](#)].
- [85] M. Urano, A. Tomimatsu and H. Saida, *Mechanical First Law of Black Hole Spacetimes with Cosmological Constant and Its Application to Schwarzschild-de Sitter Spacetime*, *Class. Quant. Grav.* **26** (2009) 105010, [[0903.4230](#)].
- [86] M.-S. Ma, H.-H. Zhao, L.-C. Zhang and R. Zhao, *Existence condition and phase transition of Reissner-Nordström-de Sitter black hole*, *Int.J.Mod.Phys.* **A29** (2014) 1450050, [[1312.0731](#)].

- [87] H.-H. Zhao, L.-C. Zhang, M.-S. Ma and R. Zhao, *P-V criticality of higher dimensional charged topological dilaton de Sitter black holes*, *Phys. Rev.* **D90** (2014) 064018.
- [88] L.-C. Zhang, M.-S. Ma, H.-H. Zhao and R. Zhao, *Thermodynamics of phase transition in higher dimensional Reissner-Nordström-de Sitter black hole*, [1403.2151](#).
- [89] M.-S. Ma, L.-C. Zhang, H.-H. Zhao and R. Zhao, *Phase transition of the higher dimensional charged Gauss-Bonnet black hole in de Sitter spacetime*, *Adv. High Energy Phys.* **2015** (2015) 134815, [[1410.5950](#)].
- [90] X. Guo, H. Li, L. Zhang and R. Zhao, *Thermodynamics and phase transition in the Kerr de Sitter black hole*, *Phys. Rev.* **D91** (2015) 084009.
- [91] X. Guo, H. Li, L. Zhang and R. Zhao, *The critical phenomena of charged rotating de Sitter black holes*, *Class. Quant. Grav.* **33** (2016) 135004.
- [92] D. Kastor and J. H. Traschen, *Cosmological multi - black hole solutions*, *Phys. Rev.* **D47** (1993) 5370–5375, [[hep-th/9212035](#)].
- [93] S. Bhattacharya, *A note on entropy of de Sitter black holes*, *Eur. Phys. J.* **C76** (2016) 112, [[1506.07809](#)].
- [94] H.-F. Li, M.-S. Ma and Y.-Q. Ma, *Thermodynamic properties of black holes in de Sitter space*, *Mod. Phys. Lett.* **A32** (2016) 1750017, [[1605.08225](#)].
- [95] R. Clarkson and R. B. Mann, *Eguchi-Hanson solitons in odd dimensions*, *Class. Quant. Grav.* **23** (2006) 1507–1524, [[hep-th/0508200](#)].
- [96] T. Eguchi and A. J. Hanson, *Asymptotically Flat Selfdual Solutions to Euclidean Gravity*, *Phys. Lett.* **B74** (1978) 249–251.
- [97] R. Clarkson and R. B. Mann, *Soliton solutions to the Einstein equations in five dimensions*, *Phys. Rev. Lett.* **96** (2006) 051104, [[hep-th/0508109](#)].
- [98] V. Balasubramanian, J. de Boer and D. Minic, *Mass, entropy and holography in asymptotically de Sitter spaces*, *Phys. Rev.* **D65** (2002) 123508, [[hep-th/0110108](#)].
- [99] A. W. C. Wong and R. B. Mann, *Five-Dimensional Eguchi-Hanson Solitons in Einstein-Gauss-Bonnet Gravity*, *Phys. Rev.* **D85** (2012) 046010, [[1112.2229](#)].

- [100] R. B. Mann and C. Stelea, *New multiply nutty spacetimes*, *Phys. Lett.* **B634** (2006) 448–455, [[hep-th/0508203](#)].
- [101] W. G. Brenna, R. B. Mann and M. Park, *Mass and Thermodynamic Volume in Lifshitz Spacetimes*, *Phys. Rev.* **D92** (2015) 044015, [[1505.06331](#)].
- [102] G. T. Horowitz and T. Jacobson, *Note on gauge theories on $m /$ and the ads/cft correspondence*, *Journal of High Energy Physics* **2002** (2002) 013.
- [103] S. Das and R. Mann, *Conserved quantities in Kerr-anti-de Sitter space-times in various dimensions*, *JHEP* **0008** (2000) 033, [[hep-th/0008028](#)].
- [104] G. W. Gibbons and S. W. Hawking, *Action integrals and partition functions in quantum gravity*, *Phys. Rev. D* **15** (May, 1977) 2752–2756.
- [105] R. Clarkson, A. M. Ghezelbash and R. B. Mann, *Entropic N bound and maximal mass conjectures violation in four-dimensional Taub-Bolt(NUT)- dS space-times*, *Nucl. Phys.* **B674** (2003) 329–364, [[hep-th/0307059](#)].
- [106] R. Clarkson, A. M. Ghezelbash and R. B. Mann, *A Review of the N -bound and the maximal mass conjectures using NUT -charged dS spacetimes*, *Int. J. Mod. Phys.* **A19** (2004) 3987–4036, [[hep-th/0408058](#)].
- [107] S. R. Coleman, *The Fate of the False Vacuum. 1. Semiclassical Theory*, *Phys. Rev.* **D15** (1977) 2929–2936.
- [108] S. R. Coleman and F. De Luccia, *Gravitational Effects on and of Vacuum Decay*, *Phys. Rev.* **D21** (1980) 3305.
- [109] J. D. Brown and C. Teitelboim, *Dynamical Neutralization of the Cosmological Constant*, *Phys. Lett.* **B195** (1987) 177–182.
- [110] X. O. Camanho, J. D. Edelstein, G. Giribet and A. Gomberoff, *A New type of phase transition in gravitational theories*, *Phys.Rev.* **D86** (2012) 124048, [[1204.6737](#)].
- [111] S. Nojiri and S. D. Odintsov, *The de Sitter / anti-de Sitter black holes phase transition?*, in *1st Mexican Meeting on Mathematical and Experimental Physics Mexico City, Mexico, September 10-14, 2001*, 2001. [gr-qc/0112066](#).
- [112] D. Lovelock, *The Einstein tensor and its generalizations*, *J.Math.Phys.* **12** (1971) 498–501.

- [113] S. R. Coleman, *The Uses of Instantons*, *Subnucl. Ser.* **15** (1979) 805.
- [114] X. O. Camanho, *Lovelock gravity, black holes and holography*. PhD thesis, Santiago de Compostela U., 2013. [1509.08129](#).
- [115] J. Crisostomo, R. Troncoso and J. Zanelli, *Black hole scan*, *Phys.Rev.* **D62** (2000) [084013](#), [[hep-th/0003271](#)].
- [116] D. Kastor, S. Ray and J. Traschen, *Smarr Formula and an Extended First Law for Lovelock Gravity*, *Class.Quant.Grav.* **27** (2010) [235014](#), [[1005.5053](#)].
- [117] R. A. Hennigar, R. B. Mann and E. Tjoa, *Superfluid Black Holes*, [1609.02564](#).
- [118] R. A. Hennigar, E. Tjoa and R. B. Mann, *Thermodynamics of hairy black holes in Lovelock gravity*, *JHEP* **02** (2017) [070](#), [[1612.06852](#)].
- [119] H. Dykaar, R. A. Hennigar and R. B. Mann, *Hairy black holes in cubic quasi-topological gravity*, *JHEP* **05** (2017) [045](#), [[1703.01633](#)].
- [120] S. Carlip and S. Vaidya, *Phase transitions and critical behavior for charged black holes*, *Class.Quant.Grav.* **20** (2003) 3827–3838, [[gr-qc/0306054](#)].
- [121] H. W. Braden, J. D. Brown, B. F. Whiting and J. W. York, Jr., *Charged black hole in a grand canonical ensemble*, *Phys. Rev.* **D42** (1990) [3376–3385](#).
- [122] F. Simovic and R. Mann, *Critical Phenomena of Charged de Sitter Black Holes in Cavities*, [1807.11875](#).
- [123] J. Oliva and S. Ray, *Conformal couplings of a scalar field to higher curvature terms*, *Class. Quant. Grav.* **29** (2012) [205008](#), [[1112.4112](#)].
- [124] L. J. Romans, *Supersymmetric, cold and lukewarm black holes in cosmological Einstein-Maxwell theory*, *Nucl. Phys.* **B383** (1992) [395–415](#), [[hep-th/9203018](#)].
- [125] R. B. Mann and S. F. Ross, *Cosmological production of charged black hole pairs*, *Phys. Rev.* **D52** (1995) [2254–2265](#), [[gr-qc/9504015](#)].
- [126] I. S. Booth and R. B. Mann, *Cosmological pair production of charged and rotating black holes*, *Nucl. Phys.* **B539** (1999) [267–306](#), [[gr-qc/9806056](#)].
- [127] A. Anabalón and A. Cisterna, *Asymptotically (anti) de Sitter Black Holes and Wormholes with a Self Interacting Scalar Field in Four Dimensions*, *Phys. Rev.* **D85** (2012) [084035](#), [[1201.2008](#)].

- [128] S. Ray, *Birkhoffs theorem in Lovelock gravity for general base manifolds*, *Class. Quant. Grav.* **32** (2015) 195022, [[1505.03830](#)].
- [129] J. Traschen, *Constraints on stress energy perturbations in general relativity*, *Phys.Rev.* **D31** (1985) 283.
- [130] D. Sudarsky and R. M. Wald, *Extrema of mass, stationarity, and staticity, and solutions to the Einstein Yang-Mills equations*, *Phys.Rev.* **D46** (1992) 1453–1474.
- [131] J. Traschen and D. Fox, *Tension perturbations of black brane space-times*, *Class.Quant.Grav.* **21** (2004) 289–306, [[gr-qc/0103106](#)].
- [132] D. Kastor, *Komar Integrals in Higher (and Lower) Derivative Gravity*, *Class.Quant.Grav.* **25** (2008) 175007, [[0804.1832](#)].
- [133] N. Goldenfeld, *Lectures on Phase Transitions and the Renormalization Group*. Westview Press, New York, 1992.
- [134] R. B. Mann and C. Stelea, *On the thermodynamics of NUT charged spaces*, *Phys. Rev.* **D72** (2005) 084032, [[hep-th/0408234](#)].

Appendix A

Generalized first law of black hole mechanics

This appendix briefly summarizes the Hamiltonian derivation of the extended first law (2.9) of black hole mechanics[51].

Consider a black hole with a killing field, solution to Einstein's field equations in d dimensional spacetime. The corresponding metric reads

$$g_{ab} = h_{ab} - n_a n_b, \quad (\text{A.1})$$

where n^a is the unit timelike normal ($n \cdot n = -1$) to a hypersurface Σ . The latter has an induced metric¹ h_{ab} that obeys $h_a{}^b n_b = 0$. In the presence of such hypersurfaces, the system evolves along the vector field

$$\xi^a = N n^a + N^a, \quad (\text{A.2})$$

where $N = -\xi \cdot n$ is the lapse function while N^a is the shift vector (that is always tangential to Σ).

The full gravitational Hamiltonian reads

$$\mathcal{H} = NH + N^a H_a, \quad (\text{A.3})$$

¹ The dynamical parameters in the phase space consist of the metric h_{ab} and its conjugate momentum $\pi^{ab} = -\sqrt{h}(K^{ab} - Kh^{ab})$, with $K_{ab} = h_a{}^c \nabla_c n_b$ being the extrinsic curvature of Σ . Note that $K = K^a{}_a$ and $\pi = \pi^a{}_a$ are the traces of these respective tensors. However h is the determinant of the metric h_{ab} restricted to Σ .

with

$$\begin{aligned} H &\equiv -2G_{ab}n^an^b = -R^{(d-1)} + \frac{1}{|h|} \left(\frac{\pi^2}{d-2} - \pi^{ab}\pi_{ab} \right), \\ H_b &\equiv -2G_{ac}n^ah_b^c = -2D_a(|h|^{-\frac{1}{2}}\pi^{ab}), \end{aligned} \quad (\text{A.4})$$

where D_a is the covariant derivative operator associated to h_{ab} on Σ and $R^{(d-1)}$ the corresponding scalar curvature of Σ . A special situation rises when considering $8\pi T_b^a = -\Lambda g_b^a$, which yields the following constraints equations:

$$H = -2\Lambda, \quad H_b = 0. \quad (\text{A.5})$$

Assuming that g_{ab} is a solution of the field equations with Killing vector ξ^a and cosmological constant Λ , its infinitesimally close solution that does not necessarily admit any Killing vector reads

$$\tilde{g}_{ab} = g_{ab} + \delta g_{ab}, \quad (\text{A.6})$$

where the corresponding $\tilde{\Lambda} = \Lambda + \delta\Lambda$, $\tilde{h}_{ab} = h_{ab} + \gamma_{ab}$ and $\tilde{\pi}_{ab} = \pi_{ab} + p_{ab}$. Note that $\gamma_{ab} = \delta h_{ab}$, $p_{ab} = \delta\pi_{ab}$ and that h_{ab} and π^{ab} are correspond to the original solution g_{ab} . Taking all of this into account, (A.5) becomes [129, 130, 131, 51]

$$D_a(B^a - 2\delta\Lambda\omega^{ab}n_b) = 0, \quad (\text{A.7})$$

with $N = -\xi^an_a = -D_c(\omega^{cb}n_b)$. Here B^a behaves as follows

$$B^a[\xi] = N(D^a\gamma_c^c - D_b\gamma^{ab}) - \gamma_c^c D^aN + \gamma^{ab}D_bN + |h|^{-\frac{1}{2}}N^b(\pi^{cd}\gamma_{cd}h^a{}_b - 2\pi^{ac}\gamma_{bc} - 2p^a{}_b), \quad (\text{A.8})$$

and $\omega^{ab} = -\omega^{ba}$ obeys [132, 51]:

$$\nabla_c\omega^{cb} = \xi^b, \quad (\text{A.9})$$

where ω^{ab} is a non-unique tensor and is only defined up to a divergence-less term.

A Gauss' law relation is displayed in (A.7) that can be integrated over a volume \hat{V} contained in Σ yielding

$$\int_{\partial\hat{V}_{out}} dS r_c (B^c[\xi] - 2\delta\Lambda\omega^{cb}n_b) = \int_{\partial\hat{V}_{in}} dS r_c (B^c[\xi] - 2\delta\Lambda\omega^{cb}n_b). \quad (\text{A.10})$$

Note that r^c is the unitary normal vector pointing into the inner boundary $\partial\hat{V}_{in}$, and out of the outer boundary of $\partial\hat{V}_{out}$ of \hat{V} .

Using $\omega^{cb} = \omega^{cb} - \omega_{AdS}^{cb} + \omega_{AdS}^{cb}$ for the $\partial\hat{V}_{out}$ part of the intergral, (A.10) becomes

$$\int_{\partial\hat{V}_{out}} d\mathcal{S}r_c (B^c[\xi] - 2\delta\Lambda\omega_{AdS}^{cb}n_b) = \int_{\partial\hat{V}_{out}} d\mathcal{S}r_c (2\delta\Lambda(\omega^{cb} - \omega_{AdS}^{cb})n_b) + \int_{\partial\hat{V}_{in}} d\mathcal{S}r_c (B^c[\xi] - 2\delta\Lambda\omega^{cb}n_b), \quad (\text{A.11})$$

with ω_{AdS}^{ab} being the Killing co-potential of the *background* AdS spacetime.

The variations in the total mass M and angular momentum J of the space-time, when setting the outer boundary at spatial infinity and respectively setting the time translation and rotations as $\xi^a = (\partial_t)^a$ and $\xi^a = (\partial_\varphi)^a$, are given by

$$16\pi\delta M = - \int_{\infty} d\mathcal{S}r_c (B^c[\partial_t] - 2\delta\Lambda\omega_{AdS}^{cb}n_b), \quad (\text{A.12})$$

$$16\pi\delta J = \int_{\infty} d\mathcal{S}r_c B^c[\partial_\varphi]. \quad (\text{A.13})$$

The ω_{AdS}^{cb} term guarantees that δM is finite [51]. Let H be the event horizon of a black hole induced by the Killing vector $\xi^a = (\partial_t + \Omega\partial_\varphi)^a$. Given that A is the area of the bifurcate Killing horizon H where ξ vanishes, its variation reads

$$2\kappa\delta A = - \int_H d\mathcal{S}r_c B^c[\partial_t + \Omega\partial_\varphi], \quad (\text{A.14})$$

here, $\kappa = \sqrt{-\frac{1}{2}\nabla^a\xi^b\nabla_a\xi_b} \big|_{r=r_+}$ is the surface gravity at this event horizon.

Since the variation of the cosmological constant $\delta\Lambda$ is spacetime-independent, the volume can be defined by

$$V = \int_{\infty} d\mathcal{S}r_c n_b (\omega^{cb} - \omega_{AdS}^{cb}) - \int_H d\mathcal{S}r_c n_b \omega^{cb}. \quad (\text{A.15})$$

Hence, the remaining terms in (A.11) can be interpreted as $V\delta P$ ². Combining all these terms, the first law of black hole thermodynamics is reproduced

$$\delta M = T\delta S + V\delta P + \Omega\delta J, \quad (\text{A.16})$$

which is in total agreement with (2.9).

² Here, V is finite due to the presence of the ω_{AdS}^{cb} term.

Appendix B

Van de Waals Fluids: A brief review

This appendix will review the Van de Waals phase transition for fluids.

The liquid/gas transition of a non-ideal fluid is described by the Van der Waals equation of state (B.1) that reads

$$\left(P + \frac{a}{v^2}\right)(v - b) = T, \quad (\text{B.1})$$

where P is the pressure, $v = V/N$ is the volume, T is the temperature and the parameter $a > 0$ and b respectively measure the attraction between particles and the volume of “fluid particles” [133]. As the nonzero size of the molecules of a given fluid is taken into account in the constant $b > 0$, The attraction between them is measured by the constant $a > 0$. Similarly, one can write this equation as a cubic equation for v yielding

$$Pv^3 - (kT + bP)v^2 + av - ab = 0. \quad (\text{B.2})$$

From the qualitative behaviour of isotherms, it is easy to see that a *critical point* takes place when $P = P(v)$ has an inflection point, i.e. at the critical isotherm $T = T_c$ yielding

$$\frac{\partial P}{\partial v} = 0, \quad \frac{\partial^2 P}{\partial v^2} = 0. \quad (\text{B.3})$$

One can write (B.2) in the form $P_c(v - v_c)^3 = 0$, then compare the coefficients to get

$$kT_c = \frac{8a}{27b}, \quad v_c = 3b, \quad P_c = \frac{a}{27b^2}. \quad (\text{B.4})$$

Note that $\frac{P_c v_c}{kT_c} = \frac{3}{8}$ is a universal number anticipated for all fluids independently of the choice a and b .

One can set

$$p = \frac{P}{P_c}, \quad \nu = \frac{v}{v_c}, \quad \tau = \frac{T}{T_c}, \quad (\text{B.5})$$

to obtain the universal *law of corresponding states*. It is valid for more general conjectures other than that of the Van der Waals equation. It reads

$$8\tau = (3\nu - 1) \left(p + \frac{3}{\nu^2} \right). \quad (\text{B.6})$$

The system undergoes a *liquid–gas phase transition* when $T < T_c$. The latter can be described by substituting the *oscillating part* of the isotherm by an isobar, as states in *Maxwell’s equal area law* that reads

$$\oint v dP = 0. \quad (\text{B.7})$$

The phase transition can be understood by analysing the (specific) Gibbs free energy, $G = G(P, T)$. For a fixed number of particles, one can integrate

$$dG = -SdT + v dP, \quad (\text{B.8})$$

while using the Van der Waals equation. Comparing the outcome with (statistical) G of the ideal gas to determine the integration function, the specific Gibbs free energy reads

$$G = G(T, P) = -kT \left(1 + \ln \left[\frac{(v - b)T^{3/2}}{\Phi} \right] \right) - \frac{a}{v} + Pv. \quad (\text{B.9})$$

The parameter v here is analyzed using P and T , via the Van der Waals equation (B.1), and Φ is a characteristic constant of the gas and it has dimensionality.

One can analyse the *coexistence line* of two phases, along which these two phases are in equilibrium. It takes place whenever two surfaces of G cross paths. It is dictated by the Clausius–Clapeyron equation

$$\left. \frac{dP}{dT} \right|_{\text{coexistence}} = \frac{S_g - S_l}{v_g - v_l}, \quad (\text{B.10})$$

where S_g , S_l , and v_g , v_l , correspond to the specific entropy and specific volume of the gas and liquid phase, respectively. Otherwise, this coexistence curve can be established using Maxwell’s law (B.7), or by finding a line in the (P, T) -plane for which the Gibbs free energy and the Van der Waals temperature coincide for two different volumes v_l and v_g .

Appendix C

Eguchi-Hanson Solitons

In this Appendix I review the derivation of the Eguchi-Hanson metric (3.4).

For this one has to use the five-dimensional generalization [134] of the Taub-NUT metric,

$$ds^2 = -\rho^2 dt^2 + 4n^2 F(\rho) [d\psi + \cos(\theta)d\phi]^2 + \frac{d\rho^2}{F(\rho)} + (\rho^2 - n^2)(d\theta^2 + \sin(\theta)^2 d\phi^2), \quad (\text{C.1})$$

with the $U(1)$ -fibration being a partial fibration over a two-dimensional subspace the $D = 3$ base space. Here, the function $F(\rho)$ is

$$F(\rho) = \frac{\rho^4 + 4m\ell^2 - 2n^2\rho^2}{\ell^2(\rho^2 - n^2)}. \quad (\text{C.2})$$

The condition $n = \frac{\ell}{2}$ must hold for this to satisfy the $d = 5$ Einstein equations with cosmological constant $\Lambda = -\frac{6}{\ell^2}$.

Setting the NUT charge, equivalent to Λ , to zero renders a degenerate metric which causes the spacetime to be non trivial. Hence one must use an ensemble of transformations yielding this “non trivial” metric in the zero cosmological constant limit, i.e. $l \rightarrow \infty$. These transformations are

$$\rho^2 = r^2 + n^2, \quad m = \frac{\ell^2}{64} - \frac{a^4}{64\ell^2}. \quad (\text{C.3})$$

Thereafter, one must set $r \rightarrow r/2$, $t \rightarrow 2t/\ell$ and obtain

$$\begin{aligned}
ds^2 &= -g(r)dt^2 + \frac{r^2 f(r)}{4} [d\psi + \cos(\theta)d\phi]^2 + \frac{dr^2}{f(r)g(r)} \\
&\quad + \frac{r^2}{4}(d\theta^2 + \sin(\theta)^2 d\phi^2), \\
g(r) &= 1 + \frac{r^2}{\ell^2} \quad , \quad f(r) = 1 - \frac{a^4}{r^4}.
\end{aligned} \tag{C.4}$$

One can easily see that (C.4) solves Einstein's equations with negative cosmological constant $\Lambda = -6/\ell^2$. Hence, one can demand $\ell \rightarrow i\ell$ transforming (C.4) into a metric that solves Einstein's equations $\Lambda > 0$.

The metric transformation (C.1) \rightarrow (C.4) yields a new way of obtaining the Eguchi-Hanson metric in $d = 4$. When imposing the limit $\ell \rightarrow \infty$ on (C.4), one obtains the Eguchi-Hanson metric

$$ds^2 = \frac{r^2}{4} f(r) [d\psi + \cos(\theta)d\phi]^2 + \frac{dr^2}{f(r)} + \frac{r^2}{4}(d\theta^2 + \sin(\theta)^2 d\phi^2), \tag{C.5}$$

as a constant t hypersurface. These steps yield a degenerate metric.

By setting $D = 2k + 2$, the metric (C.4) can be generalized to any odd dimension $(D + 1)$ where $D > 4$ must hold. This resultant set of metric then read

$$\begin{aligned}
ds^2 &= -g(r)dt^2 + \left(\frac{2r}{D}\right)^2 f(r) \left[d\psi + \sum_{i=1}^k \cos(\theta_i) d\phi_i \right]^2 \\
&\quad + \frac{dr^2}{g(r)f(r)} + \frac{r^2}{D} \sum_{i=1}^k d\Sigma_{2(i)}^2,
\end{aligned} \tag{C.6}$$

where

$$d\Sigma_{2(i)}^2 = d\theta_i^2 + \sin^2(\theta_i) d\phi_i^2, \tag{C.7}$$

and the metric functions are given by

$$g(r) = 1 \mp \frac{r^2}{\ell^2} \quad , \quad f(r) = 1 - \left(\frac{a}{r}\right)^D, \tag{C.8}$$

satisfy the $(D + 1)$ -dimensional Einstein equations for both a positive and negative cosmological constant $\Lambda = \pm D(D - 1)/(2\ell^2)$.

This is in total agreement with (3.4).

Appendix D

Thermalons

In this Appendix I derive $\pi_{\tau\tau}^{\pm}$ as discussed in [32] and I comment on the thermalon's fate at infinity.

One can start by using (4.11)

$$\frac{d}{d\tau} (a^{d-2} \pi_{\tau\tau}^{\pm}) = (d-2) a^2 \dot{a} \pi_{\varphi_i \varphi_i}^{\pm}, \quad \forall i, \quad (\text{D.1})$$

such that when $\pi_{\tau\tau}^{\pm}$ satisfies the junction condition, all the other components automatically follow. Hence, one just need to calculate $\Pi^{\pm} \equiv \pi_{\tau\tau}^{\pm}$ (This notation Π^{\pm} is simply chosen to avoid the use of indices). This only includes the *angular* parts of both the intrinsic and extrinsic curvatures; the expression then becomes

$$\Pi^{\pm} = \frac{\sqrt{\dot{a}^2 + f_{\pm}(a)}}{a} \int_0^1 d\xi \Upsilon' \left[\frac{\sigma - \xi^2 f_{\pm}(a) + (1 - \xi^2) \dot{a}^2}{a^2} \right]. \quad (\text{D.2})$$

One should impose $\Pi^+ = \Pi^-$ when not including matter which is the case here. The polynomial Υ is, as always, playing a key rôle in this computation.

Introducing $\tilde{\Pi} \equiv \Pi^+ - \Pi^-$, the junction condition and Bianchi identity (D.1) yield $\tilde{\Pi} = \frac{d\tilde{\Pi}}{d\tau} = 0$. One can easily see that this expression is miraculously independent of the spacetime dimensionality. One can introduce

$$g_{\pm} \equiv g_{\pm}(a) = \frac{\sigma - f_{\pm}(a)}{a^2}, \quad \text{and} \quad H \equiv H(a, \dot{a}) = \frac{\sigma + \dot{a}^2}{a^2}. \quad (\text{D.3})$$

Hence, (D.2) becomes

$$\Pi^{\pm} [g_{\pm}, H] = \sqrt{H - g_{\pm}} \int_0^1 d\xi \Upsilon' [\xi^2 g_{\pm} + (1 - \xi^2) H]. \quad (\text{D.4})$$

This leads to concluding that the information about the branches of the solution is hiding in g_{\pm} .

One can rewrite the difference in canonical momenta $\tilde{\Pi}$ as

$$\tilde{\Pi} = \left(\sqrt{H - g_+} - \sqrt{H - g_-} \right) \int_0^1 d\xi \Upsilon' \left[H - \left(\xi \sqrt{H - g_+} + (1 - \xi) \sqrt{H - g_-} \right)^2 \right]. \quad (\text{D.5})$$

A simple change of integration variable results in

$$\tilde{\Pi} = \int_{\sqrt{H - g_-}}^{\sqrt{H - g_+}} dx \Upsilon' [H - x^2], \quad (\text{D.6})$$

where $H = (\sigma + \dot{a}^2)/a^2$.

As the size of the bubble grows and approaches infinity, the parameter H must be computed via power law. In the limit of large bubble speed, equation (D.5) can be computed using

$$\begin{aligned} H - \left(\xi \sqrt{H - g_+} + (1 - \xi) \sqrt{H - g_-} \right)^2 &\approx \xi g_+ + (1 - \xi) g_- + \frac{1}{4H} \xi(1 - \xi) (g_+ - g_-)^2, \\ \left(\sqrt{H - g_+} - \sqrt{H - g_-} \right) &\approx \frac{1}{2\sqrt{H}} (g_- - g_+) \left(1 + \frac{1}{4H} (g_- + g_+) \right), \end{aligned}$$

One can make sure, up to an order of $1/H$, that

$$\tilde{\Pi} \approx -\frac{1}{2\sqrt{H}} \left[\Upsilon[g_+] - \Upsilon[g_-] - \frac{1}{2H} \left(\int_{g_-}^{g_+} dx \Upsilon[x] - (g_+ \Upsilon[g_+] - g_- \Upsilon[g_-]) \right) \right]. \quad (\text{D.7})$$

One needs the following variable substitution $x = \xi g_+ + (1 - \xi) g_-$ to solve for

$$H \approx \frac{1}{2(M_+ - M_-)} \left[a^{d-1} \int_{g_-}^{g_+} dx \Upsilon[x] - (g_+ M_+ - g_- M_-) \right]. \quad (\text{D.8})$$

One can get the predictable equation of H at the lightlike limit ($H \rightarrow \infty$) wherever $M_+ \rightarrow M_-$. The same happens if $a \rightarrow \infty$ and $H \sim a^{d-1}$. The asymptotic behavior of the potential in the latter case is given by

$$H \approx \frac{a^{d-1}}{2(M_+ - M_-)} \int_{\Lambda_-}^{\Lambda_+} dx \Upsilon[x], \quad (\text{D.9})$$

where H is a solution of $\tilde{\Pi} = 0$.